NATIONAL ADVISORY COMMITTEE FOR AERONAUTICS

TECHNICAL NOTE 2947

A VISUALIZATION STUDY OF SECONDARY FLOWS IN CASCADES

By Arthur G. Hansen, Howard Z. Herzig
and George R. Costello

Lewis Flight Propulsion Laboratory
Cleveland, Ohio

NACA

NATIONAL ADVISORY COMMITTEE FOR AERONAUTICS

TECHNICAL NOTE 2947

A VISUALIZATION STUDY OF SECONDARY FLOWS IN CASCADES

By Arthur G. Hansen, Howard Z. Herzig,
and George R. Costello

SUMMARY

Flow-visualization techniques are employed to ascertain the stream-
line patterns of the nonpotential, secondary flows in the boundary
layers of cascades, thereby providing a basis for more extended analyses
in turbomachines. The three-dimensional deflection of the end-wall
boundary layer results in the formation of a vortex well up in each
cascade passage. The size and tightness of the vortex generated depend
upon the main flow turning in the cascade passage. Once formed, a
vortex resists turning in subsequent blade rows. This results in
unfavorable angles of attack and possible flow disturbances on the pres-
sure surfaces of subsequent blade rows when the vortices impinge on
these surfaces.

Two major tip-clearance effects are observed: the formation of a
tip-clearance vortex, and the scraping effect of a blade with relative
motion past the wall boundary layer. The flow patterns indicate methods
for improving the blade-tip loading characteristics of compressors and
of low- and high-speed turbines.

INTRODUCTION

An important problem arising in the design of turbomachines and in
the analysis of their performance is an understanding of the nature and
influence of so-called secondary flows (those flows having components
normal to the flow direction predicted by potential flow analyses).
Various theoretical and experimental investigations have been made, each
of which, by means of various assumptions, partially describes the
manner in which secondary flows affect the performance of turbomachines.
In these analyses, usually one of two methods has been used to estimate
the deviations in the exit-flow angles and velocities due to the non-
potential flow. The first method (ref. 1) is based principally on
airfoil theory, and the flow deviations are considered as arising from

(or at least measured by) trailing-edge vortices associated with span-
wise variations in circulation. The second method (refs. 2 and 3, for
example) is based on the flow of an ideal fluid in a channel with vary-
ing inlet total pressure, and deviations arise from the appearance of
a vorticity component in the direction of the flow.

In the investigations considered, attempts were made to give a
qualitative picture of secondary-flow behavior and to provide some
foundations for approximate loss calculations. Because of the sim-
plifying assumptions involved, however, the question remains as to how
accurately these methods and various extensions of these methods
describe actual flow phenomena, for example, in a cascade. Nevertheless,
knowledge concerning the detailed streamline patterns of the actual flow
in a blade row is essential to an accurate understanding of the nature
and influence of secondary flows. Such information has not been obtained
to date from the aforementioned techniques.

As a first step in obtaining this knowledge, an experimental inves-
tigation was conducted at the NACA Lewis laboratory to determine the
streamline patterns in a cascade. The streamline patterns and the
secondary-flow behavior were determined by flow-visualization methods
using smoke and chemical traces. Photographs of the various flow pat-
terns thus obtained are presented herein. Obtaining direct evidence of
the flow paths by the careful application of these visualization tech-
niques avoided the need for the fundamental assumptions required for
theoretical analyses, which might qualify the results.

Unfortunately, because of the complicated three-dimensional flow
patterns, it is difficult to arrive at an understanding of the secondary
flows in a turbomachine by instituting the study of such flows directly
in the machine. Accordingly, for the first step in attempting to
analyze secondary flows, the visualization techniques were used to obtain
the streamline patterns in a stationary, two-dimensional cascade for a
range of Reynolds numbers. The secondary-flow behavior in the end-wall
boundary layers was thus observable without such disturbing influences
as over-all radial pressure gradients or rotative effects.

In order to extend this study to more general configurations, the
influence of blade geometry was then investigated qualitatively by inde-
pendently varying stagger angle, aspect ratio, solidity, and angle of
attack, and by the use of blade fillets in the two-dimensional cascade.
As part of a more detailed study of high-turning effects on secondary
flows, the secondary flows in rectangular bends (which have been the
subject of many recent investigations (cf. ref. 4)) were also studied
by means of flow visualization. Furthermore, a comparison is made
between the boundary-layer flows in such bends and in blade rows with
similar turning sections.

The flow-visualization technique was applied to an annular-turbine-nozzle cascade at high subsonic and at supersonic Mach numbers in order to extend the scope of this investigation into typical turbomachine flow conditions where radial pressure gradients and shock phenomena exist (refs. 5 and 6). In order to simulate more closely the mechanical conditions in a turbomachine, the two-dimensional cascade was modified to enable the study of the influence of blade-tip clearance and relative motion between wall and blades. Also, the interactions of the secondary flows in successive blade rows were investigated briefly in tandem cascades.

The results of the exploratory secondary-flow studies outlined constitute an informational unit intended to be basic to general investigations of the actual secondary flows in turbomachines.

APPARATUS AND PROCEDURES

Experimental Setups

All configurations discussed in this section will be shown in the figures throughout the report. Where necessary, an insert appears on the photographs depicting schematically an overhead view of the configuration and the smoke trace appearing in the photograph.

Basic two-dimensional cascade. - The initial experimental investigation was intended as a study of the secondary-flow phenomena in a cascade end-wall boundary layer uncomplicated by radial pressure gradients or rotative forces. Therefore, these basic tests were carried out in a two-dimensional steady-flow cascade (see fig. 1). The air to the cascade was supplied by the laboratory combustion-air system and was discharged directly into the room. Because of the construction of the cascade, the inlet-air velocities were limited to Mach numbers below approximately 0.4.

The blade row consisted of six NACA 65(12)-10 blades mounted between two channel walls at a stagger angle of 45°, an angle of attack of 11°, and a turning angle of 20°. The solidity of the cascade was 1.5; the aspect ratio for the blades was 2.34. A row of static taps was located on one wall one-half chord upstream of the blades. At this same axial location, a 1/16-inch-outside-diameter probe was mounted in a slot in the other wall for the introduction of smoke into the air stream at any desired point. All tests were conducted in the half of the passage adjacent to the smooth wall containing the static taps in order to avoid any disturbances that might arise because of the probe slot.

Modified two-dimensional cascade. - The construction of the basic two-dimensional cascade was such that the blade-geometry parameters could readily be varied independently over a wide range. In this fashion the flows through more general configurations could be studied. The geometric parameters which were varied were stagger angle, aspect ratio, solidity, and angle of attack. Other tests involved the use of fillets between the blade tips and the wall.

The 65(12)-10 blade mountings were such that the blade could be moved to provide tip clearance between the blade tips and the wall. The wall could further be replaced by an endless moving belt, the direction and speed of which could be varied in order to study the influence of relative motion between the blades and the wall. The tension on the belt was adjusted to prevent flow disturbances due to belt flap. The tests were conducted at three belt speeds: slow speed (belt speed well below airspeed), moderate speed (belt speed approximately equal to airspeed), and high speed (belt speed well above airspeed).

Three-dimensional cascade. - An annular-turbine-nozzle cascade was used to extend the investigation of secondary flows to high subsonic and to supersonic Mach numbers in a three-dimensional flow configuration (refs. 5 and 6). A schematic view of the apparatus is shown in figure 2. This cascade was supplied with air from the laboratory combustion-air system and discharged into the laboratory altitude exhaust system.

Rectangular bends. - The blade row of the two-dimensional cascade was replaced by a row of sheet-metal blades. The turning sections of these blades were concentric circular arcs having turning angles of 45°. When long straight inlet and exit guides were provided, the passages thus formed were, in effect, rectangular bends. The end wall in which the probe was mounted was replaced by a Lucite wall to make it possible to look directly into the entire bend. The overhead photographs of the bend flows were taken from this position.

Another rectangular-bend-configuration investigation was made in which the blade turning sections were 60° circular arcs, all having the same radius of curvature. The bends were made of sheet aluminum and were mounted in a two-dimensional cascade with a stagger angle of 0°.

High-turning cascades. - The boundary-layer behavior in the 60° bends was compared with that in a set of 60°-circular-arc blades. These blades were sheet aluminum and were mounted in the 0°-stagger-angle configuration. The sole difference between this 60° cascade and the 60° bends is that the cascade does not have the straight guidance sections at the inlet as do the rectangular bends.

In order to investigate the effects of relative motion between end wall and blades at high-flow-turning angles, sheet-aluminum blades with approximately 125° turning were used in the 45°-stagger-angle configuration.

Tandem cascade. - The blades for the tandem cascade were also made of sheet aluminum and were used in the 0°-stagger-angle configuration. Each of the two blade rows of the tandem cascade was mounted on an individual aluminum strip, thereby enabling the positions of the two blade rows to be shifted relative to each other in both the blade-to-blade and axial directions.

The blades in the tandem cascades were bent in circular arcs to give a turning of approximately 60° each. The upstream cascade turned the flow 60° from axial (to the left as seen in the figures of this report). The second or downstream cascade turned the flow back to the axial direction.

Flow Visualization

Three methods were used to visualize the flow patterns: (a) smoke traces in the passage and on the blades and walls, (b) hydrogen sulfide gas reacting with a lead carbonate suspension in glycerin painted on the walls and blades, and (c) paint-flow traces on the surfaces at the higher gas-flow speeds. The smoke flow-visualization method was used in the two-dimensional cascades for tests made at low speeds (30 ft/sec). At the higher speeds (Mach numbers of approximately 0.4 in the two-dimensional configuration and higher Mach numbers in the annular cascade), the hydrogen sulfide - lead carbonate visualization method was used. At the highest speeds studied in the annular cascade, the flow of the paint on the shrouds and blades provided additional information concerning the secondary-flow behavior.

Photographs were taken of the traces obtained by admitting smoke or hydrogen sulfide through the wall static taps and through the probe at either the wall itself or in the passage. As will be demonstrated, the agreement between the probe and static-tap traces showed that the probe did not disturb the flow in the passage sufficiently to affect these tests.

Smoke traces. - Smoke was produced by burning oil-soaked cigars with service air (fig. 3). This method of generating smoke was found to be superior, for this application, to other methods which have been used elsewhere. In particular, the smoke was nontoxic, noncorrosive, easily generated, and of sufficient intensity to be photographed. The

rate of smoke production and injection into the air stream were carefully controlled by means of settling bottles, pressure regulators, and bleeds so as to make it possible to match closely the local direction, velocity, and density of the air stream. In order to maintain the smoke traces intense enough for photographing, the inlet-air velocity was held at approximately 30 feet per second when the smoke-visualization method was used. The smoke-trace method was particularly advantageous because it was possible thereby to visualize the streamlines any place in the passage as well as directly on the walls and blades. No difficulty was encountered with diffusion of smoke into air. However, it is difficult to present the results photographically because the photographs cannot show the three-dimensional movement of the traces which appear, instead, as projections against the passage walls or against the blades. In addition, suitable photographs are difficult to obtain for regions of low contrast.

Hydrogen sulfide traces. - In order to obtain flow traces at higher airspeeds, the following procedure was adopted. The wall and the blades were covered with a paint of lead carbonate in glycerin and alcohol. As the hydrogen sulfide was introduced through the static taps, or through the probe, its path along the blades and on the wall was observable as a brown trace on a white background. This reaction is semipermanent and accumulative. The procedure, therefore, was to introduce the hydrogen sulfide at such rates that the local velocity and direction of the air stream could be matched closely, and the disturbance of the local flow minimized. This was continued until a photographable trace was obtained. Furthermore, the molecular weight of hydrogen sulfide is close to that of air, which minimizes the diffusion due to density differences. Disadvantages of the method are that the gas is highly toxic and corrosive and the reaction must proceed for a long time in order to obtain sufficient color contrast for photographing.

Paint-flow traces. - At the higher Mach numbers, the soft, nondrying paint used in these tests would flow along the painted surfaces and trace out flow patterns. It will be demonstrated by comparison with hydrogen sulfide traces that the paint-flow traces can indicate the flow conditions directly at the surfaces involved.

Test Procedures

In any experimental investigation it is necessary to establish the validity of the procedures involved in order to insure the reliability of the results. In the following paragraphs the test procedures are discussed, and the bases for trust in the results obtained are briefly indicated. References are made to the various sections of the report where each of the considerations involved here is discussed in greater detail.

Probe investigation. - The experimental investigation of secondary flows was begun with the basic two-dimensional cascade at low airspeeds. Smoke-visualization techniques were employed to trace out the flow patterns in the end-wall boundary layer of this cascade in which such complicating factors as radial pressure gradients or rotative forces were eliminated. It was considered desirable to use the probe for the introduction of the smoke for the low-speed tests because with the probe, a point-by-point traverse across the inlet section just upstream of the blades could be made. Thus it was necessary to establish that the probe results are reliable. This was done by comparison of the streamline patterns obtained by use of the probe and the static taps for introducing smoke. Figures 4 through 7, which show the deflection patterns in the wall boundary layer, are used for this purpose and will be discussed fully in the Initial Low-Speed Investigation section of RESULTS AND DISCUSSION. (Throughout this report, except when specified otherwise, the photographs presented were taken with a camera downstream looking up into the discharge section.) Examples of probe surveys of the secondary-flow patterns in the basic two-dimensional cascade wall boundary layer are shown in figures 8 and 9.

Hydrogen sulfide investigation. - As noted earlier, the use of smoke traces proved unsuitable at the higher air velocities and under these conditions one method of visualizing the flow was by means of hydrogen sulfide. The H_2S trace was found to have a tendency to spread out, making it impossible to maintain the trace as a well-defined line. Because of the increased turbulence at the higher air velocities, the H_2S could not be confined to a layer at a specified distance from the wall but was distributed throughout the entire height of the boundary layer. Therefore the H_2S traces indicate the flow paths of a region of the entering boundary layer instead of an individual path. Hence, pictures of the H_2S traces, in general, resemble figures 4(b) and 6(b) where the smoke was introduced at some position away from the wall. Figures 10 through 12 illustrate the kind of "wide" trace typically obtained when H_2S is used.

Paint-trace investigation. - Justification for considering that the patterns obtained by the flow of the nondrying paint are indicative of boundary-layer flow paths directly at the surface was obtained by a comparison of the hydrogen sulfide trace with the paint trace in figure 10(c), where the similarity between the patterns obtained is noteworthy. The obvious precautions are that the paint must be nondrying and capable of flowing when subjected to the air-flow gradients, and also that the test duration must be sufficient to insure that the paint attains a final pattern rather than merely some intermediate patterns. Nevertheless, the assumption that paint-flow traces correspond to air-flow paths can be considered valid only when confirmed by additional experimental evidence.

Inlet boundary-layer conditions. - For convenience, in the course of making the modifications to the cascade as required for the geometric configurations under study, various lengths of inlet section, constructed of different materials, were used because preliminary checks showed (within wide limits) that the thickness of the inlet boundary layer did not affect the type of results obtained. This conclusion is affirmed by noting that the general character of the fundamental secondary-flow phenomena is unchanged over the wide range of conditions investigated here.

RESULTS AND DISCUSSION

Initial Low-Speed Investigation

The first stage of the experimental investigation of secondary flows was the visualization of the streamline patterns in the wall boundary layer of the basic two-dimensional cascade. The main-stream air velocity was approximately 30 feet per second, which permitted the use of smoke for the visualizing.

Spanwise variation of deflection. - The initial phase of the experimental program was concerned with determining the nature and magnitude of the deflection of the wall boundary layer from the pressure surface of one blade toward the suction surface of the adjacent blade. The progressive increase in flow deflection as the wall is approached is qualitatively discussed in the literature. The flow deflection of smoke traces for three spanwise positions is shown in figure 4. In figure 4(a), the smoke is admitted from the static tap with a velocity sufficient to project the smoke stream approximately 1/4 inch from the wall. In figure 4(b), the smoke velocity is reduced to the point where the smoke is projected approximately 1/8 inch from the wall. In figure 4(c), the smoke velocity is further reduced so that the smoke tube lies against the wall in the vicinity of the tap. By superimposition of these three photographs, the magnitude of the variations in deflections is evident (fig. 4(d)).

The results of the spanwise survey, shown in figure 4, demonstrate visually the increase in flow deflection in the wall boundary layer as the wall is approached, as anticipated in the literature. In figure 4(c), the streamline path in the boundary layer very near the wall is clearly seen to cross the passage and to arrive at the suction surface of the passage well upstream of the blade trailing edge.

Reliability of probe and static tap results. - The deflection in the boundary layer along the wall when smoke was admitted through a static tap located upstream of the blades is shown in figure 5. The smoke trace in figure 5(b) was made by the smoke that remained

in the static tap from the time of the previous photograph, fig-
ure 5(a). In figure 5(b), the pressure drop from outside the tunnel
to the static pressure at the wall inside was negligible, and so the
residual smoke must be considered to assume the direction of the air
flow at the wall, that is, it is not projected out into the air stream.
Figure 5(c), made by superimposing figures 5(a) and 5(b), indicates that
as these tests were conducted, each of the smoke traces so represented
must be considered as lying along the wall in the neighborhood of its
respective tap. This procedure was useful in establishing that the flow
patterns at the wall itself could be visualized properly by means of
smoke traces.

The deflection patterns obtained by a spanwise survey through the
boundary layer, using the probe to introduce the smoke, are shown in
figure 6. Paralleling the tests for figure 4, the probe was positioned
so that the smoke was admitted 1/4 inch from the wall (fig. 6(a)),
1/8 inch from the wall (fig. 6(b)), and at the wall (fig. 6(c)). The
superimposition of figure 4 on figure 6 is shown in figure 7. The close
agreement between the streamline patterns obtained demonstrates that the
presence of the probe does not unduly disturb the flow, and that under
the test conditions, the probe results are reliable.

Deflections along wall. - Spanwise surveys through the boundary
layer at other positions across the passage yielded patterns essentially
similar to those seen in figures 4 and 6. In each case, the streamlines
at the wall arrived at the suction surface of the blade at some point
upstream of the trailing edge.

Figure 8 enables a direct comparison of representative paths of the
streamlines obtained in one passage by a probe traverse along the wall.
In each case shown in figure 8, the smoke was introduced with the probe
directly against the wall which, as was demonstrated by figure 7, serves
to trace out the streamline of flow in the boundary layer on the wall
itself at the probe location. These paths are seen in figure 8(e), made
by superimposing figures 8(a) to 8(d), to be confluent in the corner at
the suction surface of the passage near the trailing edge. This parti-
cular phenomenon of the convergence of these streamlines to a small
region in the corner was neither anticipated nor implied elsewhere.

Passage vortex formation. - One of the chief drawbacks of the
photographic presentation is that the smoke traces are seen in the
photographs only as projections against the passage walls or against
the blades. To an actual observer present at the time the tests were
made, the streamlines pictured in figures 8(a) to 8(d) appeared to be
drawn, as if by a flow sink, to the corner made by the suction surface
of the passage and the wall, as shown in figure 8(e). As the stream-
lines approached this region, their paths took on a spiral twist

(counterclockwise in the figures presented herein). Thus, the smoke
streamline crossing the passage in figure 8(d) remained on the wall
until it reached the corner. Upon reaching the corner, the major por-
tion of the smoke trace rolled up in a vortex and came off downstream;
however, the smoke in this vortex (fig. 8(d)) was diluted by the rest
of the boundary-layer air comprising the vortex to the extent that it
could not be perceived photographically at this camera angle.

As the smoke, during the probe traverse, was introduced progres-
sively closer to the suction surface of the blade (figs. 8(c), 8(b),
and 8(a), respectively), the smoke streamlines were observed to deflect
away from the wall as they proceeded downstream. The spanwise deflec-
tion of these smoke traces increased in this order, while the curva-
ture of their paths of approach to the blade decreased in the same
order. Therefore, in figure 8(e), although the streamline of fig-
ure 8(a) appears to cross the other streamlines, which is patently impos-
sible, it actually deflected away from the wall farther than the other
streamlines and passed over them. This process, whereby the boundary-
layer streamlines at and near the wall cross the passage while some of
them are displaced spanwise farther from the wall than others, results
in the formation of the so-called passage vortex. The patterns shown
in figure 8 illustrate how part of the inlet boundary layer rolls up
to form part of the passage vortex.

The vortex formation, as described here, occurred well in the pas-
sage and not as a trailing-edge phenomenon. When a smoke stream was
introduced near the blade leading edge in the corner formed by the suc-
tion surface and the wall, it was observed to assume the same type of
counterclockwise spiral rotation in the passage axially at approximately
the blade midchord position. Because of the tightness of the spiral,
and because the photographs show only path projections, it has not been
possible to obtain a suitable photograph of this evidence of vortex
formation within the passage of the basic two-dimensional cascade.
Photographic evidence of passage vortex formation will be presented in
the section on bends.

At the flow speeds used for these tests, laminar separation prob-
ably occurred on the suction surfaces of the blades near the trailing
edges. When smoke was introduced into the wall boundary layer (fig. 8),
a small portion of this smoke eddied out onto the blades into the
separated-flow region. This slow accumulation of smoke in the stagnant
region produced the dense traces seen on the blades.

Deflections on blades. - The streamline deflection on the blades
caused by secondary flow has been noted and pictured in reference 1.
Figure 9 presents the smoke-trace patterns of this deflection on the
blades. The smoke (fig. 9(a)) was admitted through the probe approxi-
mately 3/16 inch from the wall and in such a position that the smoke

stream split and divided on the blade. In figure 9(b), the probe was 1/2 inch from the wall, positioned so that the smoke path lay on the pressure surface of the blade. In figure 9(c), with the probe at the wall, the smoke follows the suction surface of the blade.

The manner in which the flow on the blade was deflected spanwise toward the wall on the blade pressure surface and spanwise away from the wall on the blade suction surface is clear in figure 9. A comparison of figures 9(b) and 9(c) shows that the deflection on the suction surface was much greater than that on the pressure surface. Such large deflection differences were not to be anticipated from secondary-flow mechanisms similar to that described in reference 1. The large deflection difference evident in figure 9 is here principally attributed to the area-blockage effect of the passage vortex near the suction surface, which causes a large deflection of the flow on the blade suction surface. The region between the smoke trace in figure 9(c) and the wall is, therefore, a rough measure of the size of the passage vortex.

As a result of the flow deflection off the blade pressure surface, air flowed onto the passage wall and was observed to become the wall boundary layer for the region downstream of the smoke trace of figure 8(d). The presentation of this phenomenon photographically was prevented by the rapid thinning of the smoke as it left the blade and diffused on the wall. This will be shown photographically later with the higher-turning configurations.

Remarks on initial low-speed investigation. - The secondary-flow pattern in the basic two-dimensional cascade at low airspeeds is a three-dimensional deflection of the flow in the end-wall boundary layer, both in the spanwise direction normal to the wall and across the passage along the wall. As a result, the boundary layer rolls up to form a passage vortex well up in the passage and not as a trailing-edge phenomenon. In the region near the low-pressure side of the passage where the vortex forms, large gradients of pressure and flow direction make it difficult to take accurate measurements. The complicated three-dimensional nature of this flow makes questionable, too, the applications to date of any two-dimensional, or quasi-three-dimensional, analyses of the flow patterns in the wall region and certainly influences the entire flow through the passage.

Initial High-Speed Investigation

In order to visualize the flow patterns at higher air velocities (larger Reynolds numbers), it was necessary to use the H_2S trace method and the paint-flow-trace method. The construction of the two-dimensional cascade precluded its use for flows above a Mach number of approximately 0.4. The annular-turbine-nozzle cascade rig was therefore used for the higher subsonic and for the supersonic Mach numbers.

Deflections on wall in two-dimensional cascade. - The visualization of the flow along the passage wall and blade at Mach numbers of approximately 0.4 is shown in figure 10. The pattern in figure 10(a) was made by H_2S introduced through a static tap upstream of the blades. A portion of the H_2S trace actually reached and flowed onto the suction surface of the blade but was too faint to photograph and so is shown by the dotted line in figure 10(a). The toxicity and obnoxious odor of the H_2S prevented its use in this cascade (which discharges into the room) for the extended period of time required to darken the trace further.

In order to circumvent this difficulty, an effort was made to concentrate the H_2S trace in the region of chief interest by use of a passage wall static tap. In figure 10(b), the H_2S was introduced through a static tap in the passage; the flow to the corner and onto the blade can be seen somewhat more clearly.

The dark trace on the first blade on the left, shown in figure 10(c), was due to H_2S released from a wall static tap so located that the flow divided on the blade. A faint H_2S trace is, of course, obtained immediately upon release of the gas but it was necessary to run the test for a prolonged period of time in order to intensify the trace sufficiently for photographing. During this protracted run, the paint on the rest of the blades in figure 10(c) was observed to flow slowly until it assumed the final pattern apparent in the picture. The similarity between the H_2S trace and the paint patterns is noteworthy.

Deflections on shrouds of three-dimensional cascade. - The deflection patterns at Mach numbers higher than 0.4 were obtained by applying the H_2S flow-visualization method to the annular nozzle ring of a typical modern high-speed turbine. In the annular-turbine-nozzle cascade it was possible to use the H_2S for a sufficient length of time to make the clear, dark traces presented in figures 11 and 12. Figure 11 shows the H_2S traces obtained with this annular cascade at a hub-discharge Mach number of approximately 0.9 and a tip-discharge Mach number of approximately 0.7. A view of the cascade inner shroud at the blade-row inlet is shown in figure 11(a). The H_2S was admitted through one wall static tap in each of two adjacent passages, and the tap positions relative to the blades can be seen in figure 11(a).

The results of figure 11(b) show that again the pattern has been repeated: In each case the flow deflects across the passage, arrives at the suction surface of the blade, and flows out on the blade. The shape of the flow traces on the blades and shrouds indicates the formation of a vortex within the passage in the annular cascade as well as in the two-dimensional cascade. In figure 11(c), the pattern is repeated at the outer shroud with high subsonic Mach numbers.

The H₂S traces for the same annular cascade when the approximate hub- and tip-discharge Mach numbers were 1.5 and 1.2, respectively, are presented in figure 12. The same inner- and outer-shroud static taps were used here as were used for figure 11. Despite flow discontinuities caused by the supersonic flow velocities involved, the deflection pattern on the shrouds is nevertheless repeated and the formation of passage vortices is indicated.

Remarks on initial high-speed investigation. - The pattern of deflection of the wall boundary-layer flow across the passage was repeated at Mach number 0.4 in the two-dimensional cascade and again at the high subsonic and supersonic Mach numbers in the annular cascade. Although, strictly speaking, the H₂S and paint-flow-visualization methods used in this section show what happens in the boundary layer only at the boundary itself, the indications are strong that passage vortex formation occurs at the high speeds too.

Cascade Parameter Investigation

In this section the effects of variations of the cascade parameters (blade geometry) on the secondary flows are investigated.

In the region of extremely large velocity gradients and angle deflections, where the passage vortex is formed, the accuracy of total pressure and flow angle measurements is severely limited and the interpretation of such quantitative measurements must be made with care.

For these reasons the influence of blade geometry on secondary flows was investigated qualitatively by means of appropriate modifications to the basic two-dimensional cascade. The cascade was modified for the investigation of the following numerical values of parameters in addition to those already reported for the basic two-dimensional cascade (the parenthetical values are those of the basic cascade): stagger angle, 0° (45°); aspect ratio, 1.67 (2.34); solidity, 2.0 (1.5), and 0.75; angles of attack, 4°, 7°, (11°), 15°, and 20°. Also, blade fillets were added on the suction surface, on the pressure surface, and on both surfaces, respectively, to evaluate their effects on the secondary flows.

In each case with the main-stream velocity about 30 feet per second, the secondary-flow patterns were observed by the smoke-flow-visualization techniques, and the results are presented photographically.

Stagger angle. - The deflections of the streamlines in the inlet boundary layer which join in a region near the suction surface are demonstrated in figures 13(a) to 13(c), for a cascade with a stagger

angle of 0° (where stagger angle is the angle between the cascade axis and the incoming air). The values of the parameters are given in the legend for each photograph of this section. The streamline pattern can be seen, by comparison, to be essentially identical with the pattern in figure 8, where the stagger angle is 45°. Therefore, for convenience in photographing, the 0°-stagger-angle configuration was used for the remainder of the tests.

The path of a streamline in the main flow through the cascade with a stagger angle of 0° is shown in figure 13(d). It was observed during the tests that the total turning of the flow is essentially unchanged from that of the cascade with a stagger angle of 45°.

Aspect ratio. - The aspect ratio for the two-dimensional cascade was reduced from 2.34 to 1.67 by means of specially devised inserts along the end walls. The boundary-layer streamlines (fig. 14) remained unaffected. It was observed during the test that the spanwise deflection of corresponding streamlines in the boundary layer was also unaffected by the change in aspect ratio.

Solidity. - With the solidity (ratio of blade chord to blade spacing) reduced from 1.5 to 0.75, the main portion of the inlet boundary-layer streamline at a blade nose was not deflected completely across the channel (fig. 15(a)). Most of the smoke was deflected part way across the channel and then proceeded downstream. The wisp of smoke seen at the trailing edge reached there by flowing upstream in the separated region behind the suction surface of the blade. For the case with the solidity reduced to 0.75, it was observed that the three-dimensional aspects of the boundary-layer flow, namely, the deflection of streamlines near the suction surface in a direction away from the wall, had decreased considerably and the passage vortex was smaller. Because the camera shows only projections, the deflections away from the wall could not be photographed here. Consequently, the photographs show only cross-channel deflection, but the three-dimensional aspects of the flow cannot be ignored for proper interpretation of the phenomena reported.

The streamline for the first probe location at which the suction surface was reached by cross-channel flow is shown in figure 15(b). The turning of the main stream (fig. 15(c)), is less at the low solidity of 0.75 than at the design solidity of 1.5 (fig. 13(d)).

The results of tests at a solidity of 2.0 are shown in figure 16. Figure 16(a) shows, as might be expected, that the boundary-layer streamline at the nose of one blade is deflected all the way across the channel. The deflections of the secondary-flow streamlines in the spanwise direction were observed to have increased over those in the basic cascade. The main-stream flow illustrated in figure 16(b) is turned somewhat more than in the basic cascade (solidity, 1.5).

Angle of attack. - The streamline patterns were investigated for
the cascade at the original solidity of 1.5 and at angles of attack of
4°, 7°, 15°, and 20° (original angle of attack, 11°). Figures 17 and 18
show the results of the tests at 4° and 20°, respectively. At a 4°
angle of attack (fig. 17), it was necessary to move the probe halfway
across the channel at the inlet in order to find a streamline which
would deflect to the suction surface. As the angle of attack increased,
the cross-channel and away-from-the-wall deflections increased, and the
passage vortex became larger.

Combined solidity and angle of attack. - The streamline paths for
the cascade with solidity of 0.75 and angle of attack of 4° are shown
in figure 19. Again, it is necessary to move the probe almost halfway
across the channel at the inlet in order to find a streamline which is
deflected to the suction surface. It was observed that in this case the
deflections away from the wall were smaller than for the basic configura-
tion. At a solidity of 2.0, an angle of attack of 20°, and with the
probe away from the wall (fig. 20(a)), some streamlines in the blade
boundary layer well up on the pressure surface of a blade deflect to the
wall and cross the channel to the suction surface of the next blade,
there to comprise part of the passage vortex. A comparison of the
amount of turning of the main streams for the two configurations, which
represent the extremes of the ranges investigated, is possible with the
use of figures 19(c) and 20(b).

This study of solidities and angles of attack indicates that the
over-all turning of the main streams of the blade rows is a major factor
in the cross-channel and spanwise deflections of the inlet wall boundary
layer. Furthermore, it was observed during these tests that, for the
configurations which involved greater turning of the main stream, the
spanwise deflection of the corresponding streamlines in the boundary
layers increased, the roll-up into the passage vortex was tighter, and
the vortex was larger.

The study of flows through bends in a later section of this report
will present more qualitative information on the effects of main-stream
turning variation on secondary flows.

Blade fillets. - Streamlines for configurations having fillets of
approximately 3/16-inch radius of curvature on the blade pressure sur-
face, blade suction surface, and on both blade surfaces are shown in
figures 21(a), 21(b), and 21(c), respectively. The fillets apparently
had little effect upon the formation of the passage vortices. Similar
results were obtained with larger fillets, as well.

Remarks on cascade parameter investigation. - Throughout the investigation of various geometric configurations of the two-dimensional cascade, the basic mechanism of the formation of a secondary-flow passage vortex was unchanged; however, the degree to which the wall boundary layer deflected away from the wall and across the channel, as well as the size and tightness of the passage vortices, was influenced by those parameters which involved the turning of the main flow. These parameters, as illustrated by the figures, were solidity and angle of attack. Parameters, such as aspect ratio and stagger angle, that did not alter the turning had no apparent influence on this secondary flow. Furthermore, the fillets on the blades had no appreciable effect on the passage vortex roll-up.

Secondary Flows in Bends and High-Turning Cascades

Secondary flow in bends. - It has been noted in the literature (cf. ref. 4) that low-stagnation-pressure fluid in the end-wall boundary layers of rectangular bends moves across the passage from the pressure toward the suction side. It has been indicated further that, upon reaching the suction surface, the low-stagnation-pressure fluid is displaced away from the wall and out into the main stream.

The smoke-visualization technique was applied to the study of the boundary-layer flow in two sets of rectangular bends with the following results.

As noted earlier, the curved walls of the 45° rectangular bends are concentric circular arcs so that the main-flow streamlines may be as nearly circular as possible in the turning section of the elbow.

Figure 22 shows the typical passage vortex formation pattern described for cascades earlier in this report. The smoke was introduced at the wall and near the pressure surface of the bend. It can be seen to cross the passage and to roll up near the suction surface. Because of the greater turning involved in this case than heretofore, the roll-up and vortex formation are much more distinct, enabling more satisfactory photographs of the passage vortex phenomenon than those obtained earlier.

The smoke filament in any of these pictures actually traces out the path of only one of the streamlines which comprise a passage vortex. Because of the symmetry of the flow in such a vortex, however, the behavior of any one streamline can be considered representative of the entire vortex flow. Accordingly, in this report, when the roll-up of a streamline into a vortex is shown, it will be characterized as the entire vortex in the discussion of the figure.

Figure 23 shows another view of a part of the passage vortex taken with the camera pointed almost directly upstream into the vortex. Careful examination of this figure discloses that the portion of the passage vortex shown here does not actually touch the suction surface. The outer portion of the passage vortex which does contact the suction surface was obtained by admitting smoke away from the wall up on the pressure surface of the passage. This is in accordance with the pattern of passage vortex formation described earlier, that is, the boundary-layer roll-up is such that the outer layers of the passage vortex are derived from inlet boundary-layer flow near or on the pressure surface side of the passage; the central portions of the passage vortex are derived from the inlet boundary layer nearer the suction side of the passage.

Another part of the passage vortex in the 45° rectangular bend is presented in figure 24. Here the vortex is clearly shifting in a direction away from the wall and also away from the suction surface.

The formation of a passage vortex in the wall boundary layer of the 60° rectangular bend is shown in figure 25. The turning sections of these passages are circular arcs, all having equal radii of curvature. The introduction of a large quantity of smoke made it possible to observe the continued twisting of the vortex downstream of the blade row (fig. 26).

An overhead view of the deflection of a boundary-layer streamline across the passage is presented in figure 27(a). When viewed in this direction, perpendicular to the surface in which the streamlines are flowing, the streamlines appear quite faint and so it is considerably more difficult to obtain good, high-contrast pictures from above than from downstream.

This streamline (fig. 27(a)) does not actually contact the suction surface of the passage, that is, this streamline is not in the outermost layer of the vortex. For figure 27(b), the smoke was admitted up on the pressure surface of the bend, about 1/4 inch away from the end wall. In this case, the streamline pictured is one which actually does reach the suction surface across the passage.

Comparison of secondary flow in bends and cascades. - A comparison is made in this section of the secondary-flow patterns obtained with the rectangular bends having a turning angle of 60° and with a two-dimensional cascade of sheet-metal blades having a turning angle of 60°. The total turning, the rate of turning, and the blade spacing are the same for both configurations. With the exception of the leading-edge region, the main-flow streamline patterns were likewise found to be essentially the same.

Figures 28(a) and 28(b) show two of the streamlines in the end-wall boundary layer of the 60° cascade and how they roll up in the passage vortex. Figure 28(c) shows that some of the fluid in the passage vortex of this configuration comes from up on the pressure surface of the blade at a distance from the wall.

In figure 29, the smoke is admitted at the inlet to the blade row and at the wall, but closer to the pressure surface than in figures 28(a) and 28(b). It appears from figure 29 that in this 60° turning cascade of sheet-metal blades (with the tangent to the blades at the inlet being in the axial direction), a well-defined stagnation region exists near the blade leading edge on the pressure side. The smoke trace, in the photograph, approaches this region, divides in two, and flows around it. One part of the smoke follows a cross-channel flow pattern; the other part flows around the blade leading edge and downstream along the blade suction surface in the adjoining passage. An overhead view of this phe-nomenon appears in figure 30. This difference in behavior of the bound-ary layers of the cascade and the bends can be explained qualitatively as follows. The main streamline pattern for the given cascade should have the form depicted in figure 31(a), that is, a stagnation point should exist on the pressure surface of the blade slightly downstream of the leading edge. The high pressures which must exist in this region force some of the smoke (fig. 30) on one side of the stagnation stream-line to flow upstream and around the nose of the blade. On the other side of the stagnation streamline, smoke flows across the channel. The adverse pressure gradients in the vicinity of the wall in the region immediately upstream of the stagnation point give rise to a relatively large separated-flow area. In the elbow configuration previously dis-cussed, such a stagnation region on the pressure surface does not exist. The main streamline pattern should have the form shown in figure 31(b) because the straight entrance section affords a gradual loading of the turning surfaces. Thus, despite the fact that the mean streamlines through the passages are relatively the same for the 60° bends and for the corresponding cascade, the boundary-layer flows are noticeably different.

In figure 32(a), the probe admitting the smoke has been shifted toward the suction side of the passage, just enough for the smoke trace to clear the stagnation region. The path of the smoke trace, by compari-son with figure 27(a) of the 60° bend, can be seen to be somewhat dis-torted. In figure 32(b), the probe has been moved even closer to the suction side, yet the flattened trajectory still is evidence of the effects of the separated-flow region.

Remarks on flows in bends and cascades. - For purposes of photog-raphy, the tests of the secondary flows in the high-turning bends and cascades were much more satisfactory than the tests on the basic

two-dimensional cascade. As a result of the high turning involved, the
passage vortex roll-up was very well defined. Each smoke trace main-
tained its identity long enough to enable good photographic evidence of
a true vortex formation in the passage.

The accumulation near the suction surface of low-momentum fluid was
here seen to be a passage vortex. After its initial formation, the flow
in this vortex on its way downstream was seen to shift out from the end
wall.

Comparisons of the boundary-layer flows in bends and cascades dis-
closed possible large discrepancies between them. The study of secondary
flows in rectangular bends may then facilitate theoretical analyses of
flow-deflection paths, but the results may well not be applicable
directly to cascade boundary-layer flows.

Secondary Flows in Three-Dimensional Cascades

The flow-visualization technique was applied to an annular-turbine-
nozzle cascade designed for high subsonic and for supersonic Mach num-
bers in order to extend the scope of this investigation into typical
turbomachine flow conditions with radial pressure gradients and with
the complicating addition of shock phenomena. The information concern-
ing cross-channel deflections and passage vortex formation obtained in
the basic two-dimensional cascade, together with the results obtained
using H_2S and paint-flow traces, provided a clear understanding of
secondary flows in three-dimensional cascades (refs. 5 and 6). In
reference·5, careful surveys of total pressure and flow angle made at
the discharge of the turbine-nozzle blades revealed the presence of a
sizable loss core near the inner shroud. The loss core near the outer
shroud was very much smaller than this at the lower pressure ratio inves-
tigated in reference 5 and decreased almost to the vanishing point at
the higher pressure ratio. (Fig. 5 of ref. 5, which presents these
results of the surveys, is reproduced for convenience herein as fig.
33.) This was considered to indicate the presence of sizable inward
radial flows in the cascade. Accordingly, the H_2S and the paint-flow-
trace methods were applied to the cascade. Figures 11 and 12 are the
results of the H_2S tests and demonstrate the typical cross-channel
deflection pattern. Paint-trace evidence of radial flows in the blade
wakes and on the blade suction surfaces is presented in figures 11
and 12 of reference 5. In particular, figure 11(b) of reference 5,
reproduced herein as figure 34, is a striking indication of radial flows
along the blade suction surface in a region of thickened boundary layer
produced by the intersection of a flow discontinuity (at the supersonic
Mach number) with the suction surface.

Reference 6 attempts to evaluate these radial flows and concludes "The inner-wall loss core associated with a blade of the turbine-nozzle cascade is largely the accumulation of low-momentum fluids originating elsewhere in the cascade. This accumulation is effected by the secondary-flow mechanism which acts to transport the low-momentum fluids across the channels on the walls and radially in the blade wakes and blade boundary layers. . . . At one flow condition investigated, the radial transport of low-momentum fluid . . . . accounted for 65 percent of the (inner wall) loss core . . . . "

Figure 35 (fig. 6 of ref. 6) presents an over-all sketch of the secondary-flow components in the annular-turbine-nozzle cascade. Similar tests on another annular-nozzle configuration (as yet unpublished data) disclosed the same pattern of secondary flows but with better evidence of radial flows in the blade wakes at the lower pressure ratios.

Tip-Clearance Effects in Two-Dimensional Cascade

with Low-Turning Blades

In order to simulate more closely the conditions in a turbomachine, tip clearances of 0.060 and 0.014 inch were provided in the two-dimensional cascade. The effects of this tip clearance were studied by means of the smoke-visualization method. One of the end walls of the cascade was then replaced by an endless moving belt whose direction and speed could be varied, in order to study the tip-clearance effects with relative motion between blades and wall.

Tip clearance. - The possibility that blade-tip-clearance flow might oppose the formation of the passage vortices and thus reduce these flow disturbances was investigated. The flow patterns at clearances of 0.060 and 0.014 inch (1.7 and 0.4 percent span, respectively), are shown in figures 36 and 37, respectively. The point of principal interest arising from this study was the fact that with tip clearance the passage vortex heretofore observed was displaced but was neither eliminated nor apparently reduced in magnitude.

The deflection of the flow along the pressure surface (fig. 36(a)) is greater than for blades without tip clearance because a large part of the flow under the blade tip comes from flow off the blade pressure surface. For this particular probe location, the flow was observed to cross under the blade tip at the midchord position. This blade boundary-layer flow, which crosses under the blade, forms a vortex lying against the suction surface. This tip-clearance vortex rotates in a direction opposite to that of the secondary-flow vortex and preempts the region where the secondary-flow vortex would form if no tip clearance were present. Nevertheless, figure 36(b) shows that the usual passage vortex

still exists and is merely displaced by the tip-clearance vortex. Essentially, the same phenomenon for 0.060-inch blade tip clearance is illustrated in figures 37(a) to 37(c). The tip-clearance vortex in figure 37(a) was traced out by smoke admitted through a probe. Figure 37(b) is a side view of the displaced passage vortex and was obtained when the smoke was admitted through wall static taps upstream of the blades. Figure 37(c) depicts the pattern obtained from smoke admitted through the probe to show the tip-clearance vortex, while smoke admitted simultaneously through a wall static tap shows the usual secondary-flow vortex. The manner in which the tip-clearance vortex flows contiguous to the secondary-flow vortex can be seen in the figure.

A particularly striking picture of the tip-clearance vortex forming in a cascade with 0.060-inch blade clearance is shown in figure 37(d).

Relative motion between blades and wall. - The investigation of the flow behavior when relative motion existed between the cascade blades and the cascade end wall disclosed some unexpected results. In particular, it had been assumed a priori that the moving wall would tend to increase the flow of the wall boundary layer as well as of the blade boundary layer off the leading surface and to pull them under the blade tips in the direction of the wall motion. However, figure 38 indicates that this assumption is invalid. Comparison of the smoke deflection in figure 38(a), where the wall is stationary, with figures 38(b) and 38(c), where the motion of the wall is such as to make the pressure surface the leading surface, shows that flow on the blade is actually deflected away from the wall. Similarly, figure 39, where the suction surface is leading, shows increased deflection of the flow away from the wall with increasing wall speed; figures 39(a), 39(b), and 39(c) illustrate the patterns for the stationary wall, for the wall moving at moderate speed, and for the wall moving at high speed, respectively.

The explanation of the observed phenomenon is that the blades have a scraping action on the flow near the moving wall. The blade leading surface scrapes up fluid entrained on the moving wall thus imparting a rolling motion to the air in the vicinity of the leading surface. Figure 40 shows this roll-up when the pressure surface is leading. Figure 41 portrays the same type of roll-up when the suction surface is leading. One consequence of this scraping effect is the virtual elimination of the tip-clearance vortex associated with a stationary wall for this configuration (figs. 36 and 37).

The patterns on the pressure surface of a blade when the suction surface is leading are shown in figure 42. In a comparison of the flow deflection in figure 42(a) (wall stationary) with figures 42(b) and 42(c) (wall moving), the wall motion increases the flow deflection on the pressure surface toward the wall. Smoke injected near the moving wall actually flowed down the blade onto the wall and was carried across to the adjacent blade suction surface.

Similarly, figure 43 shows that the moving wall, with the pressure surface leading, deflects the flow on the suction surface toward the wall. In this case, it was also observed that smoke flowed down the blade suction surface onto the wall and was carried over to the pressure surface of the adjacent blade. A photograph of this effect was unobtainable because of the severe diffusion that existed when smoke was so introduced. Furthermore, this action of the moving wall with the pressure surface leading removed the stagnant air region previously existing on the blade suction surface near the trailing edge so that the flow now remains attached to the entire blade suction surface.

Remarks on tip-clearance effects. - Instead of reducing secondary-flow effects, tip clearance in the basic two-dimensional cascade resulted in merely displacing the secondary-flow vortex and provided another vortex rotating in the opposite direction. The two vortices rotated side by side without much mixing and thus constituted a considerably larger flow disturbance than did the secondary flows alone.

When the wall moved past the blade tips, the net effect was that flow near the wall was scraped off and was rolled up by the blade leading surfaces, while the low-momentum fluid on the blade trailing surfaces was pulled off the blades.

In the case where the pressure surface was leading (e.g., as in a compressor), this behavior acted in this configuration: (a) to improve flow characteristics on the blade suction surface even at some spanwise distance from the tip by reducing the boundary layer which exists when the wall is stationary (this is good because it reduces the tendency toward separation on the blade suction surface), (b) to replace the secondary-flow vortex and tip-clearance vortex on the suction surface by a different roll-up near the blade leading surface, and (c) to improve generally the tip flow on the pressure surface and the blade tip loading in the sense that it prevents the tip flow from deflecting under the blade which would reduce the pressure difference across the blade tip. The patterns of the flow obtained with the pressure surface leading simulate, to a degree, the absolute fluid motion in an axial-flow compressor stator or the relative motion in the compressor rotor.

When the suction surface was leading, for the configuration tested, this behavior acted: (a) to aggravate the effects at the suction surface by piling up low-energy fluid there which increased the secondary-flow effects while adding a new roll-up near the leading surface (this is bad because it increases the tendency toward separation on the blade suction surface), and (b) to aggravate the tip effects at the pressure surface by increasing the deflection of the flow and thereby impairing the blade loading at the tip. In this case, where the suction surface is leading, the flow patterns simulate to a degree the relative motion of the fluid at the blade tips of a turbine rotor.

The foregoing observations offer a possible explanation for the larger tip losses encountered in turbines as compared with compressors. They also indicate that, whereas shrouding appears to be undesirable in compressors, it may be beneficial for turbine configurations similar to the one studied herein with low turning and low blade tip stagger.

Tip-Clearance Effects with High-Turning Blades

Preliminary considerations. - As noted in the previous section, the blade-tip-clearance flows and the scraping effects produced by relative motion between blades and wall may lead to boundary-layer separation and reduced tip loading in a turbine rotor. This condition would result in less work being extracted from the gas at the tip section. Total-temperature measurements behind turbine rotors generally indicate that this is actually the case.

However, in several recent experimental investigations of high-speed turbines at the NACA Lewis laboratory, this quite typical decline in turbine blade performance at the tip section was notably absent. The turbine blading configurations involved were fairly typical of high-speed turbine rotors, that is, large-turning, high-twist blades. Consideration of these results along with those of the previous section suggested the possibility that, under certain conditions, a balance between the passage vortices, the tip-clearance vortices, and the scraping effects might be established which would enhance good blade tip loading.

It was reasoned that the scraping effect, which in the configuration of the previous section was so large that it masked completely the passage and tip-clearance vortex effects, would be reduced considerably when the blade tip orientation was more tangential in direction. The chord line of the tip sections of high-twist blades is pointed more nearly in the direction of relative blade-wall motion than in the case examined in the previous section. Physically, the blades might be considered to have a slicing action on the wall boundary layer rather than the kind of scraping action seen before. It was reasoned further that the tip-clearance vortex would become larger with higher turning in the blades as a result of the increased gradient of pressure through the clearance space from the pressure surface to the suction surface of the blade. It has already been established that the passage vortex became larger with increasing turning. As has been previously noted, some of the flow forming the passage vortex comes off the pressure surface of the blade. This effect might be somewhat reduced by the tip-clearance action to divert into the tip-clearance vortex some of the boundary-layer flow which would, in the case with zero clearance, otherwise deflect off the blade pressure surface, onto the wall, and across into the passage vortex.

Tests with moving wall and high-turning blades. - Smoke studies were conducted in the two-dimensional cascade, with the moving wall, to investigate the possibilities discussed in previous sections. The 45°-stagger-angle configuration was used to permit large turning. Figure 44 presents photographs of the results of an investigation of blades with approximately 125° turning. In this configuration, the leading edges of the blades have zero angle of incidence with the main flow and the trailing edges of the blades point approximately 10° from the direction of the moving-wall motion. A schematic sketch of the apparatus appears in figure 44(a).

Because of the high turning of the cascade blades, the camera had to be directed broadside at the smoke and could not be aimed along smoke paths. This necessitated the use of large quantities of smoke to obtain any photographs at all. The pictures which were obtained are pictures of projected smoke patterns only.

In figure 44(b), the smoke was introduced with the probe at the leading edge of the middle blade of the cascade on the pressure surface side (the photographs show suction surfaces only), and spanwise about one-third of the way up the blade. The wall is stationary. Some of the smoke deflected down the pressure surface and through the tip-clearance space, forming a very large tip-clearance flow region on the suction side of this middle blade. This tip-clearance flow can be seen near the wall against the suction surface of the middle blade in figure 44(b). The excess of smoke which did not follow this pattern can be seen passing downstream to the right in the photograph. No suitable photographs could be obtained of the passage vortex roll-up. This was observed during the tests to occur in the upstream third of the passage and to roll around the large region occupied by the tip-clearance flow, making a sharp surface of demarcation defining this region.

With the wall moving at moderate speed (fig. 44(c)), the tip-clearance flow, seen against the suction surface, was observed to decrease considerably. The region occupied by this flow was correspondingly reduced with the result that smoke introduced in the boundary layer at the passage inlet could now approach closer to the suction surface than with the wall stationary.

With the wall at a higher speed (fig. 44(d)), no tip-clearance flow to the suction surface was observed. Smoke introduced in the inlet boundary layer for the most part flowed quite smoothly downstream. This indicates that such a balance was established between the passage vortex and the scraping effects on the one hand, with the powerful forces tending to create tip-clearance flow on the other hand, as to produce relatively undisturbed flow throughout the passage. As a matter of fact, the flow through the passage under these conditions was smoother than in earlier configurations where less turning and smaller tip-clearance forces were involved.

Remarks on tip-clearance effects in turbine rotors. - In a very
preliminary sort of investigation, it was found that a balance between
the passage vortex, the tip-clearance vortex, and the scraping effects
of the blades on the moving wall could be established which resulted in
improved flow conditions throughout the passage and its boundary-layer
regions. It may be inferred, therefore, that the possibility certainly
exists of designing high-speed turbine-rotor configurations in such
fashion as to reduce separation and to prevent reduced loading on the
blades at the tip section. This possibility depends upon evaluating
and regulating the relative sizes of the secondary and blade-tip-
clearance flow effects. This also suggests a reason for apparently
conflicting experimental results concerning the effects of tip clear-
ance on turbomachine performance.

In more moderate-speed turbine rotors, with typically less blade
stagger at the tip than is usual with the high-speed rotors, it may not
be possible to reduce the scraping effects sufficiently. For such tur-
bines where the centrifugal stress problems are not too acute, shroud-
ing of the rotors appears to be a more likely method of blade-tip-
loading control.

Secondary Flow in Tandem Cascades

Flow patterns in tandem cascades. - The construction of the tandem
cascades was described in the Experimental Setups section of this
report. Smoke traces disclosed that the main stream followed the turn-
ings through both cascades quite smoothly.

The secondary-flow pattern in the wall boundary layer for each 60°
cascade by itself was the same as shown previously (figs. 25 to 28);
that is, each generated its own passage vortex which then extended
downstream.

The behavior of the vortex generated by the upstream cascade pro-
vided the chief interest in this flow-visualization study. This vortex
did not turn as much as the main flow as it passed through the down-
stream cascade. Instead, it displayed a strong tendency to continue in
the same direction as when it left the upstream cascade. When the rela-
tive spacing of the cascades was such that this vortex passed through
the downstream cascade without touching a blade there, it was not turned
back to the axial direction. Because of the setup used, it was not
possible to get overhead pictures of this phenomenon so that the dis-
charge angle of the vortex might be ascertained. The best estimate that
could be made in this series of qualitative studies is that the vortex
tube does turn somewhat in passing through the second blade row but that
the discharge angle of the vortex is nearer 60° from axial than axial.

A striking manifestation of the resistance to turning of the vortex tube is provided in figure 45. In figure 45(a), the smoke was introduced at the inlet to the upstream cascade and at the wall. The smoke trace is seen to cross the passage in this cascade. The deflection of the streamline away from the wall also is apparent from its spanwise position in the photograph as it enters the second or downstream cascade. Then (see fig. 45(a)), the vortex tube, instead of turning with the main flow, proceeds in its path until it collides with the pressure surface of a blade in the second cascade. An observer could see the flow in the vortex tube strike the pressure surface and deflect off downstream. At the low airspeeds of these tests, flow separation was observed on the pressure surface of the blade in the region of the impact.

Figure 45(b) shows the same phenomenon when the smoke is introduced at a different position in the inlet boundary layer of the first cascade.

Remarks on secondary flows in tandem cascades. - This tandem cascade investigation demonstrates the peculiar resistance to turning of the secondary-flow vortices as they extend downstream. The preliminary results of these tests indicate one way in which the secondary flows, with little actual energy involvement per se, may give rise to considerable losses as a result of their behavior in subsequent stages of turbomachines. This behavior pattern of the vortex tubes suggests the need for further investigations into the nature of the vortices, how they penetrate the main-flow field, and what becomes of the main flow in the vicinity of the origin of the rolled-up vortex and along the path it traverses.

CONCLUSIONS

1. The pattern of secondary-flow behavior in boundary layers of cascades and rectangular elbows, which occurs whenever there is turning of the main stream, consists of a three-dimensional roll-up of end-wall boundary layer into a region near the suction surface to form a passage vortex. No trailing-edge vortex phenomenon was observed. The size and tightness of this passage vortex depends principally upon the amount of turning of the main stream.

2. It is a characteristic of a passage vortex to shift in a direction away from the end wall and from the blade suction surface as it moves downstream and to resist subsequent turnings with the main stream. The latter result is particularly evident in the tandem-cascade studies where a vortex passing from one cascade through another is shown striking the pressure surface of a blade in the downstream cascade causing flow disturbances. These disturbances may account for a large part of the losses attributed to secondary flows in turbomachines.

3. The existence of blade tip clearance in a cascade induces a vortex near the suction surface (formed from flow under the blade tip) which rotates in a direction opposite to the passage vortex. The tip-clearance vortex displaces the passage vortex from the region near the blade suction surface and rotates side by side with it without appreciable mixing. The magnitude of the tip-clearance vortex varies with blade loading.

4. When relative motion exists between the cascade blades and the cascade end wall, the leading surfaces of the blades with moderate blade tip stagger "scrape" up entrained fluid near the wall and impart a rolling motion to the air in this region while on the trailing surface, boundary-layer fluid is aspirated off the blade onto the wall. With the pressure surface leading (compressor case), the scraping effect was shown to improve blade tip loading characteristics. With the suction surface leading (turbine case) the scraping effect was shown to be detrimental to blade tip loading characteristics. For turbines with high blade tip stagger, it appears possible to obtain a balance between passage vortex forces, tip-clearance forces, and blade scraping effects. As a result, the normally large disturbed flow area (and fall-off of turbine-blade performance at the tip) near the suction surface can be virtually eliminated.

5. The passage vortex formation is the principal secondary-flow phenomenon in rectangular bends as it was observed to be in cascades. However, as a result of the nose effect in cascades, the boundary-layer flows are noticeably different from those in bends.

Lewis Flight Propulsion Laboratory
    National Advisory Committee for Aeronautics
        Cleveland, Ohio, February 11, 1953

REFERENCES

1. Carter, A. D. S.: Three-Dimensional-Flow Theories for Axial Compressors and Turbines. War Emergency Issue No. 41, pub. by Inst. Mech. Eng. (London). (Reprinted in U. S. by A.S.M.E., Apr. 1949, pp. 255-268.

2. Squire, H. B., and Winter, K. G.: The Secondary Flow in Cascade of Aerofoils in a Nonuniform Stream. Jour. Aero. Sci., vol. 18, no. 4, Apr. 1951, pp. 271-277.

3. Hawthorne, William R.: Secondary Circulation in Fluid Flow. Proc. Roy. Soc. (London), ser. A, vol. 206, no. A1086, May 7, 1951, pp. 374-387.

4. Eichenberger, Hans P.: Shear Flow in Bends. Tech. Rep. No. 2,
     Office Naval Res., Gas Turbine Lab., M.I.T., Apr. 15, 1952. (Con-
     tract N5ori07848.)

5. Allen, Hubert W., Kofskey, Milton G., and Chamness, Richard E.:
     Experimental Investigation of Loss in an Annular Cascade of Turbine
     Nozzle Blades of Free Vortex Design. NACA TN 2871, 1953.

6. Rohlik, Harold E., Allen, Hubert W., and Herzig, Howard Z.: Study
     of Secondary-Flow Patterns in an Annular Cascade of Turbine Nozzle
     Blades with Vortex Design. NACA TN 2909, 1953.
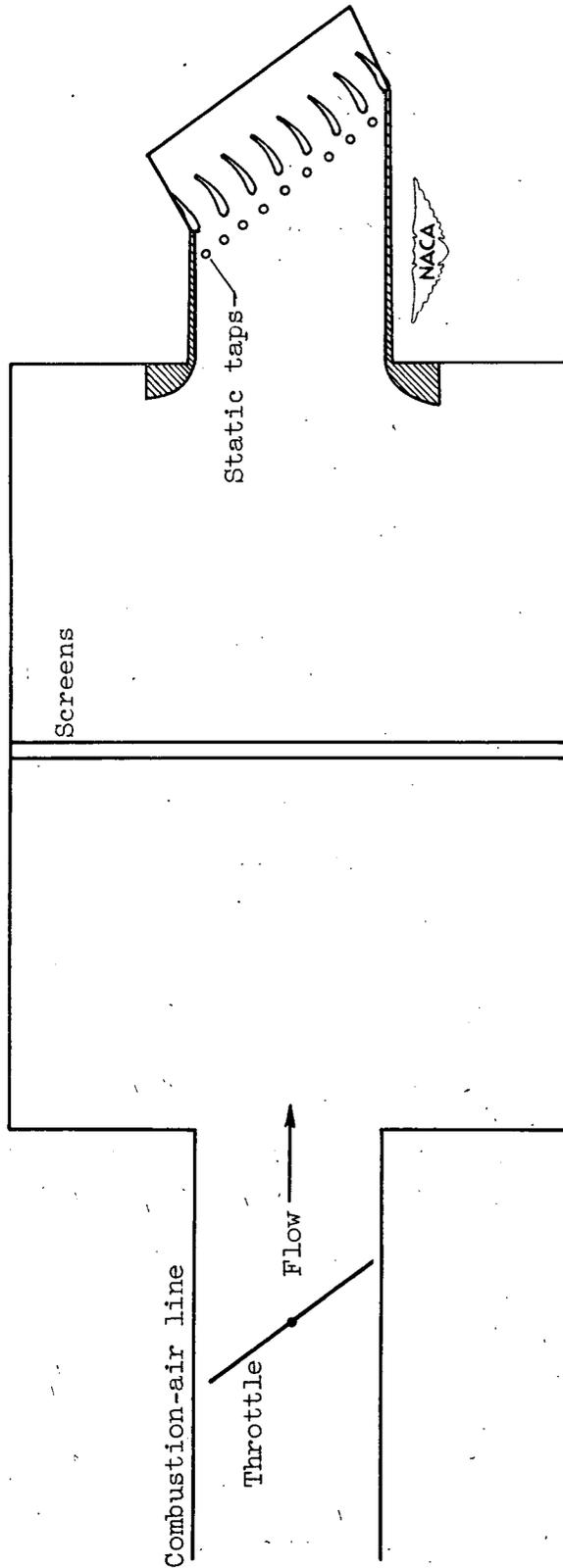
Figure 1. - Two-dimensional steady-flow cascade.
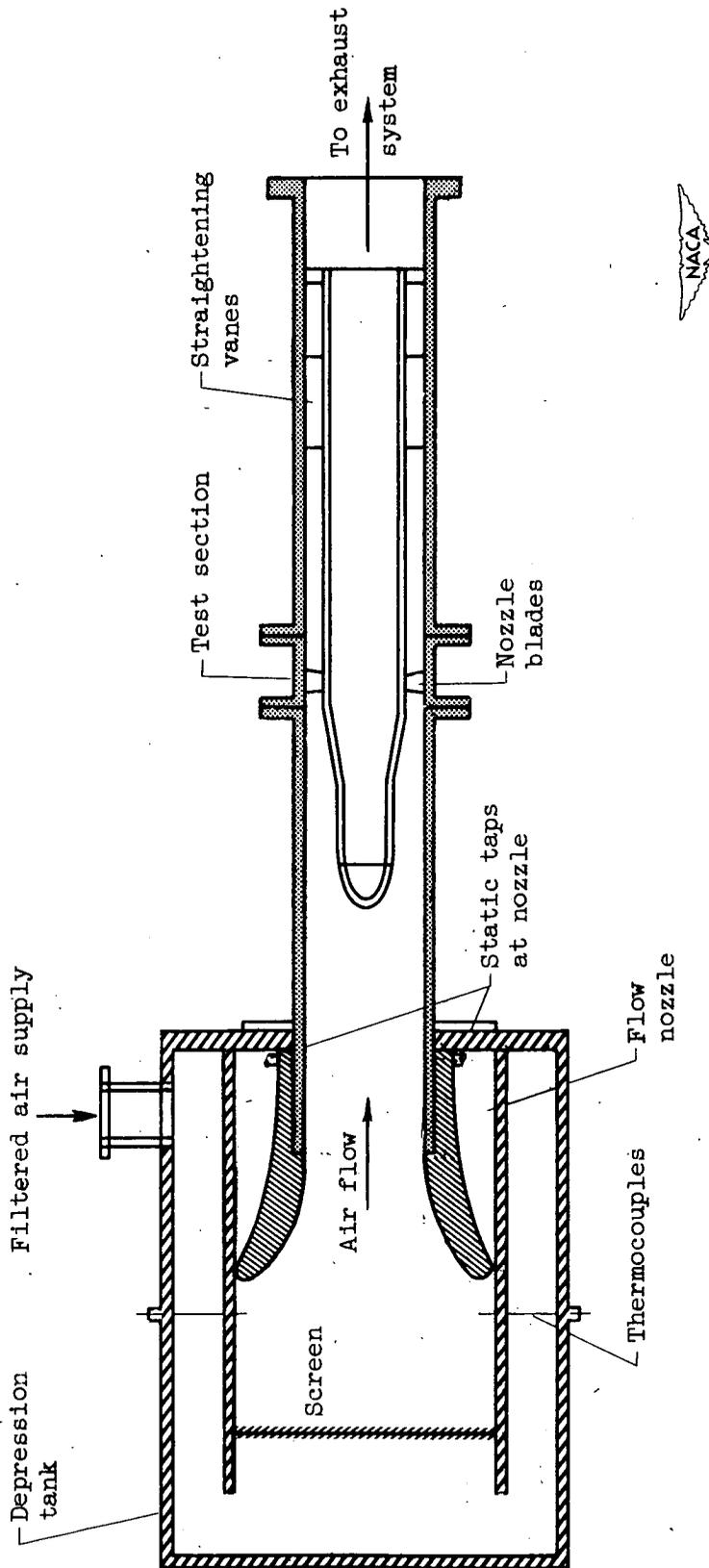
Figure 2. - Schematic view of annular-nozzle cascade test unit.
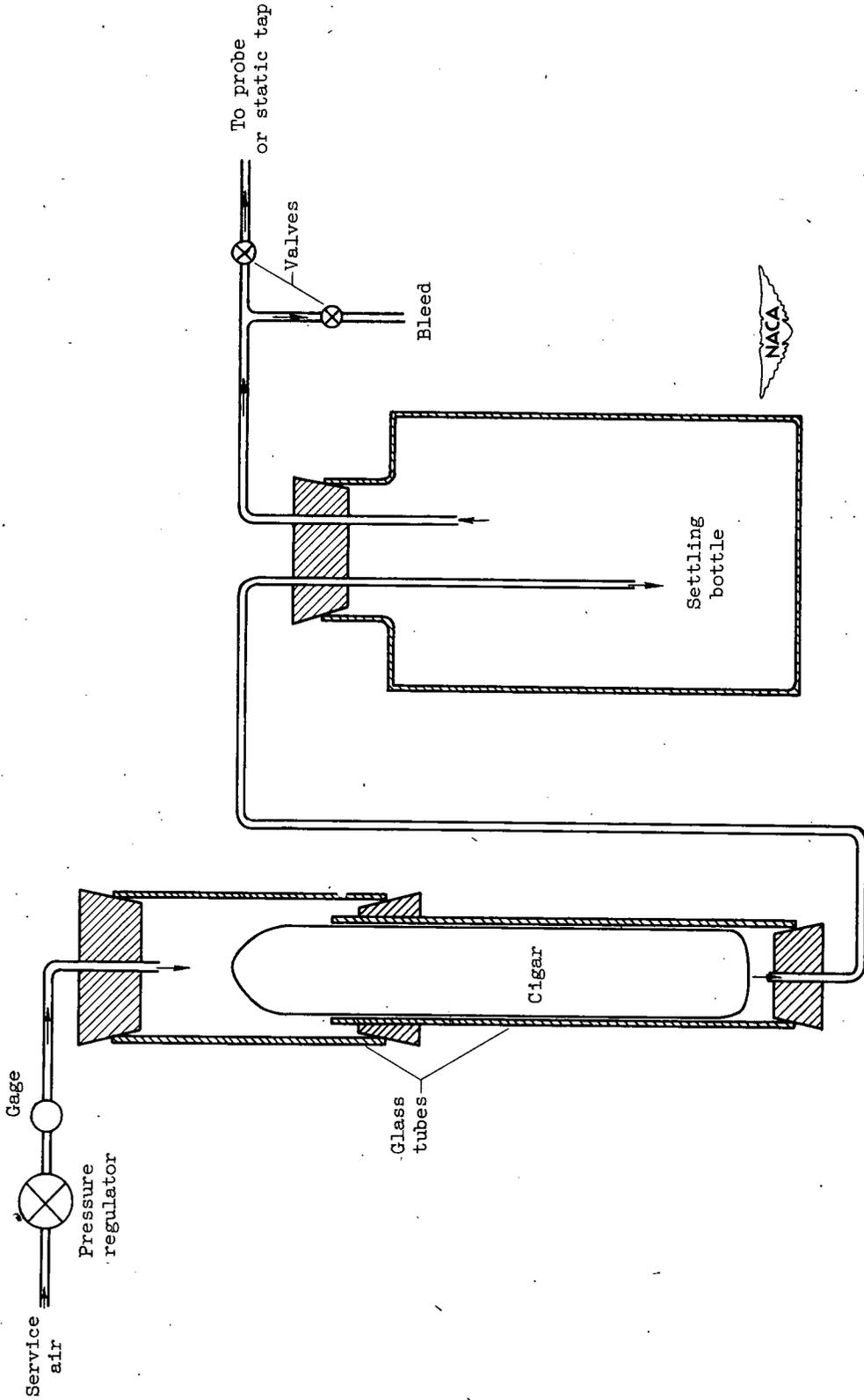
Figure 3. - Smoke generator.
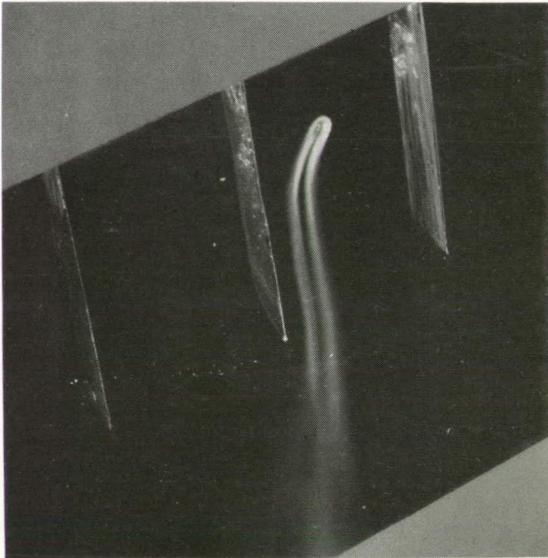
(a) Smoke trace 1/4 inch from wall.   (b) Smoke trace 1/8 inch from wall.
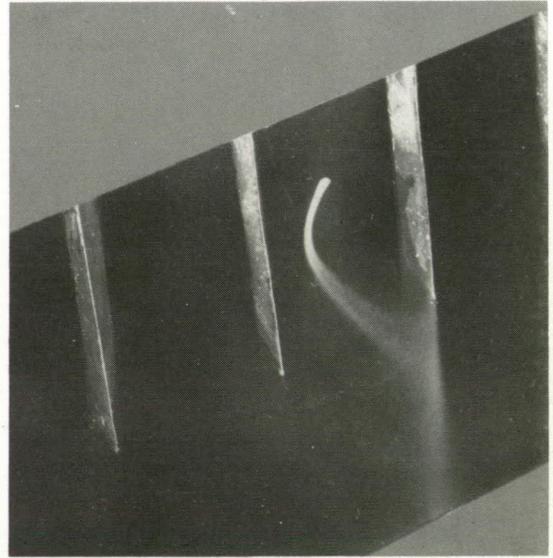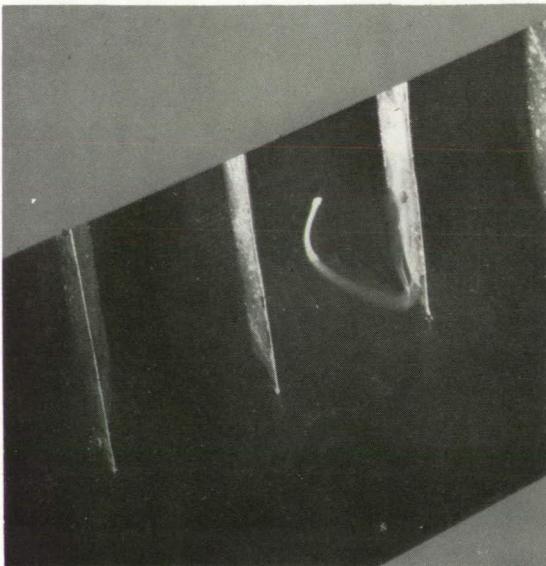
(c) Smoke trace on wall.   (d) Superimposition of (a), (b), and (c).
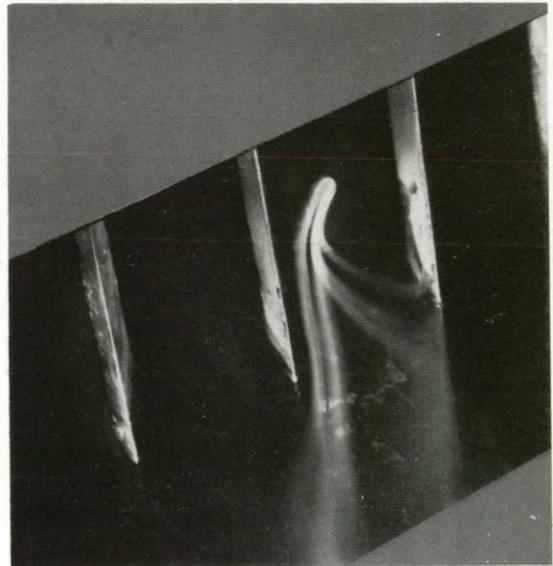
C-29952

Figure 4. - Variation of flow deflection in boundary layer. Smoke introduced through wall static tap.
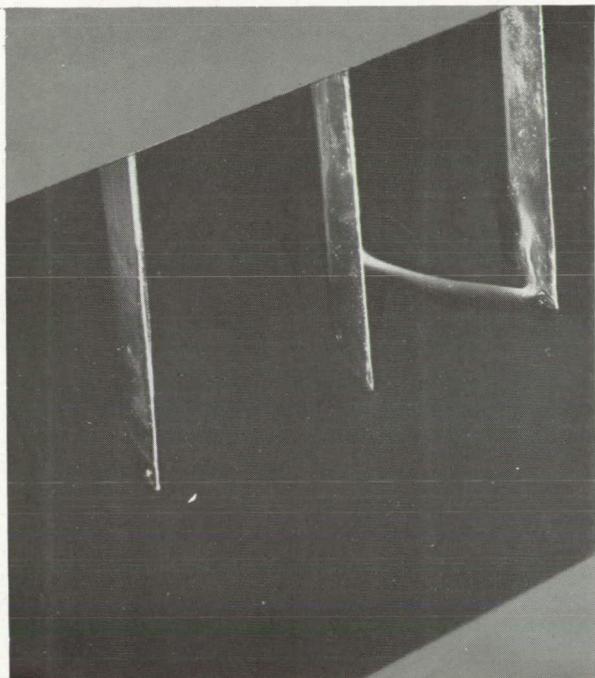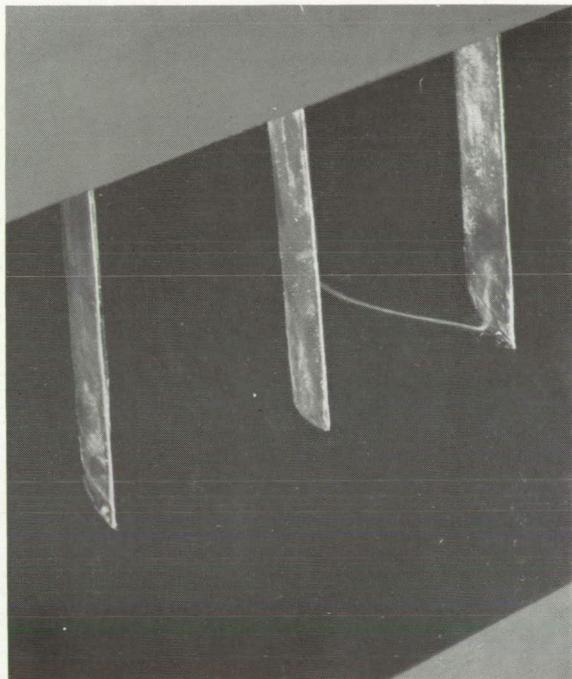
(a) Smoke through static tap.　　　　　(b) Residual smoke through static tap.
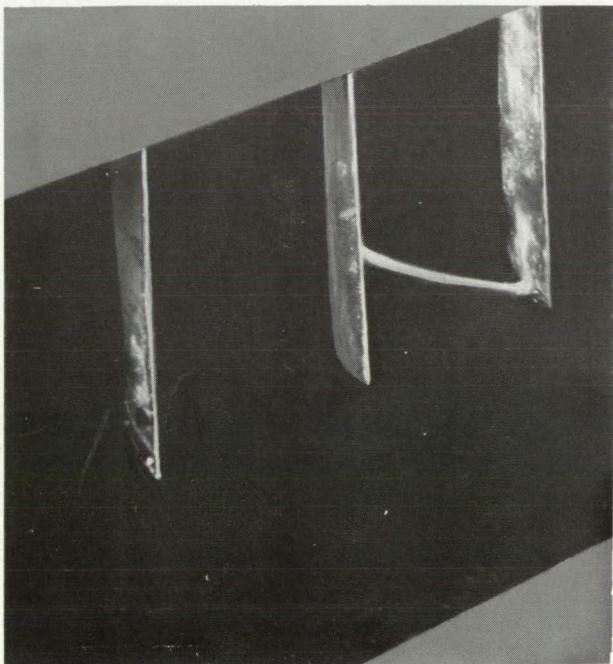
(c) Superimposition of (a) and (b).

Figure 5. - Deflection of boundary layer along wall. Smoke introduced through static
tap upstream of blades.
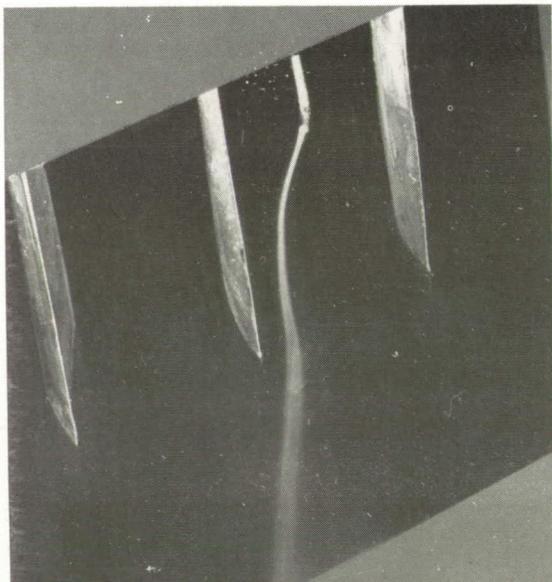
(a) Probe 1/4 inch from wall.
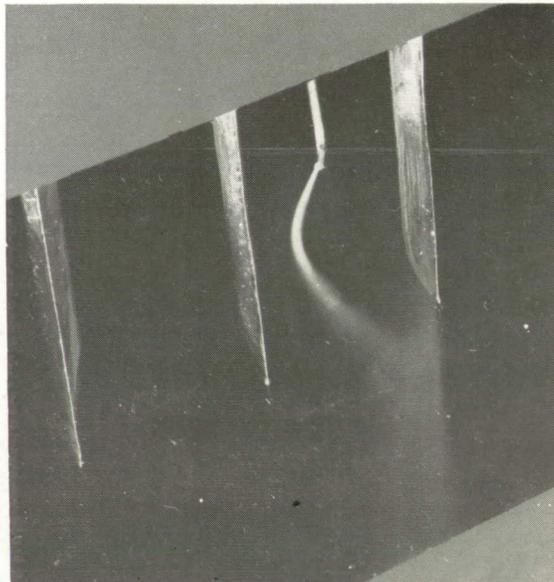
(b) Probe 1/8 inch from wall.
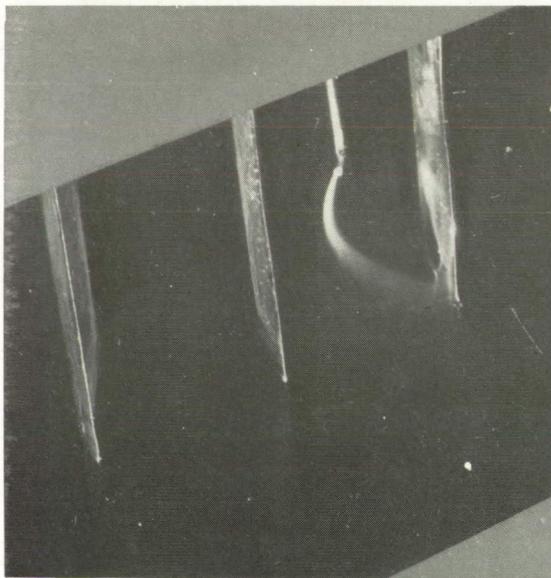
(c) Probe against wall.

(d) Superimposition of (a), (b), and (c).

C-29953

Figure 6. - Variation of flow deflection in boundary layer. Smoke introduced through
probe.
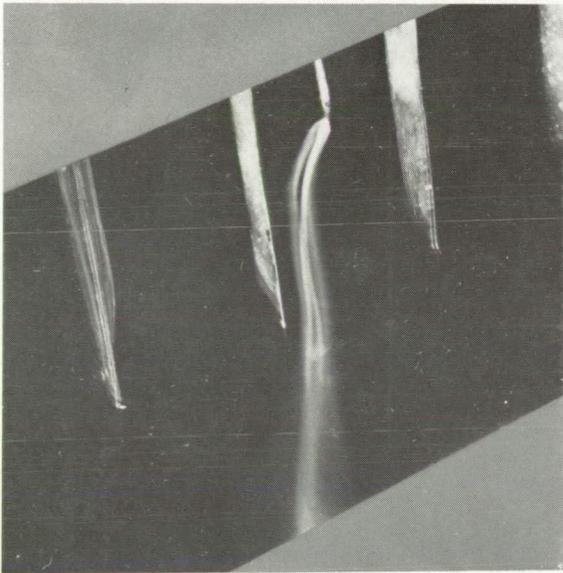
(a) Figures 6(a) and 4(a).

(b) Figures 6(b) and 4(b).
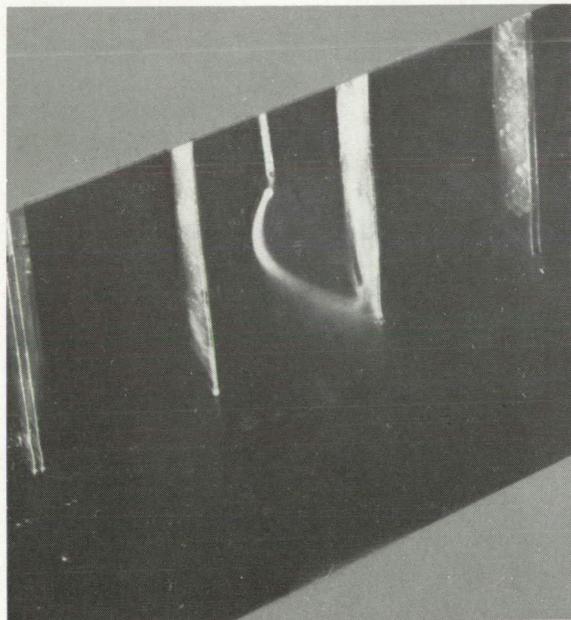
(c) Figures 6(c) and 4(c).
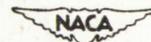
Figure 7. - Superimposition of figures 6 and 4 demonstrating the reliability of probe results for flow visualization.
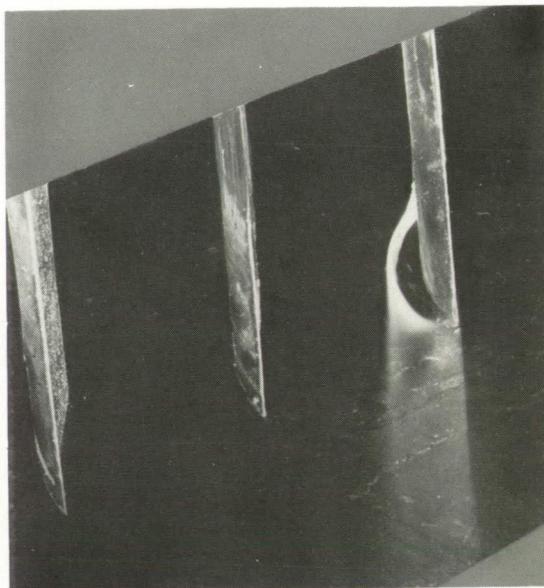
(a) Probe in position a.

(b) Probe in position b.
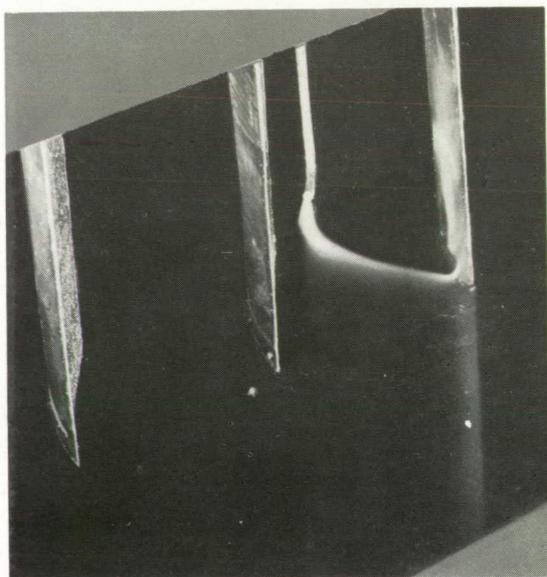
(c) Probe in position c.
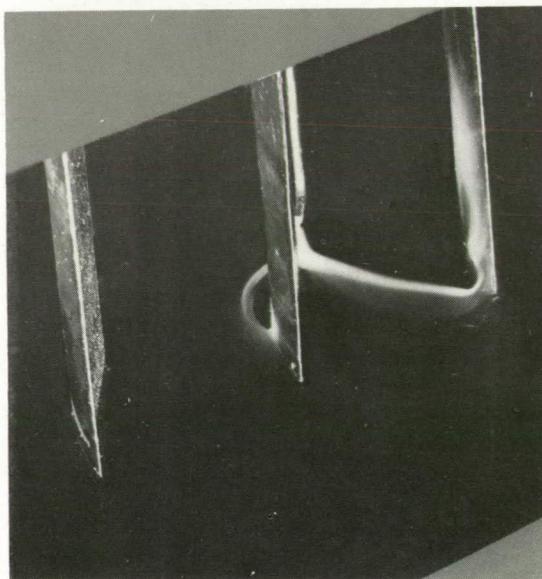
(d) Probe in position d.

Figure 8. - Flow deflection in wall boundary layer of one passage. Smoke introduced by
probe traverse along wall.
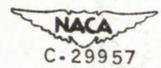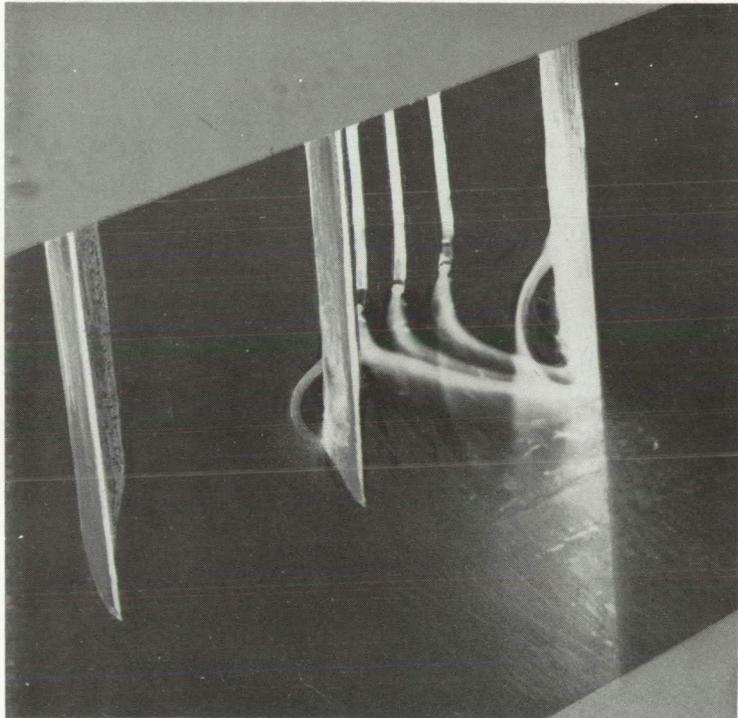
(e) Superimposition of (a), (b), (c), and (d).

Figure 8. - Concluded. Flow deflection in wall boundary layer of one passage. Smoke introduced by probe traverse along wall.
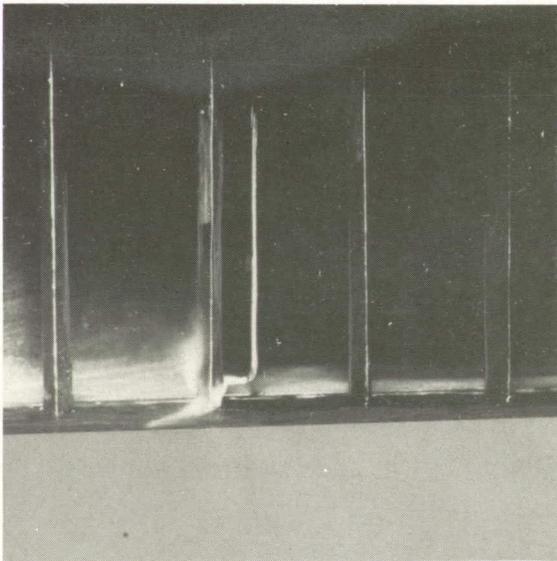
(a) Smoke tube divided on blade.
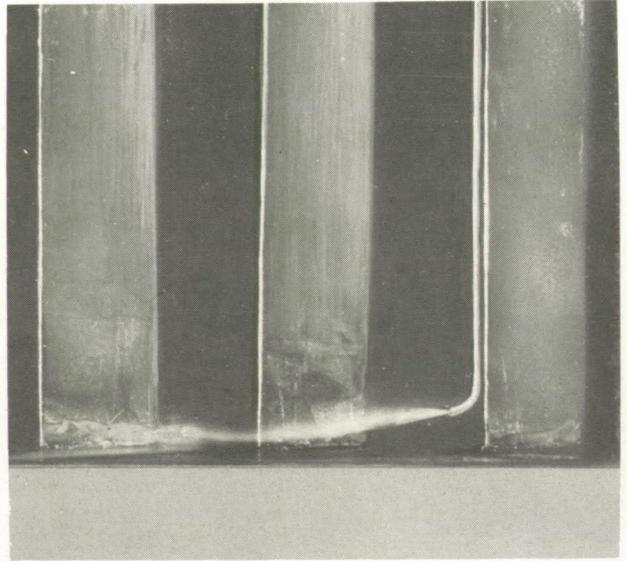
(b) Smoke tube on pressure surface of blade.
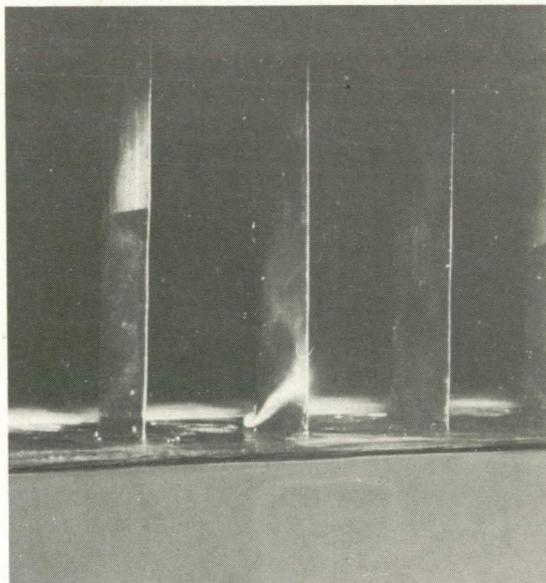
(c) Smoke tube on suction surface of blade.

Figure 9. - Flow deflections on blade.

(a) Hydrogen sulfide introduced through static tap upstream.
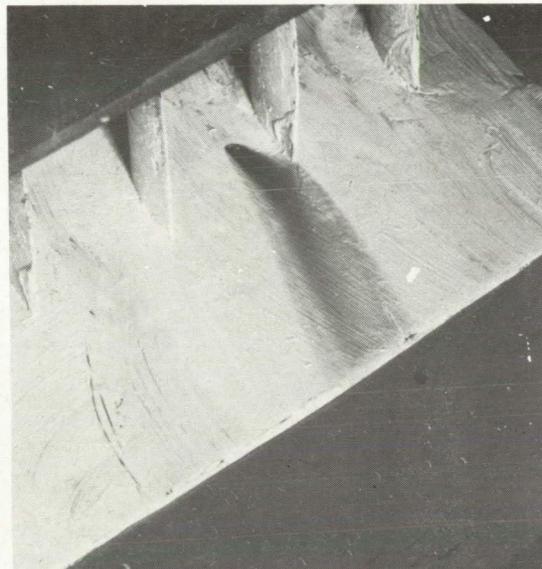
(b) Hydrogen sulfide introduced through tap in passage.
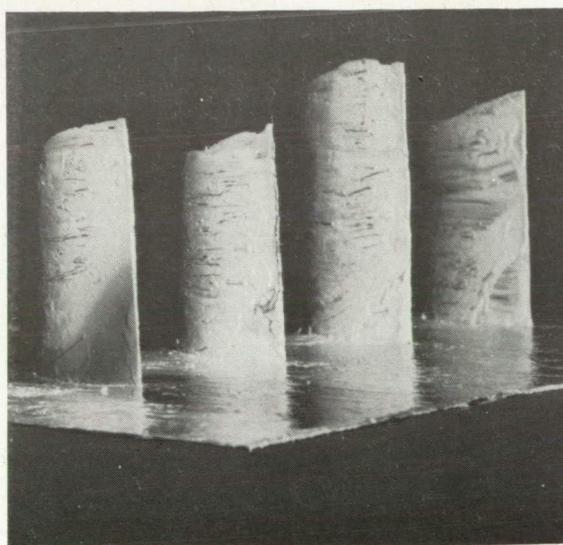
C-29959

(c) Hydrogen sulfide trace on blade suction surface.

Figure 10. - Flow traces in two-dimensional cascade at Mach numbers of approximately 0.4.
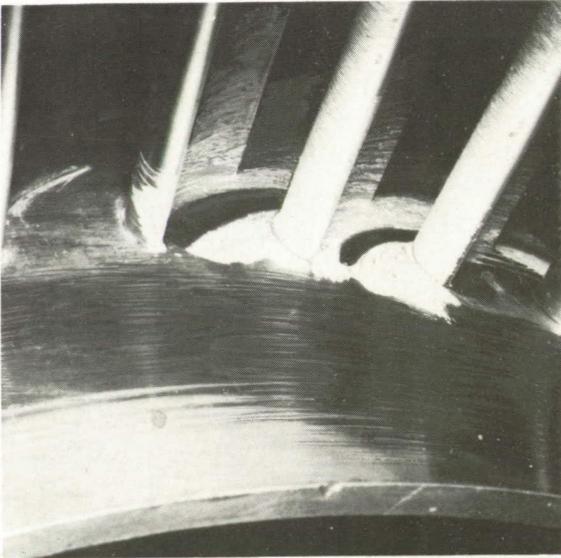
(a) Upstream view of inner shroud.   (b) Downstream view of inner shroud.
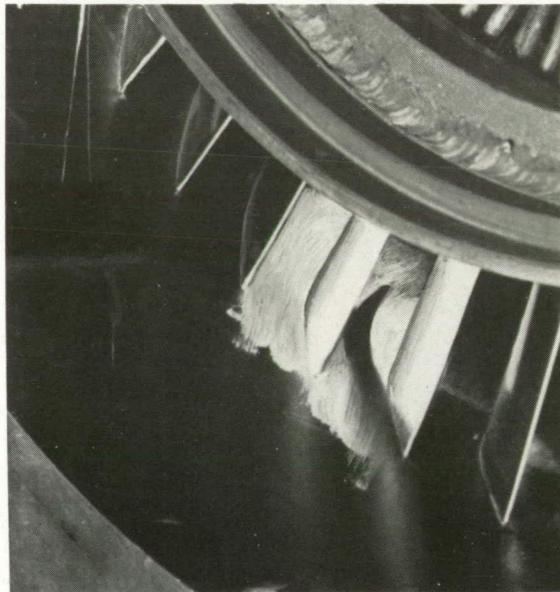
(c) Downstream view of outer shroud.

Figure 11. - Hydrogen sulfide traces in annular-turbine-nozzle cascade at high subsonic velocities. Hub-discharge Mach number, approximately 0.9; tip-discharge Mach number, approximately 0.7.
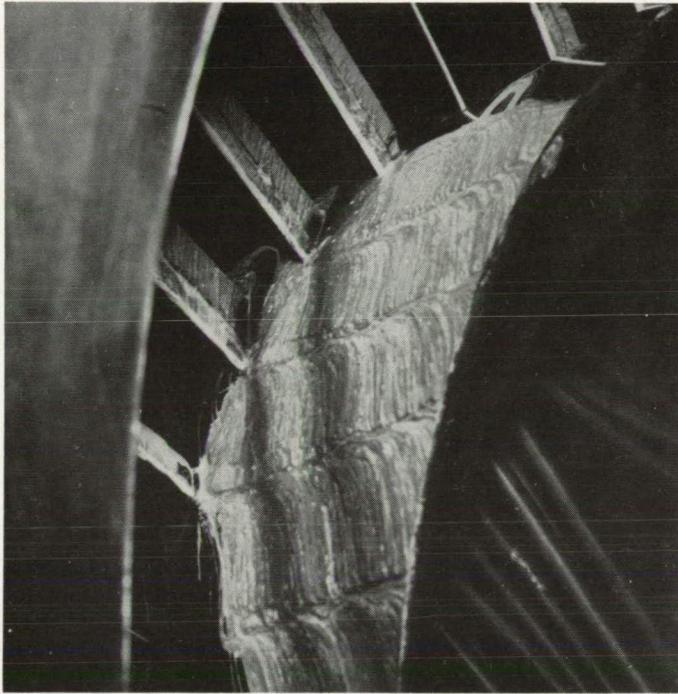
(a) Downstream view of inner shroud.

(b) Downstream view of outer shroud.

Figure 12. - Hydrogen sulfide traces in annular-turbine-nozzle cascade at supersonic
velocities. Hub-discharge Mach number, approximately 1.5; tip-discharge Mach number,
approximately 1.2.
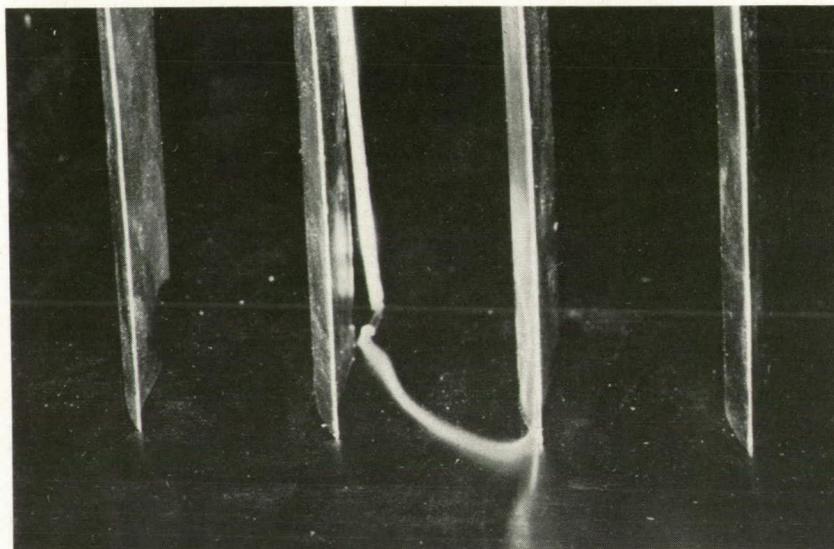
(a) Probe on wall near pressure surface.

(b) Probe on wall in midchannel.

Figure 13. - Streamline pattern in cascade with stagger angle of 0°. Solidity, 1.5; angle of attack, 11°; aspect ratio, 2.34.
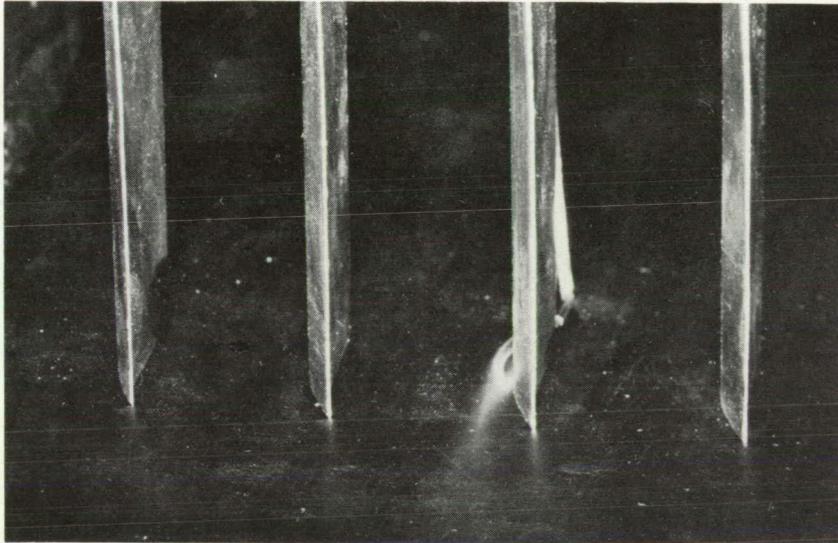
(c) Probe on wall near suction surface.
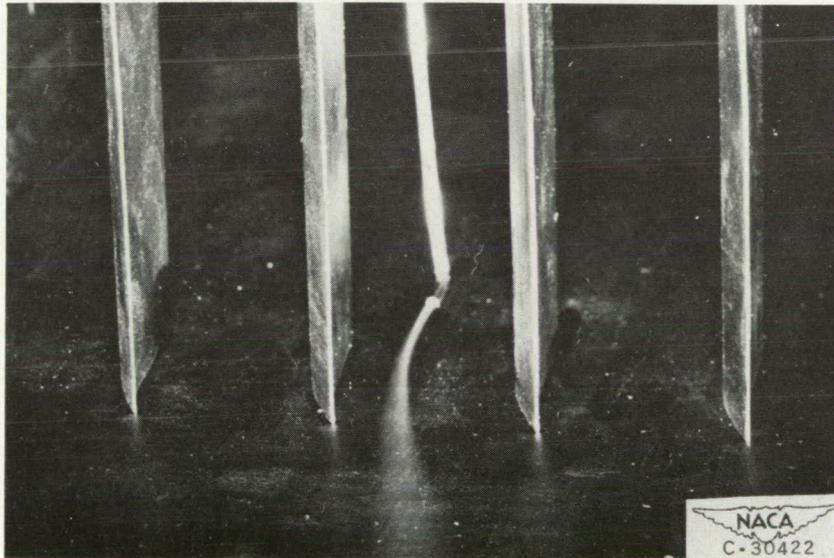
(d) Probe away from wall in main stream.

Figure 13. - Concluded. Streamline pattern in cascade with stagger angle of 0°. Solidity, 1.5; angle of attack, 11°; aspect ratio, 2.34.
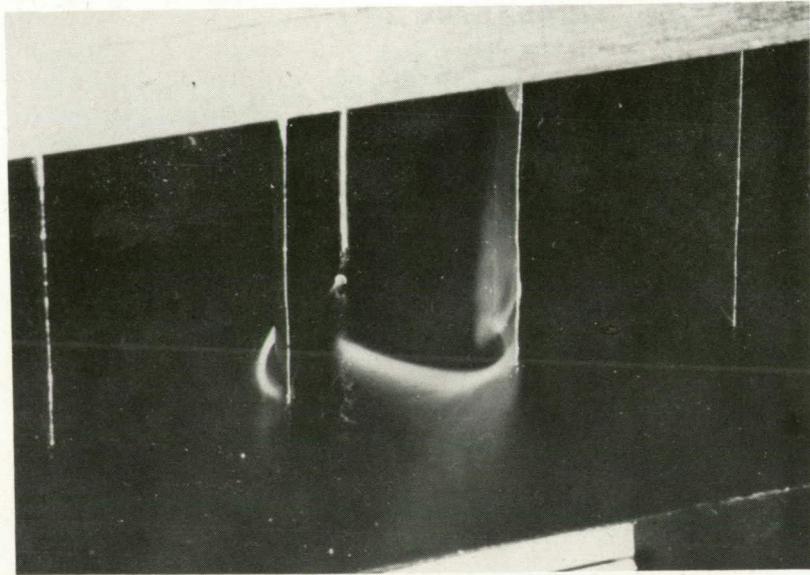
(a) Probe on wall at nose of blade.
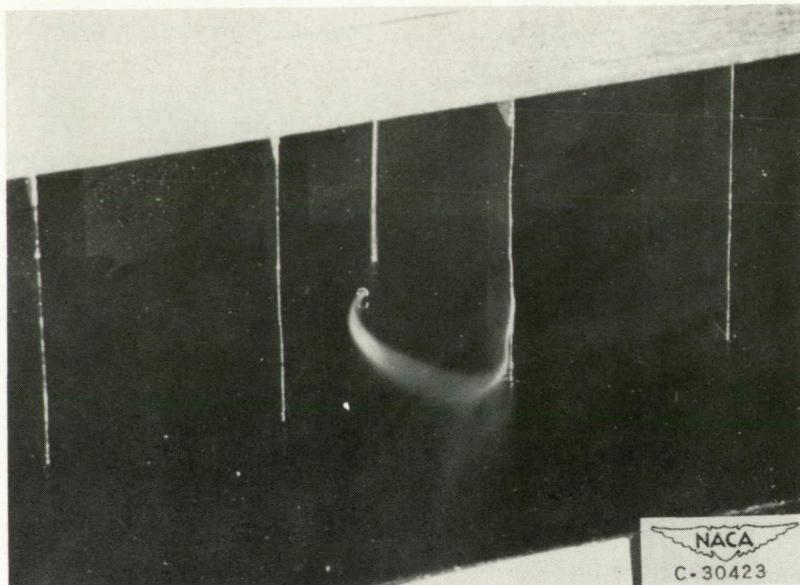
(b) Probe on wall near pressure surface.

Figure 14. - Streamline pattern in cascade with aspect ratio of 1.67. Stagger angle, 45°; solidity, 1.5; angle of attack, 11°.
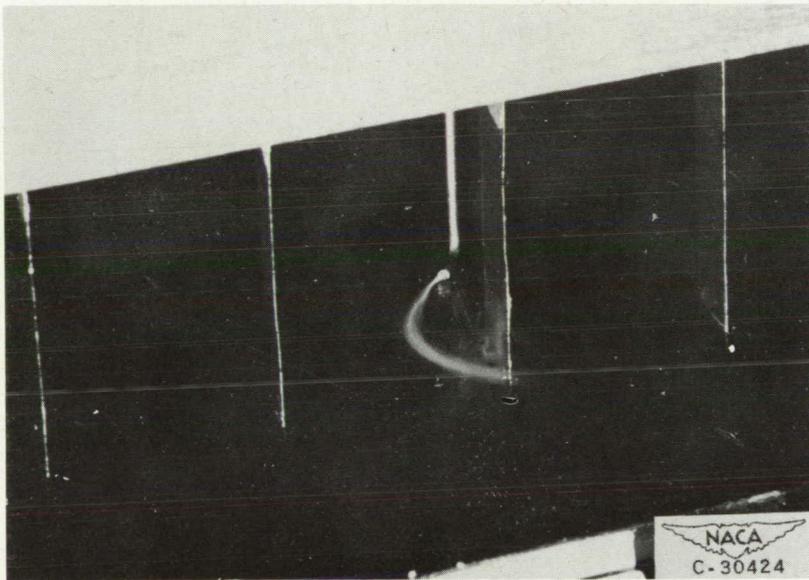
(c) Probe on wall near suction surface.

Figure 14. - Concluded. Streamline pattern in cascade with aspect ratio of 1.67. Stagger angle, 45°; solidity, 1.5; angle of attack, 11°.
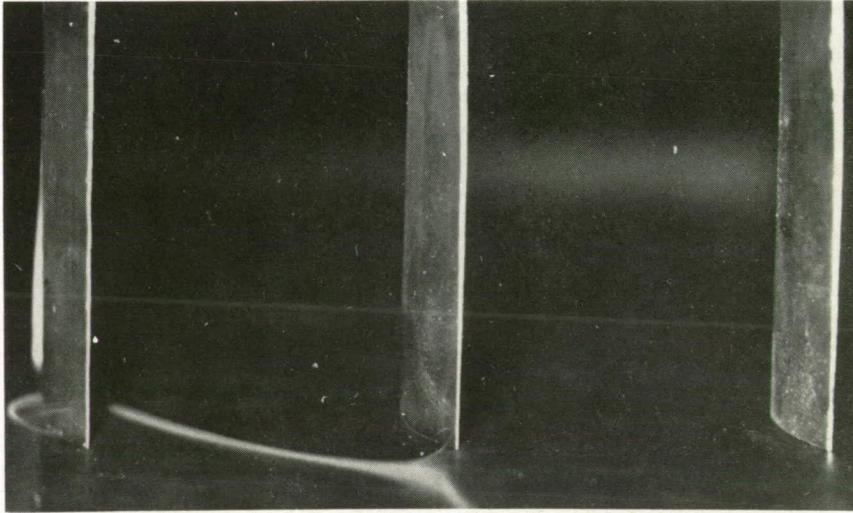
(a) Probe on wall at nose of blade.
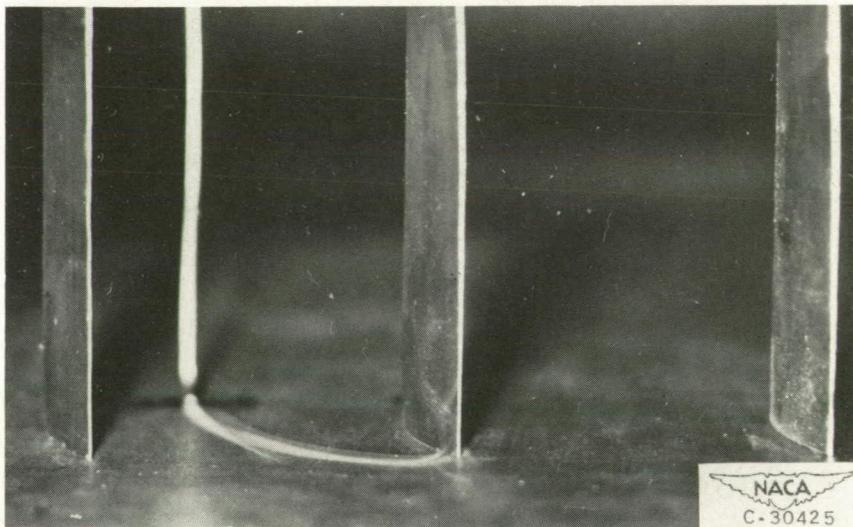
(b) Probe on wall at point where smoke first reached suction
    surface.

Figure 15. - Streamline pattern in cascade with solidity of 0.75. Stagger angle, 0°;
    angle of attack, 11°; aspect ratio, 2.34.
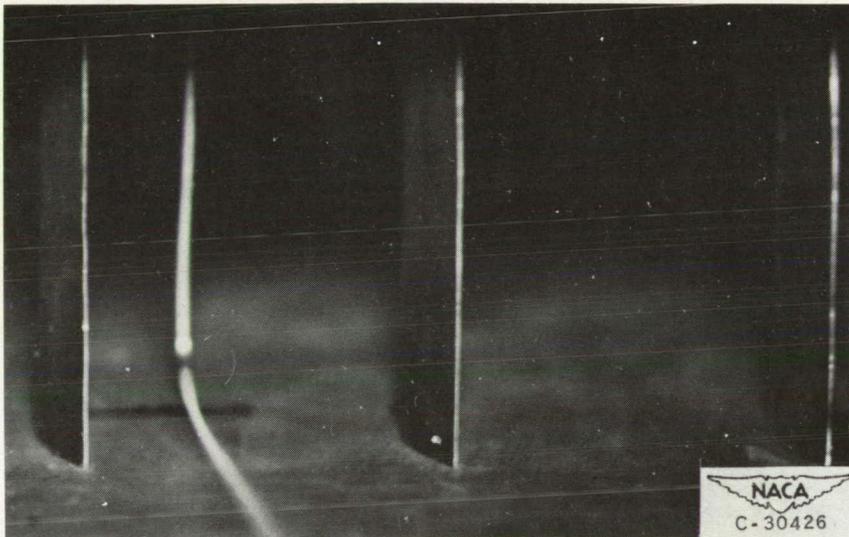
(c) Probe away from wall in main stream.

Figure 15. - Concluded. Streamline pattern in cascade with solidity of 0.75. Stagger angle, 0°; angle of attack, 11°; aspect ratio, 2.34.
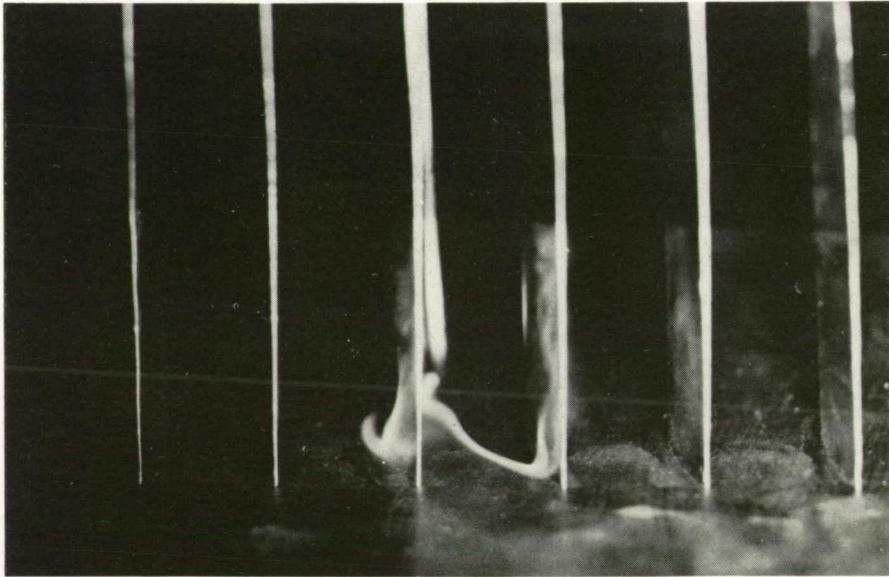
(a) Probe on wall at nose of blade.
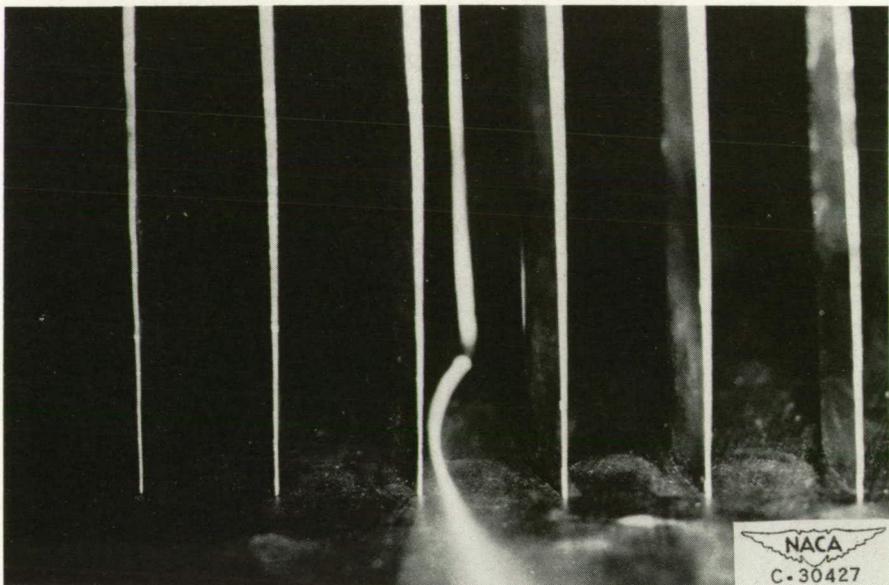
(b) Probe away from wall in main stream.

Figure 16. - Streamline pattern in cascade with solidity of 2.0.   Stagger angle, 0°;
     angle of attack, 11°; aspect ratio, 2.34.
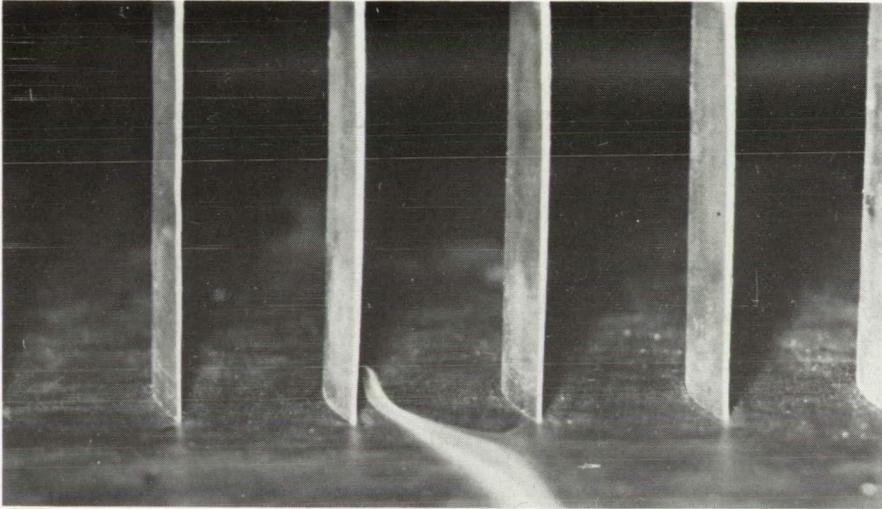
(a) Probe on wall at nose of blade.
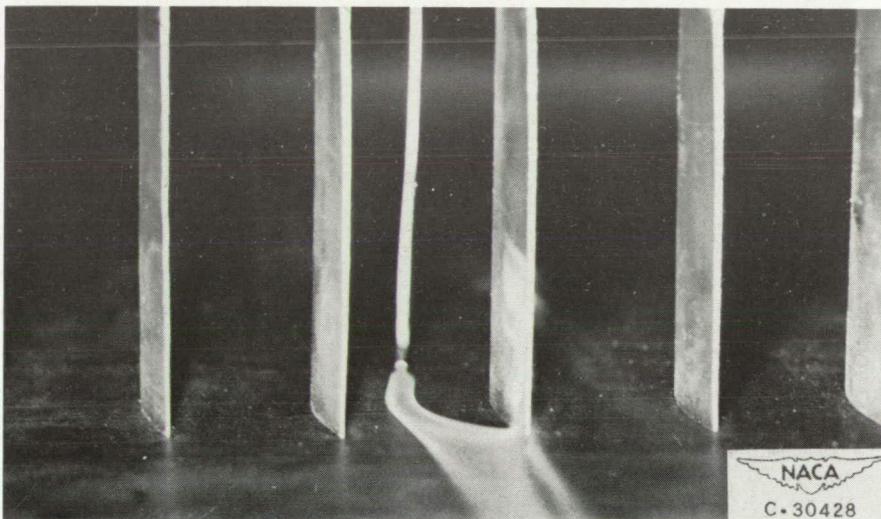
(b) Probe on wall at point where smoke first reached suction surface.

Figure 17. - Streamline pattern in cascade with angle of attack of 4°. Stagger angle, 0°;
    solidity, 1.5; aspect ratio, 2.34.
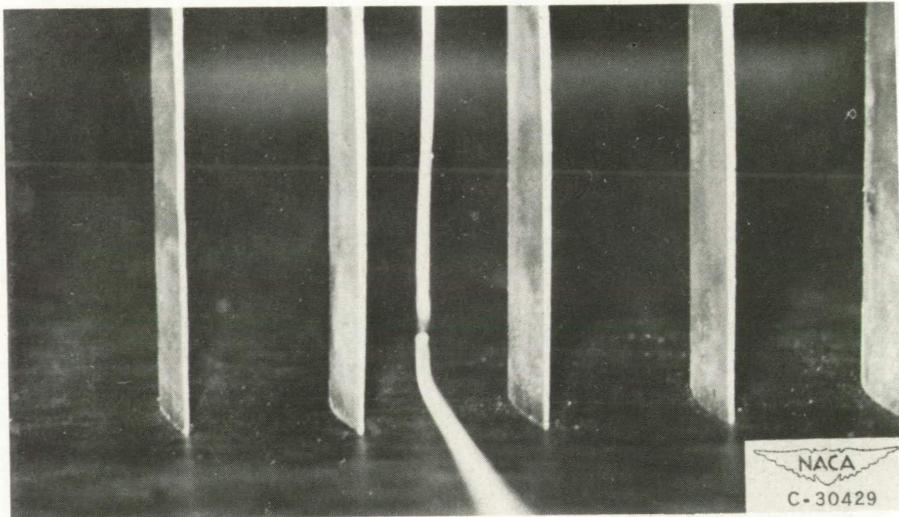
(c) Probe away from wall in main stream.

Figure 17. - Concluded. Streamline pattern in cascade with angle of attack of 4°. Stagger angle, 0°; solidity, 1.5; aspect ratio, 2.34.
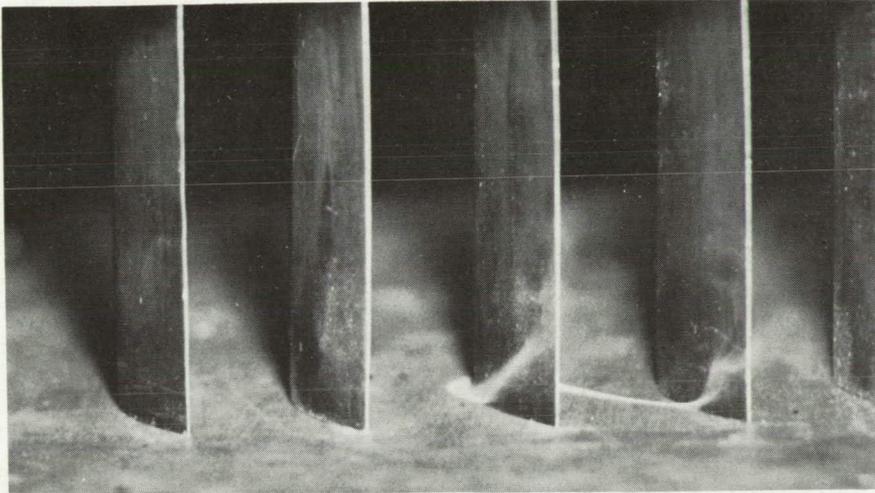
(a) Probe on wall at nose of blade.
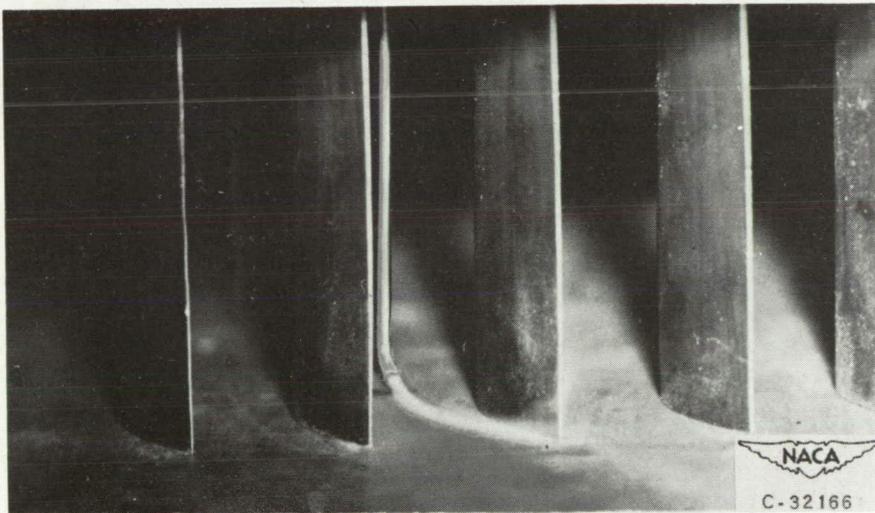
(b) Probe away from wall in main stream.

Figure 18. - Streamline pattern in cascade with angle of attack of 20°. Stagger angle, 0°; solidity, 1.5; aspect ratio, 2.34.
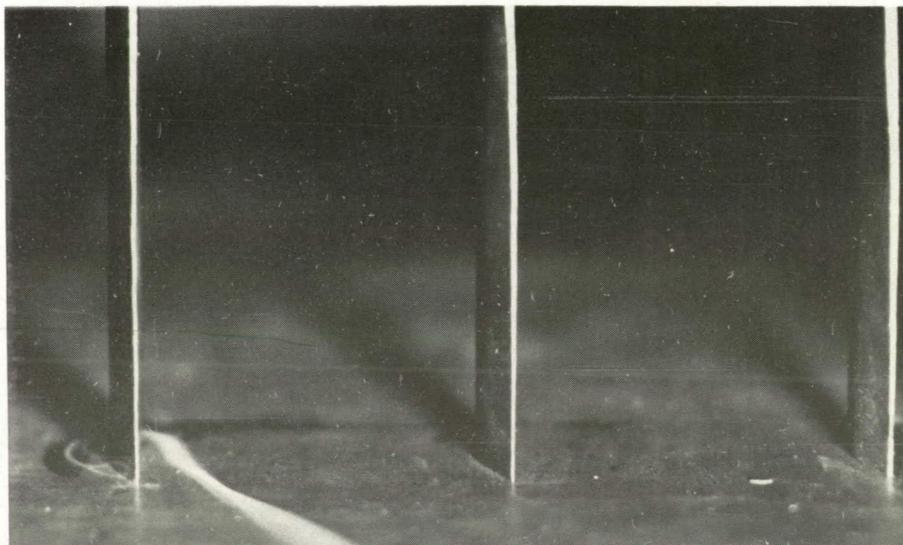
(a) Probe on wall at nose of blade.
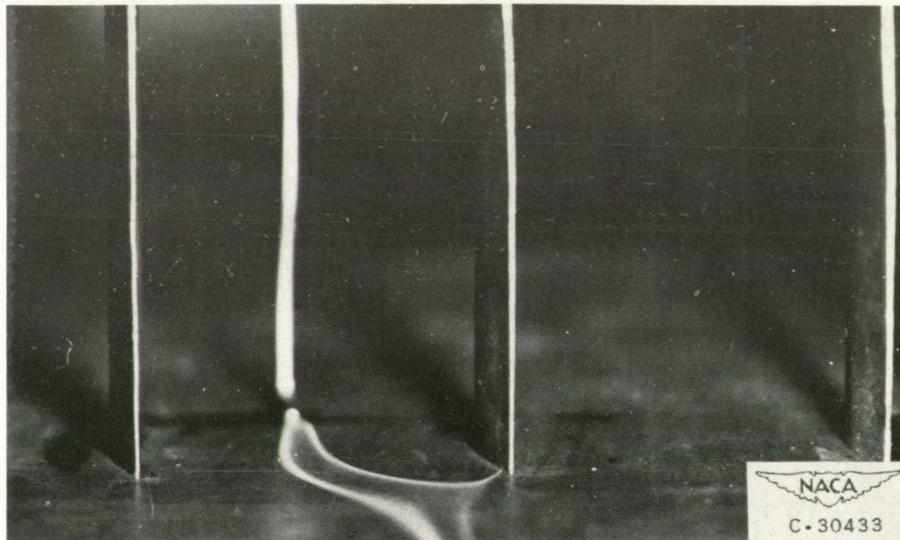
(b) Probe on wall at point where smoke first reached suction surface.

Figure 19. - Streamline pattern in cascade with solidity of 0.75 and angle of attack of
  4°.   Stagger angle, 0°; aspect ratio, 2.34.
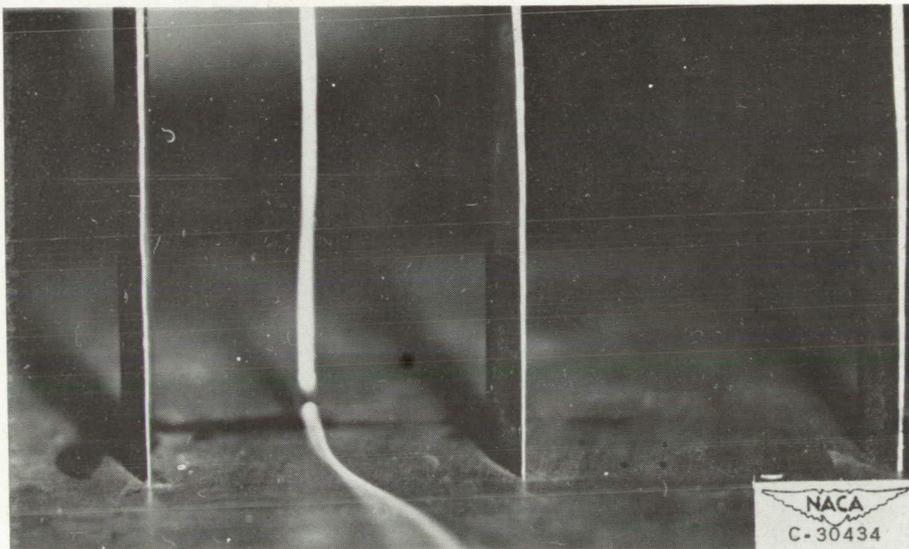
(c) Probe away from wall in main stream.

Figure 19. - Concluded. Streamline pattern in cascade with solidity of 0.75 and angle of attack of 4°. Stagger angle, 0°; aspect ratio, 2.34.
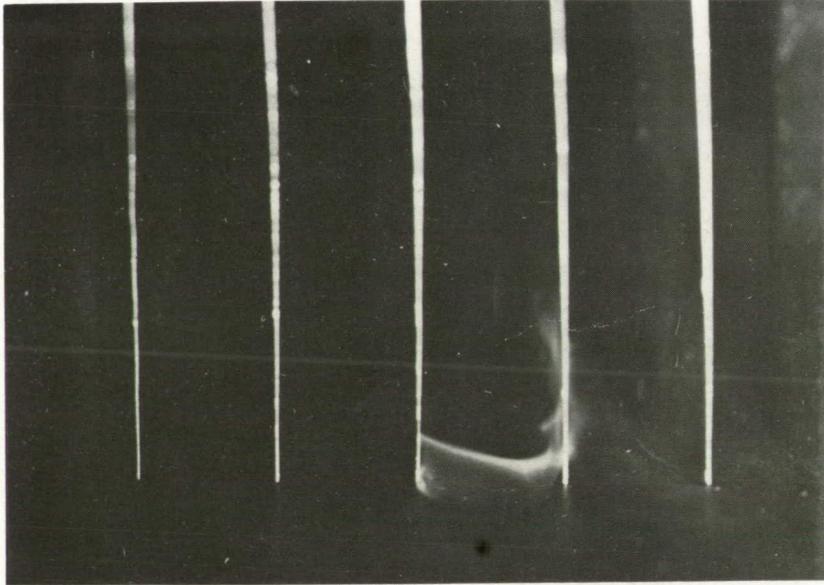
(a) Probe away from wall at nose of blade.
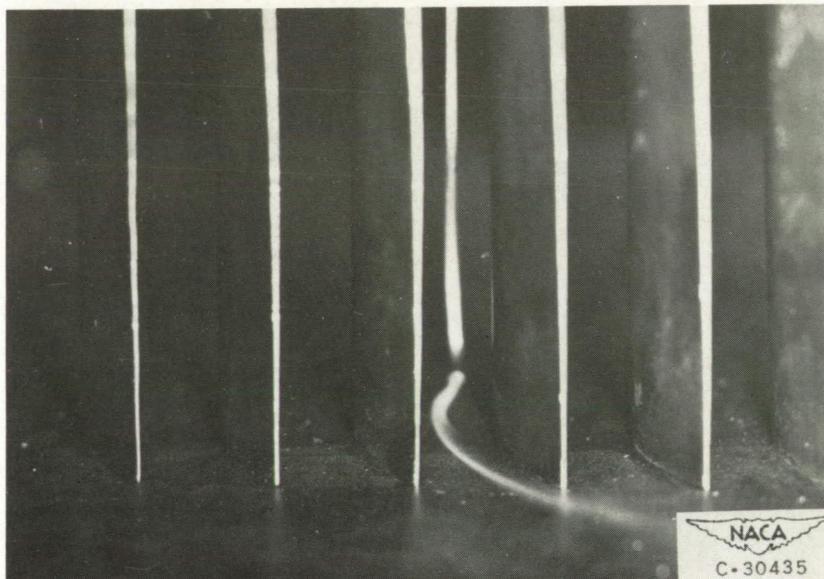
(b) Probe away from wall in main stream.

Figure 20. - Streamline pattern in cascade with solidity of 2.0 and angle of attack of 20°. Stagger angle, 0°; aspect ratio, 2.34.

(a) Fillet on blade pressure surface.
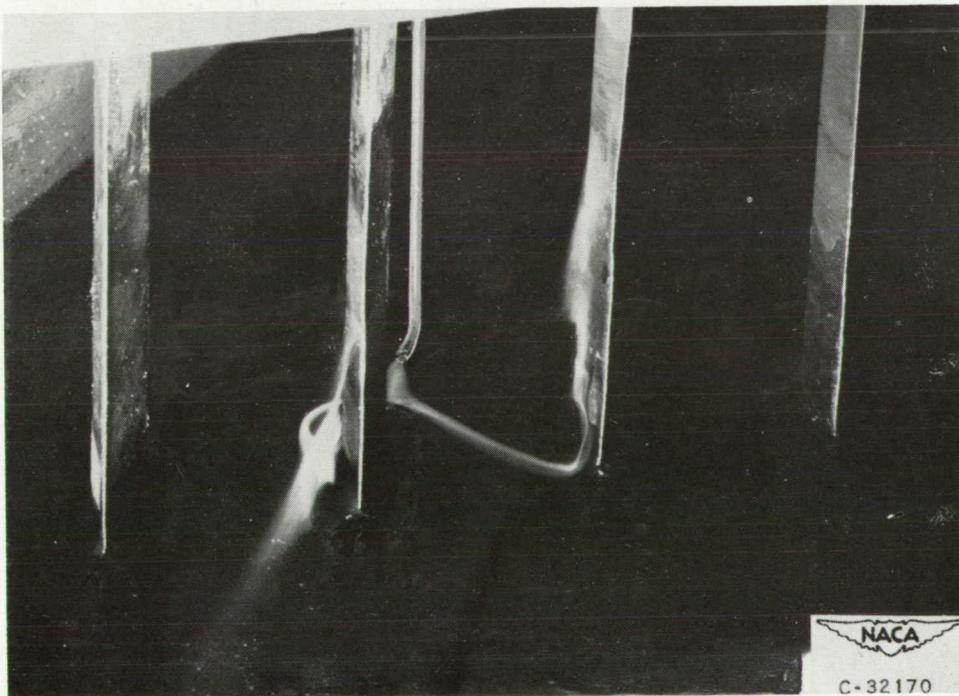
(b) Fillet on blade suction surface.

Figure 21. - Streamline pattern in cascade with blade fillets. Stagger angle, 0°; solidity, 1.5; angle of attack, 11°; aspect ratio, 2.34.
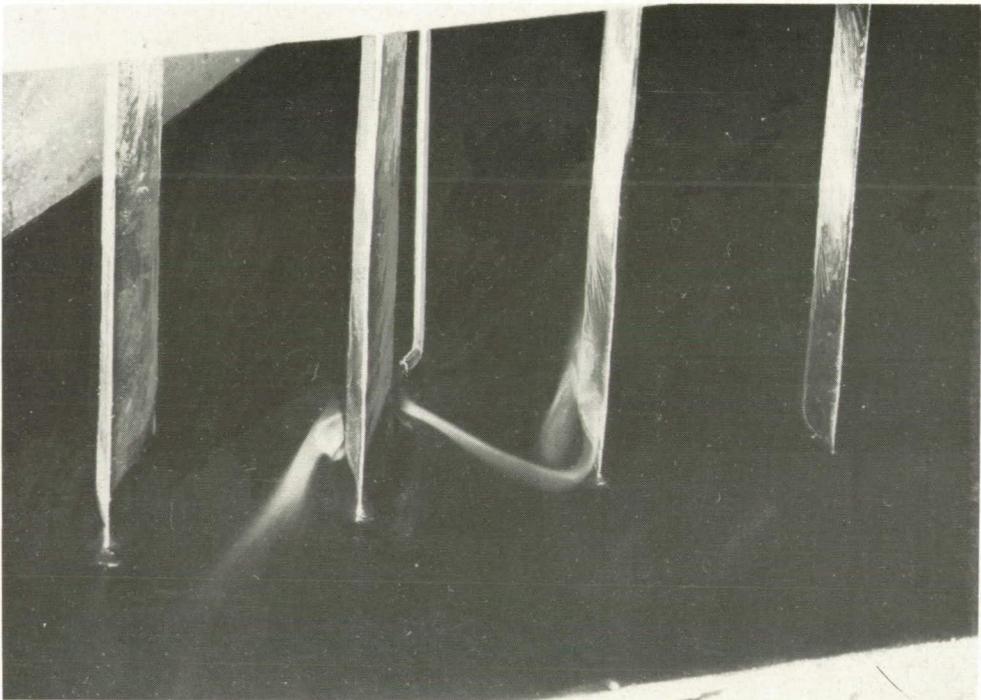
(c) Fillets on both blade surfaces.

Figure 21. - Concluded. Streamline pattern in cascade with blade fillets. Stagger angle, 0°; solidity, 1.5; angle of attack, 11°; aspect ratio, 2.34.
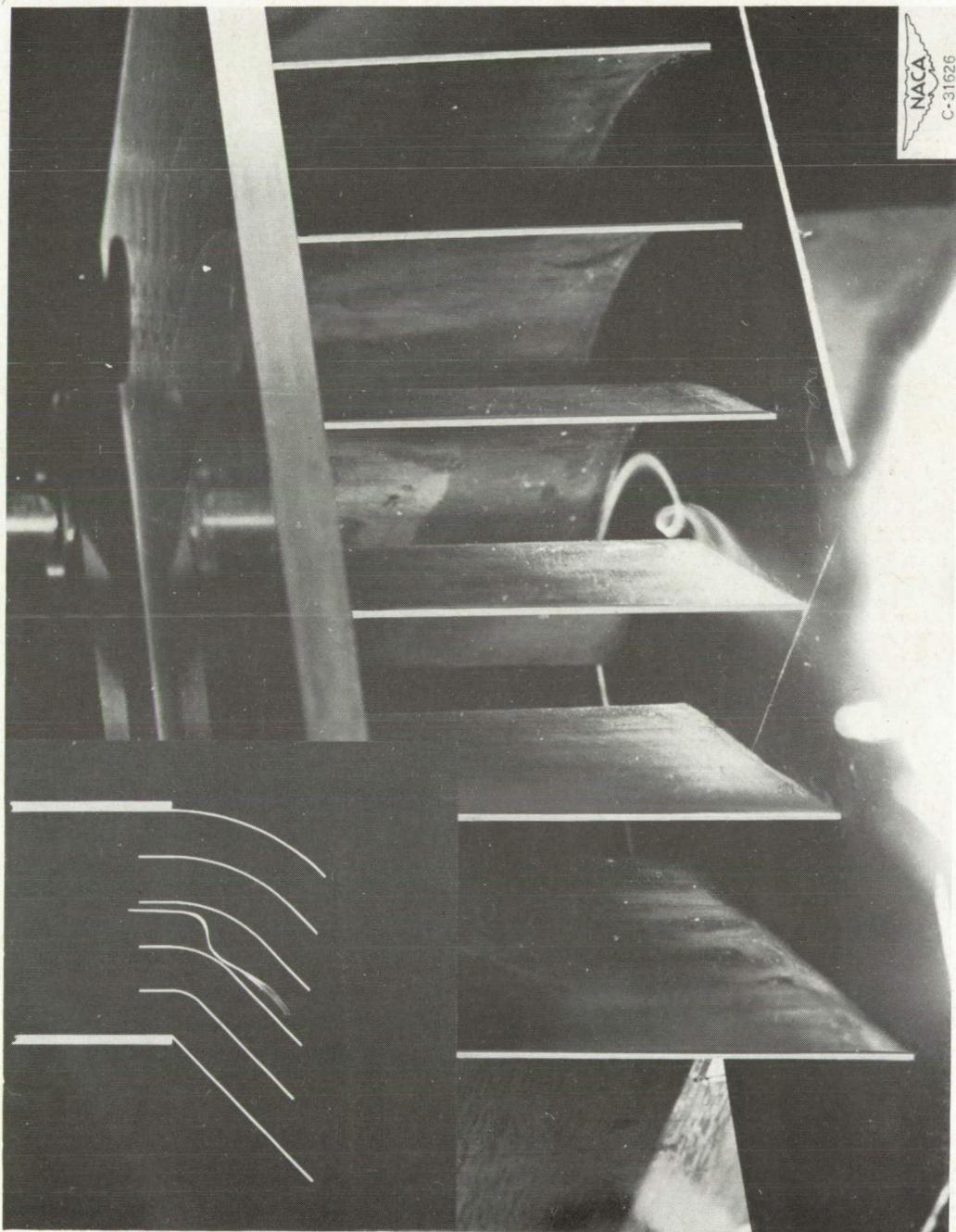
Figure 22. - Roll-up of wall inlet boundary layer to form passage vortex in 45° rectangular bend. Smoke introduced on wall near blade pressure surface.
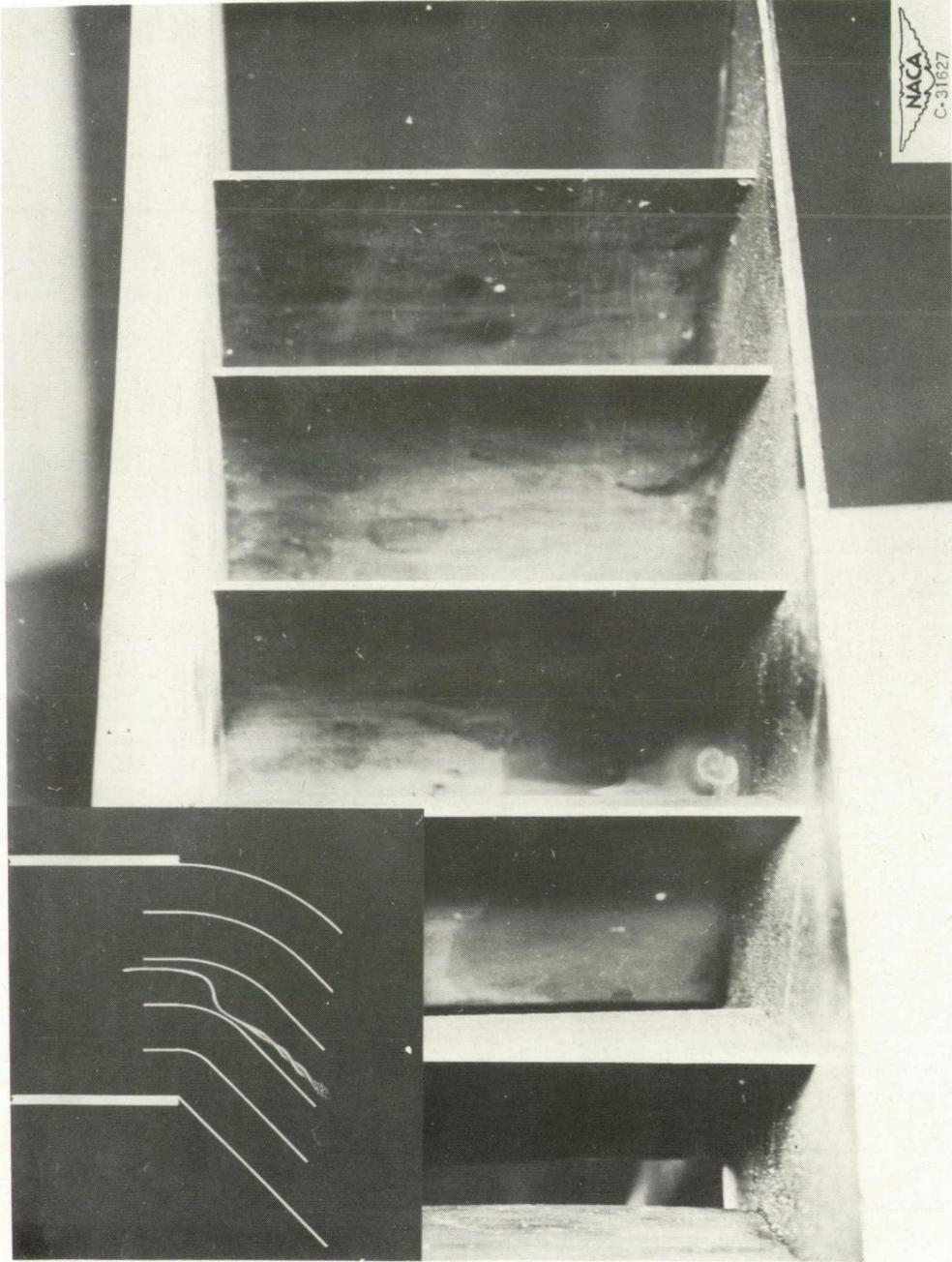
Figure 23. - Passage vortex in 45° rectangular bend. Smoke introduced on wall near blade pressure surface.

Figure 24. - Shift of secondary-flow passage vortex away from wall of 45° rectangular bend. Smoke introduced on wall near midchannel position.

Figure 25. - Roll-up of wall inlet boundary layer to form passage vortex in 60° rectangular bend. Smoke introduced on wall near blade pressure surface.
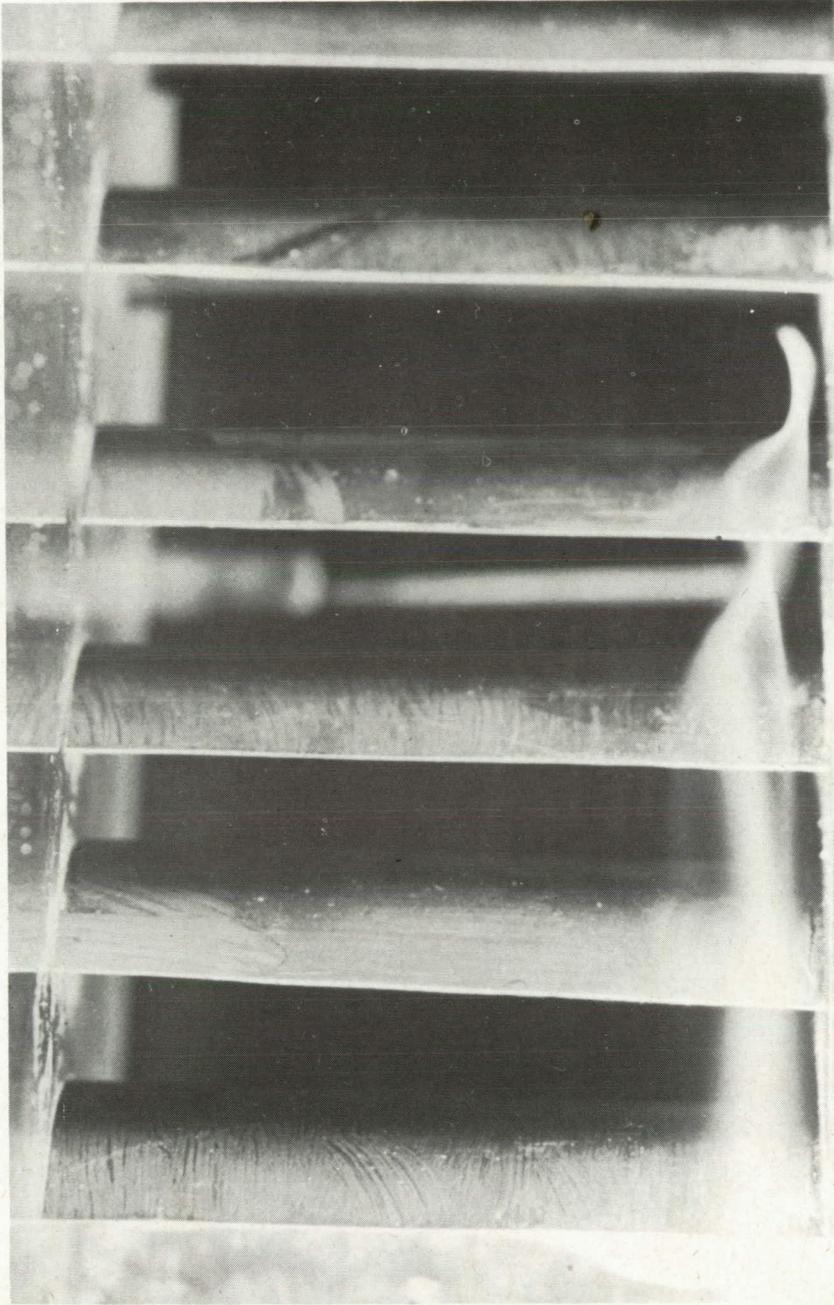
Figure 26. - Continued twisting of passage vortex downstream of blade row.
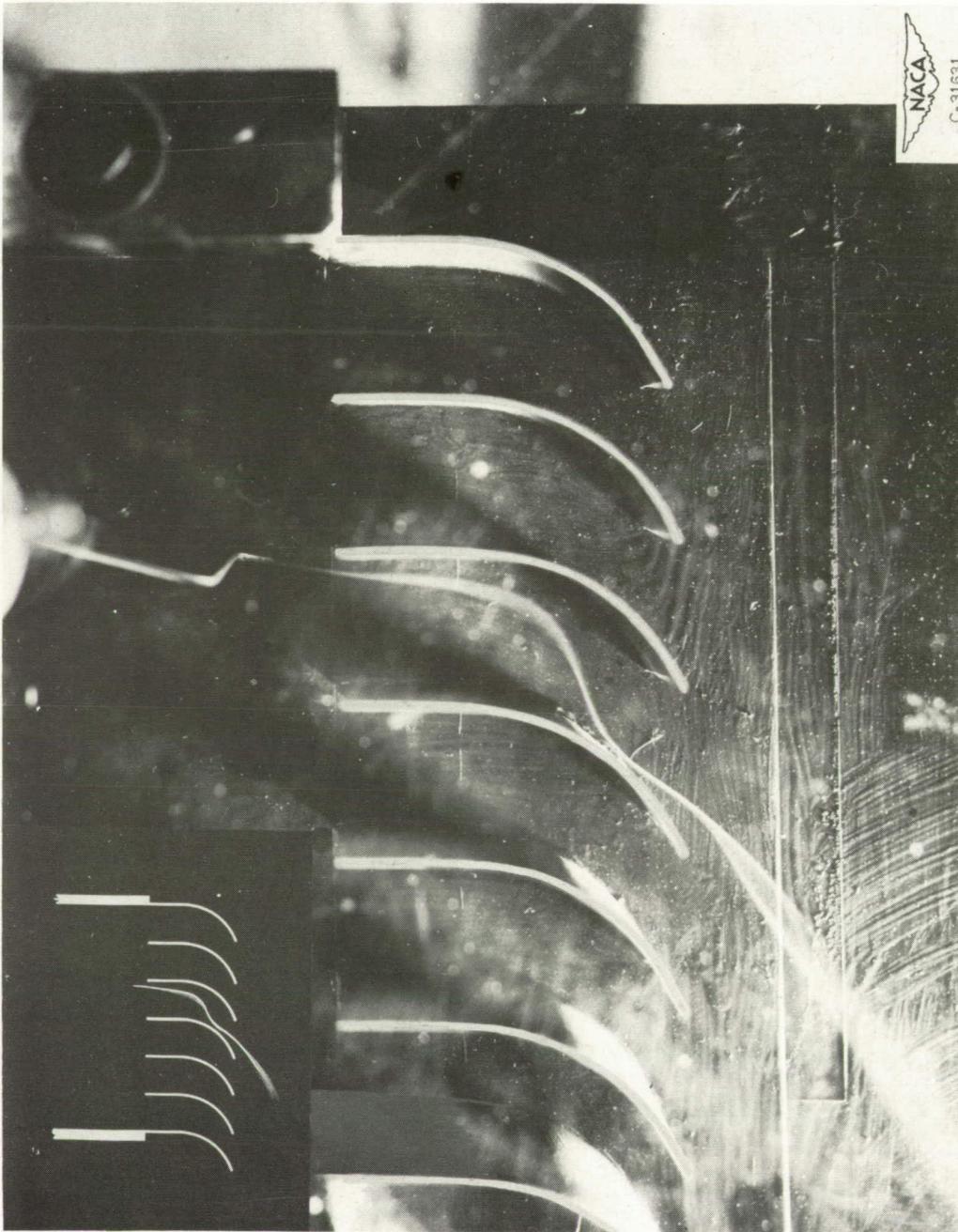
(a) Probe on wall in passage at inlet to 60° rectangular bend.

Figure 27. - Secondary-flow deflection across channel in 60° rectangular bend.
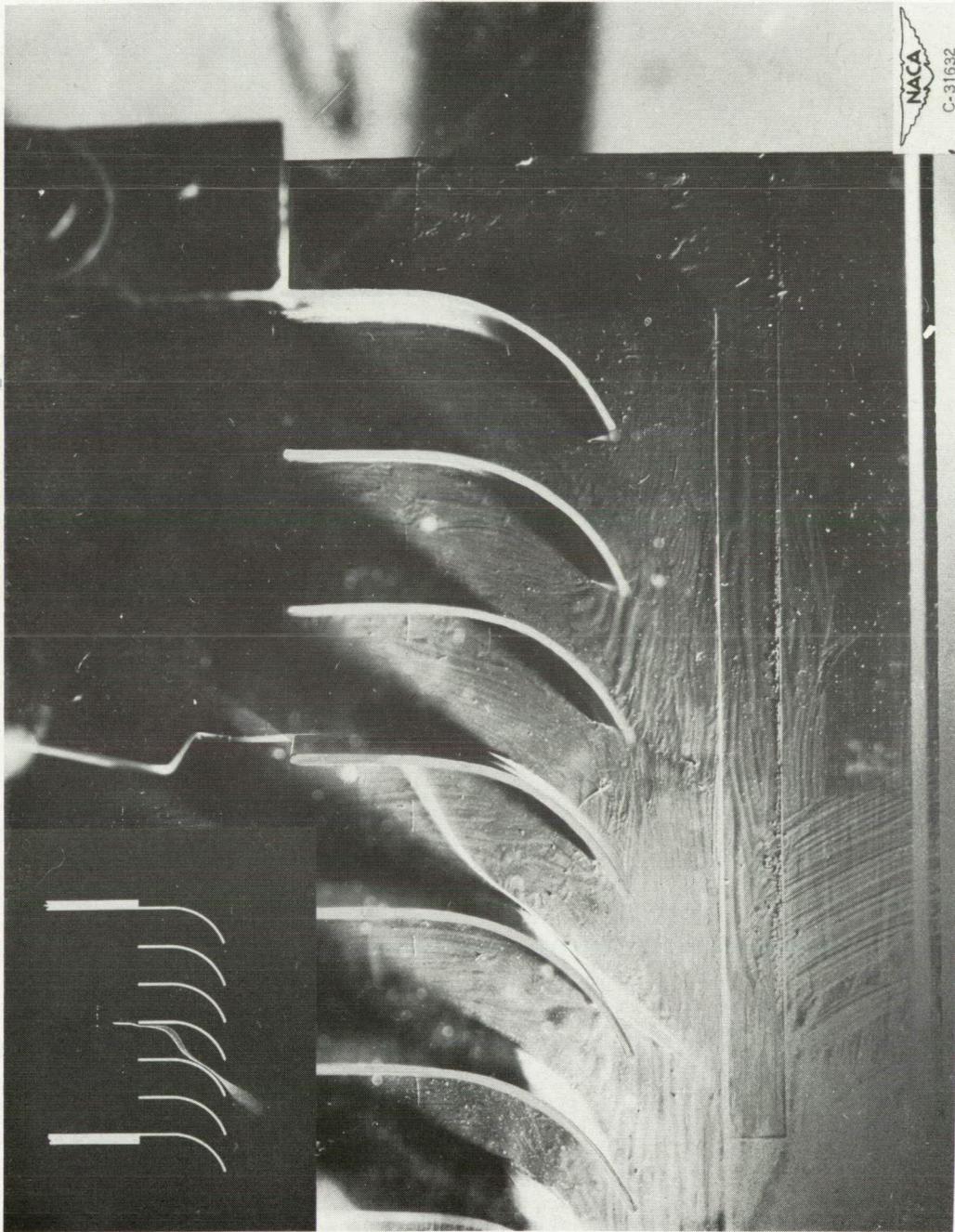
(b) Probe on pressure surface one-fourth inch from wall in 60° rectangular bend.

Figure 27. - Concluded. Secondary-flow deflection across channel in 60° rectangular bend.
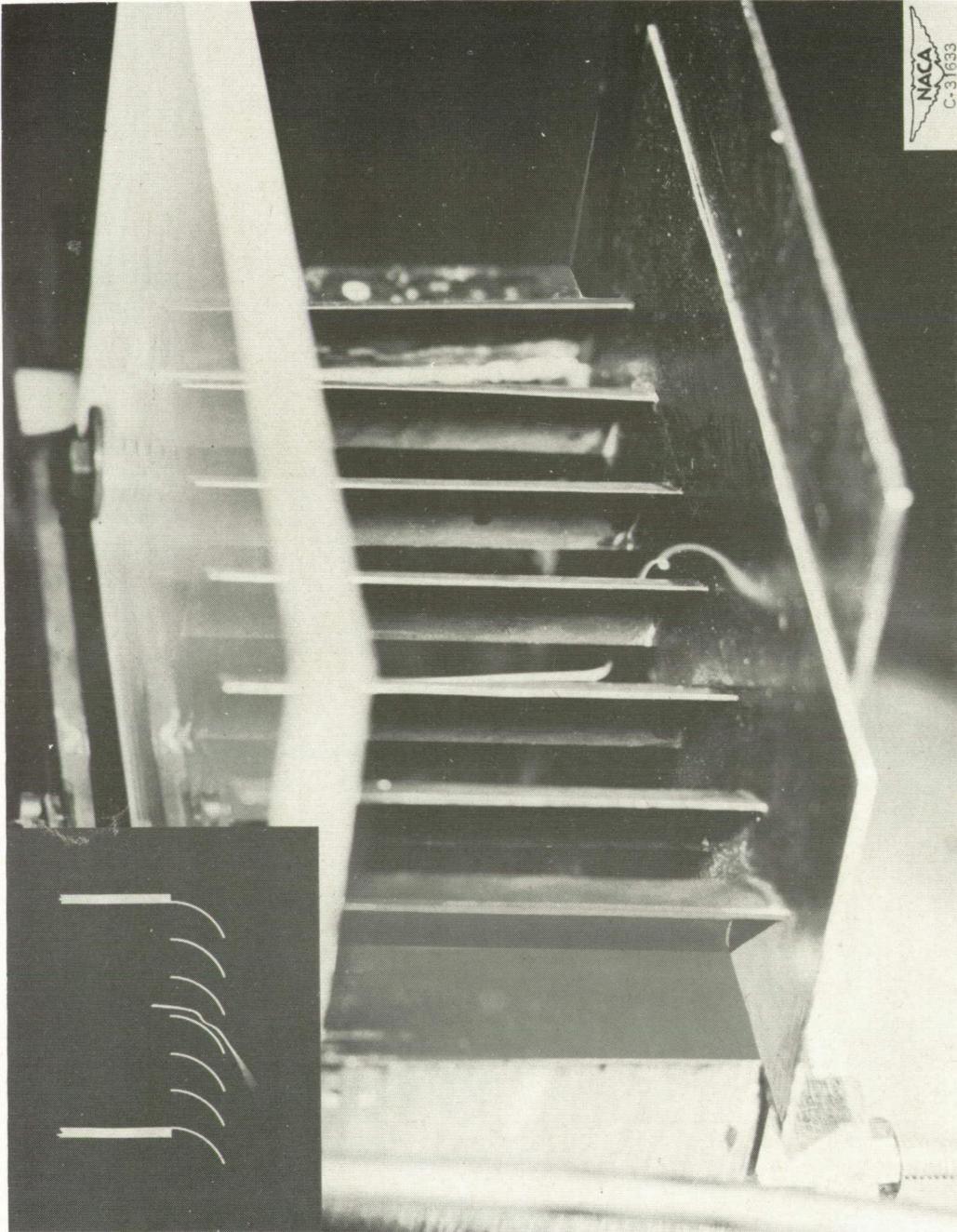
(a) Roll-up of wall boundary layer to form passage vortex. Smoke introduced on wall near suction surface.

Figure 28. - Formation of secondary-flow passage vortex in 60° cascade of blades.

(b) Roll-up of wall boundary layer to form passage vortex. Smoke introduced off wall near suction surface showing continued twisting of vortex downstream of cascade.

Figure 28. - Continued. Formation of secondary-flow passage vortex in 60° cascade of blades.
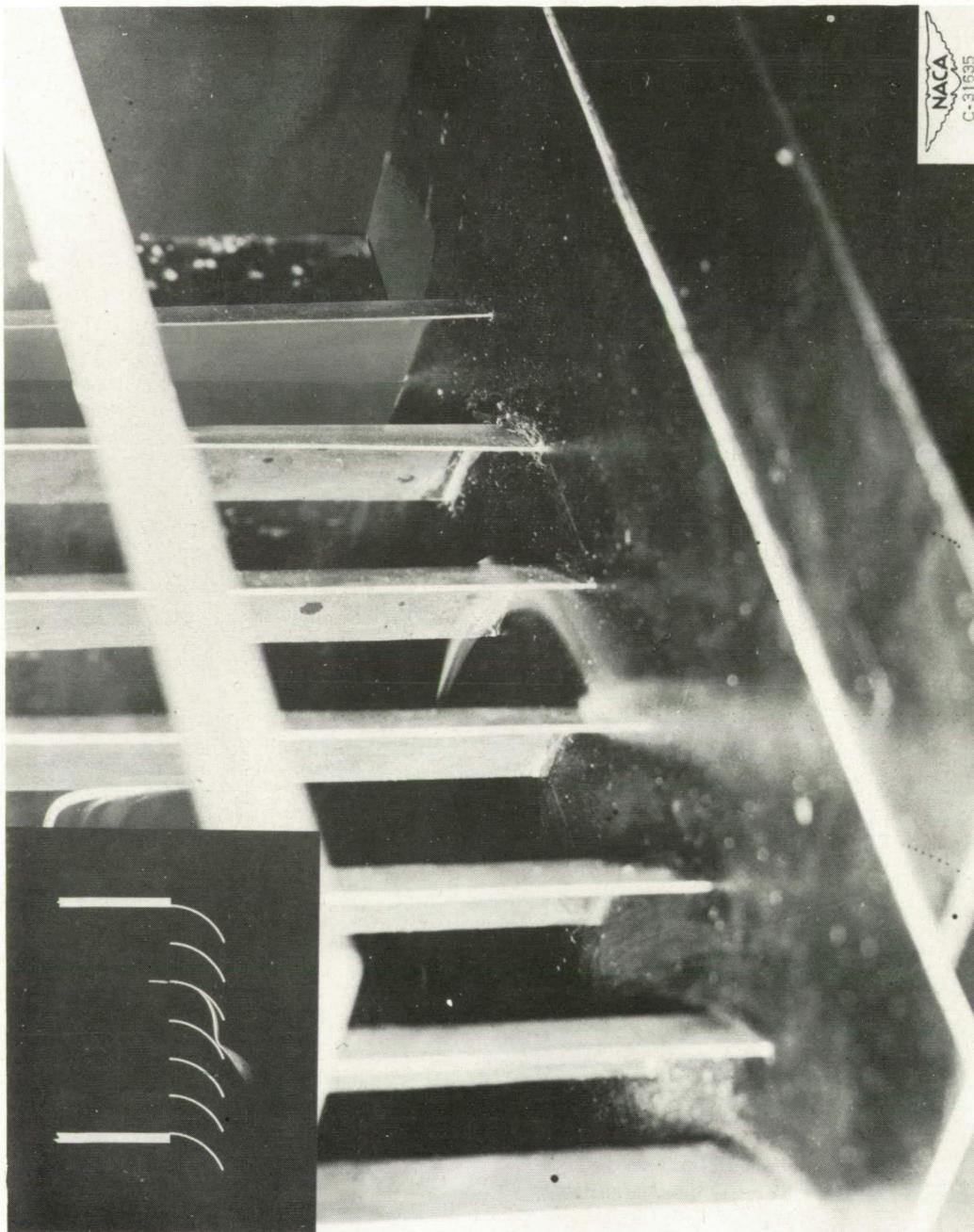
(c) Deflection of flow off blade pressure surface across passage into passage vortex.

Figure 28. - Concluded. Formation of secondary-flow passage vortex in 60° cascade of blades.

Figure 29. - Nose effects in boundary layer of 60° cascade of blades. Smoke introduced on wall near midchannel position.

Figure 30. - Overhead view of nose effect in 60° cascade of blades. Smoke introduced on wall.
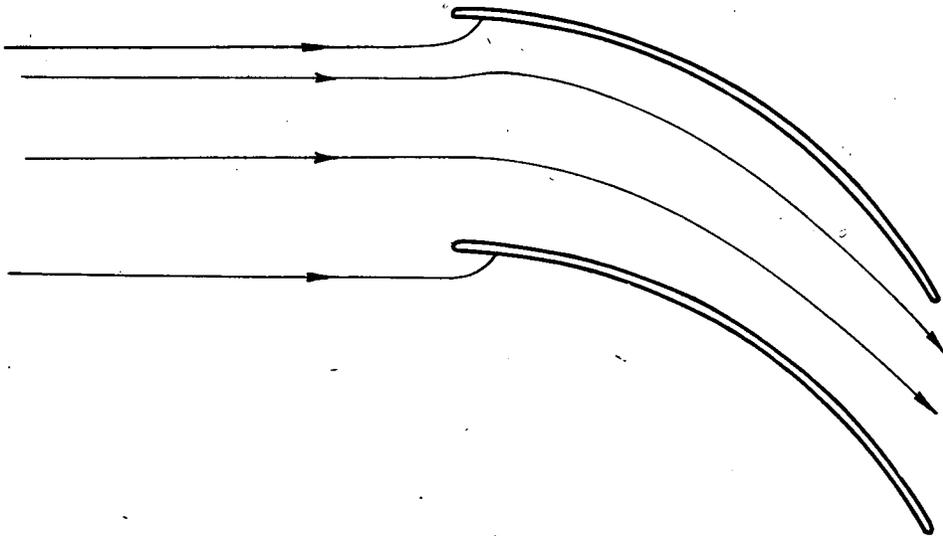
(a) Streamline pattern in 60° cascade.
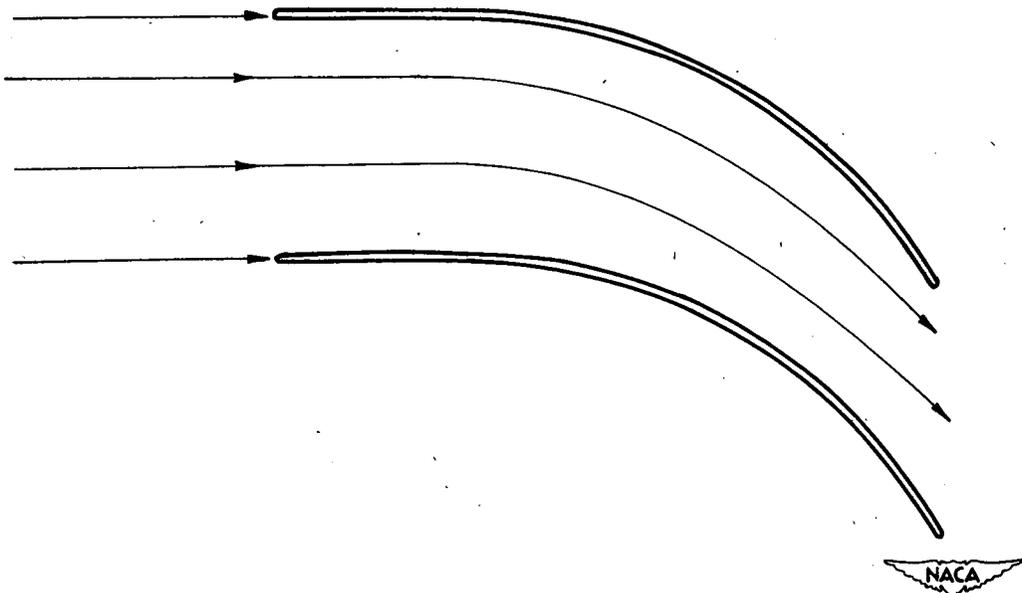
(b) Streamline pattern in 60° bend.

Figure 31. - Comparison of streamline patterns in 60° cascade and 60° bend.

(a) Smoke trace just outside nose stagnation region.

Figure 32. - Secondary-flow streamlines in boundary layer of 60° cascade showing effects of stagnation region near nose.
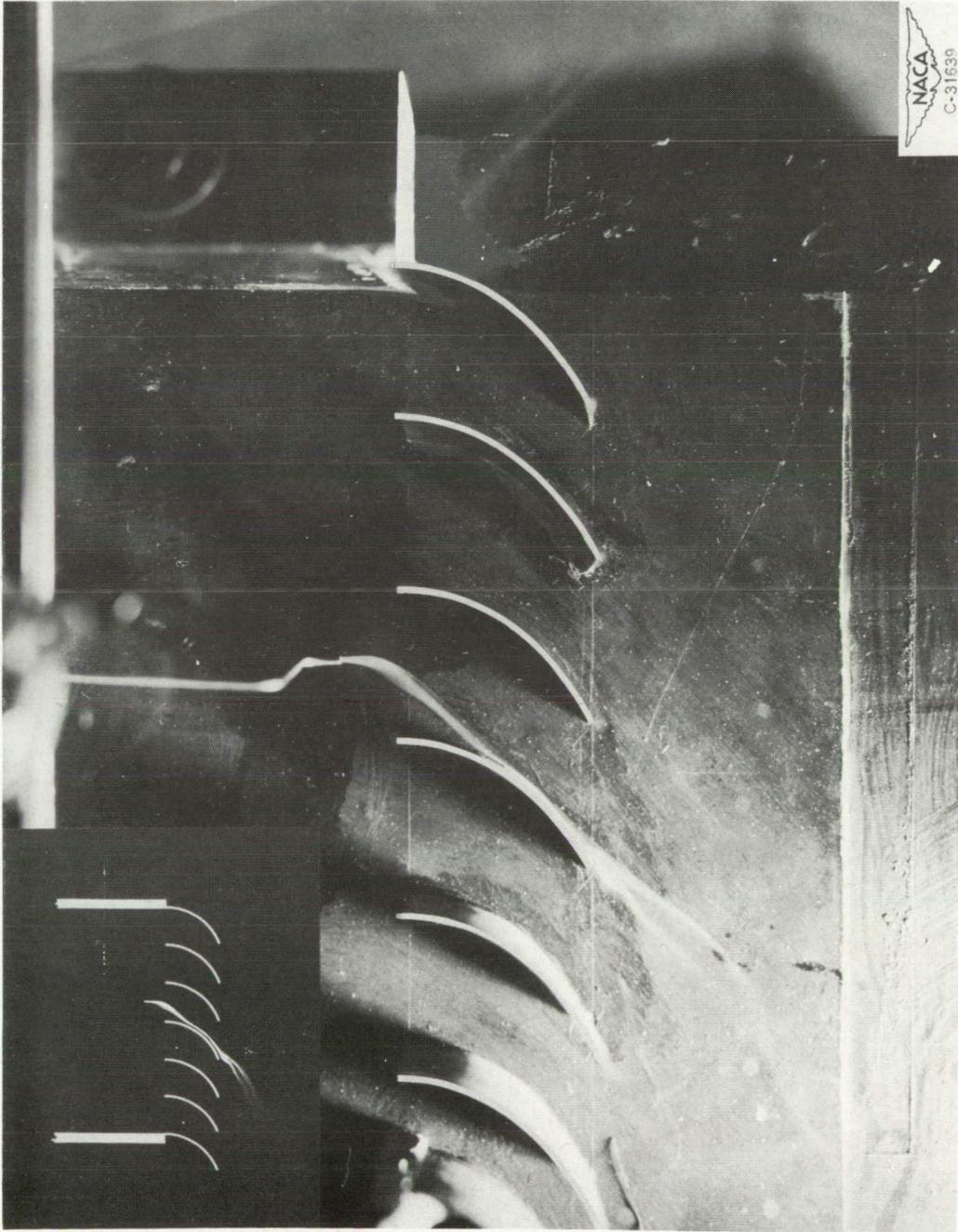
(b) Smoke trace near suction surface at inlet.

Figure 32. - Concluded. Secondary-flow streamlines in boundary layer of 60° cascade showing effects of stagnation region near nose.
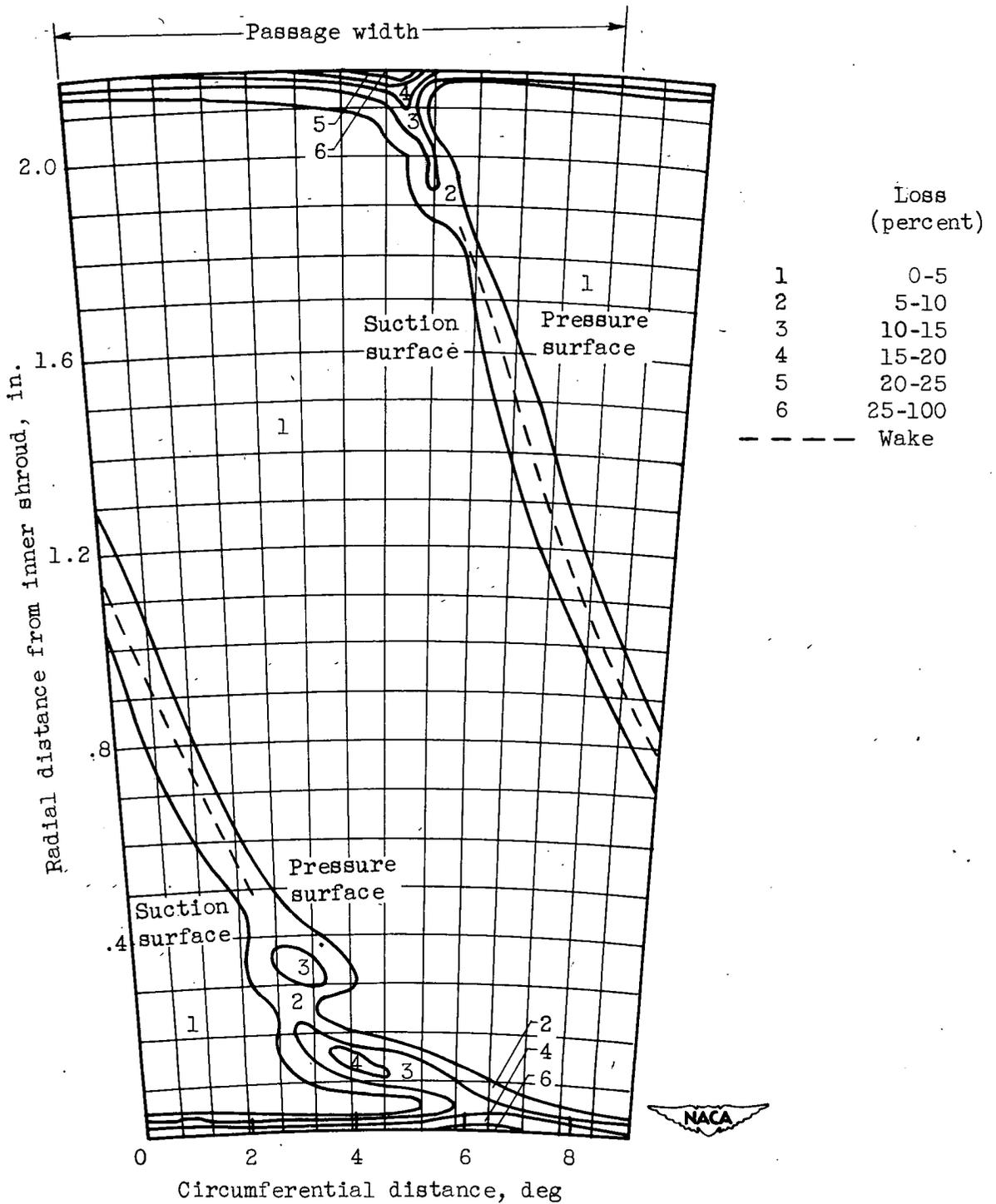
(a) Hub Mach number, 0.94.

Figure 33. - Contours of loss across one blade passage of annular-nozzle cascade.
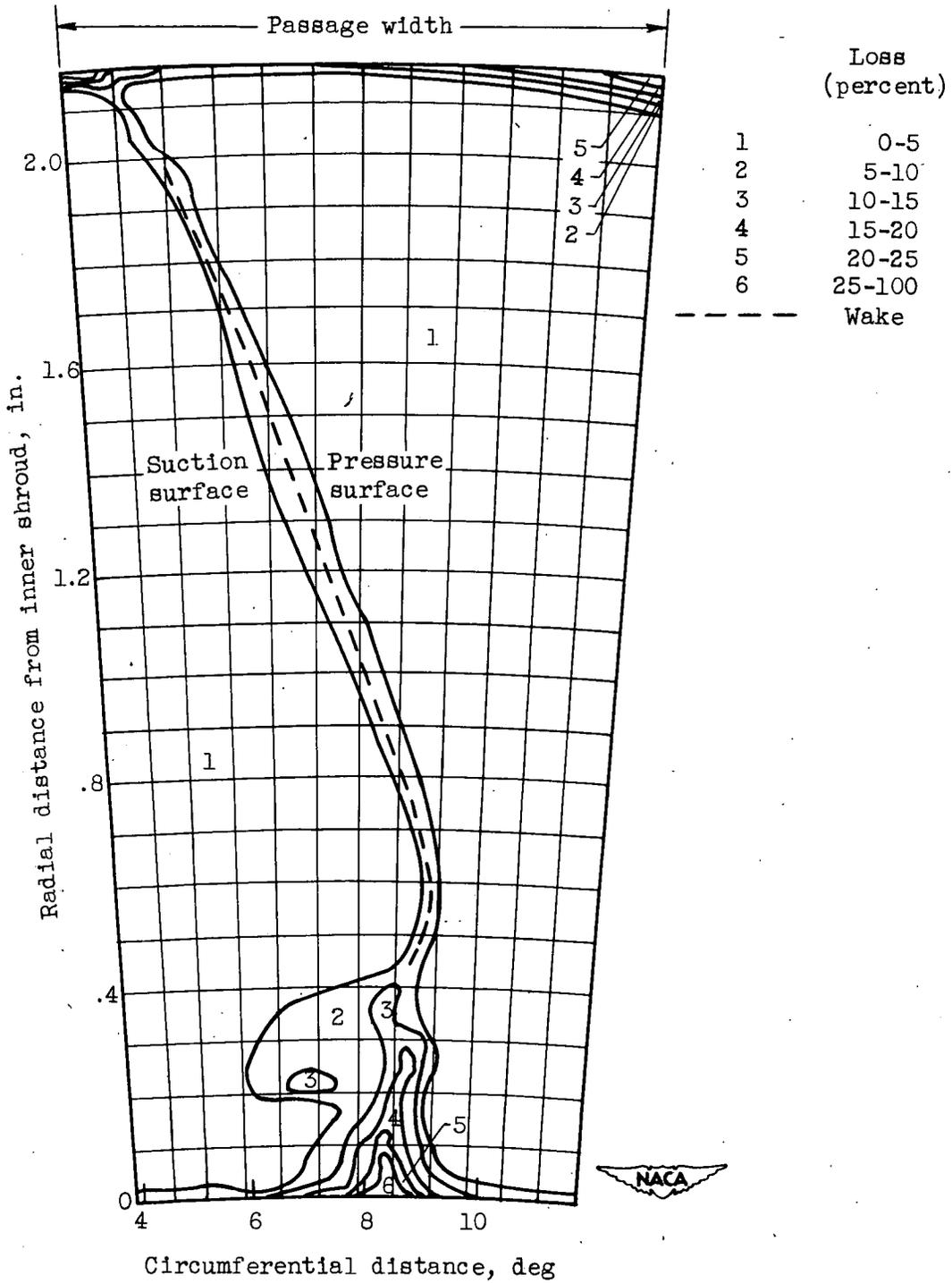
(b) Hub Mach number, 1.46.

Figure 33. - Concluded. Contours of loss across one blade passage of annular-nozzle cascade.
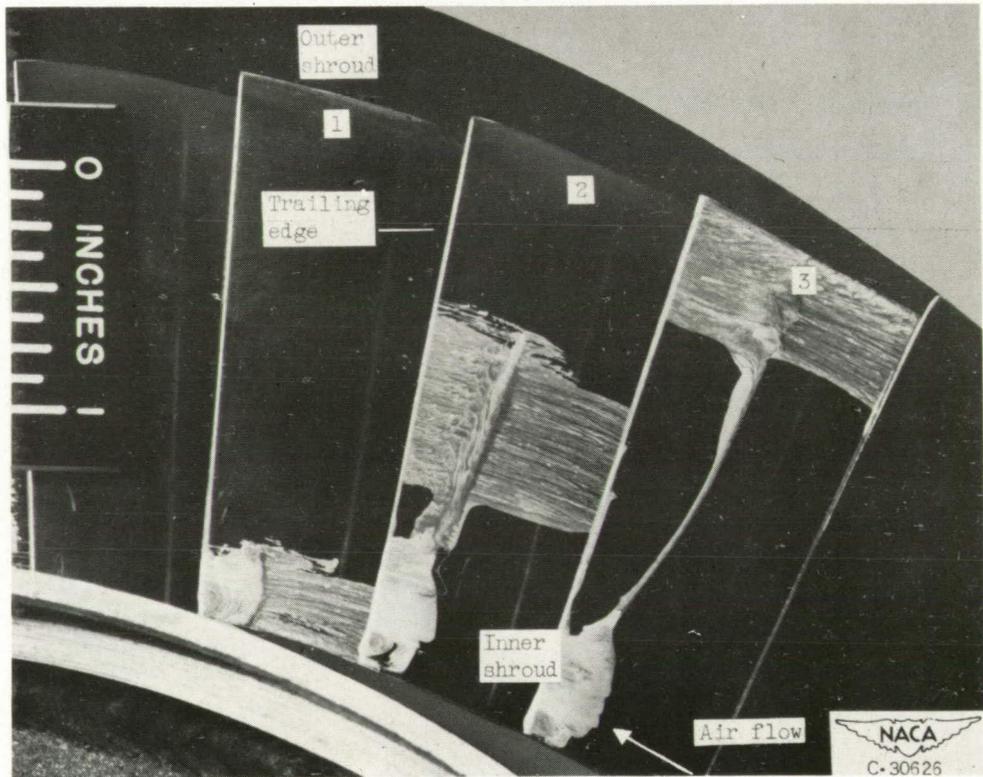
Figure 34. - Enlarged view of inward radial flow of low-momentum fluid showing paint traces of secondary flow along blade suction surface at nozzle discharge of annular—nozzle cascade.
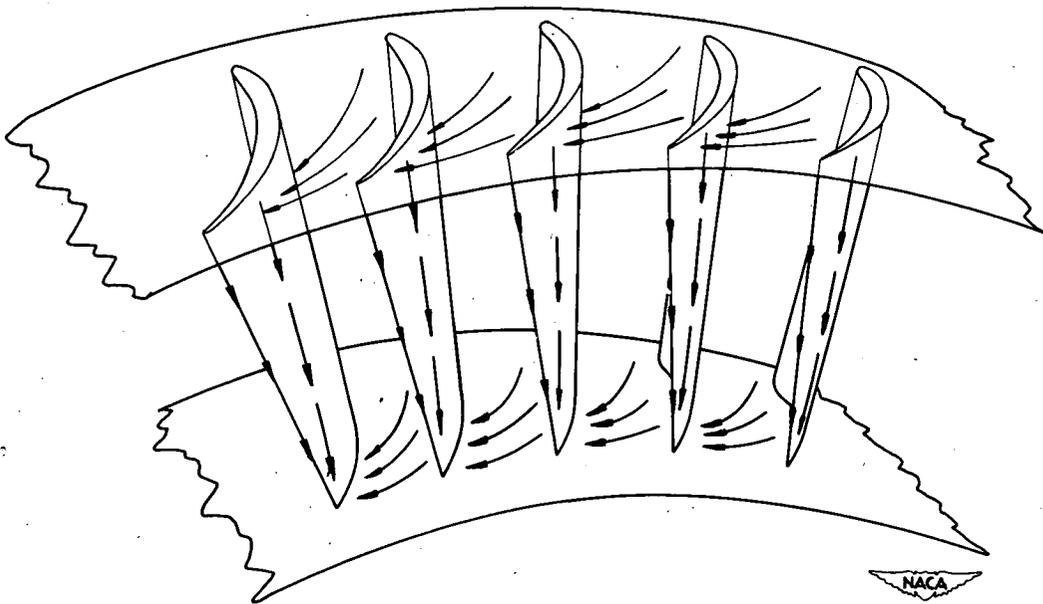
Figure 35. - Secondary-flow components in annular-nozzle cascade as indicated by paint and hydrogen sulfide traces.

(a) Probe away from wall on nose of blade.
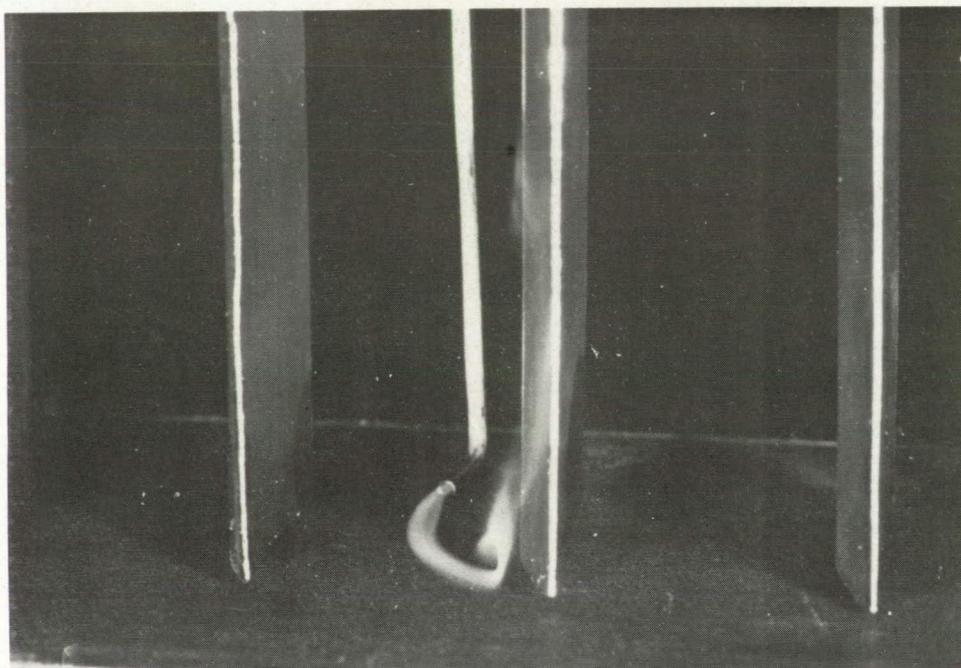
(b) Probe on wall in midchannel.

Figure 36. - Streamline pattern in cascade with 0.014 blade tip clearance. Stagger angle,
0°; solidity, 1.5; angle of attack, 11°; aspect ratio, 2.34.
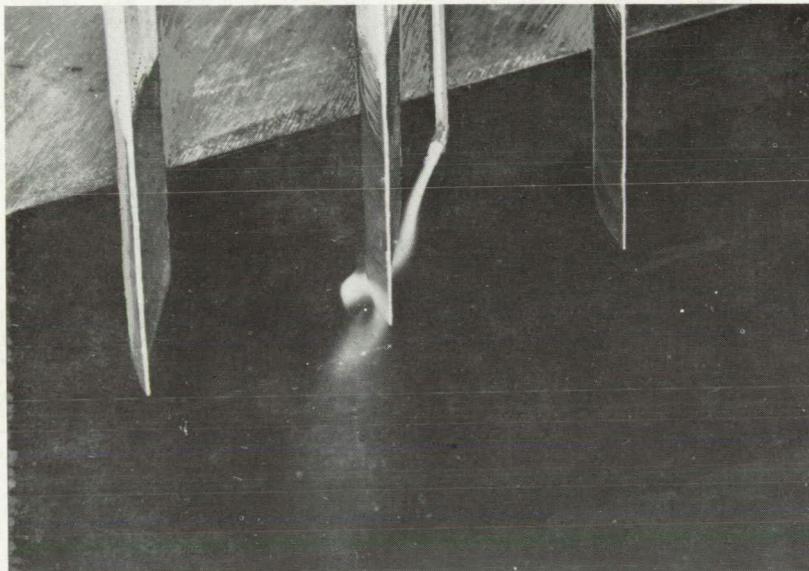
(a) Probe on wall near nose of blade; stagger angle, 45°.
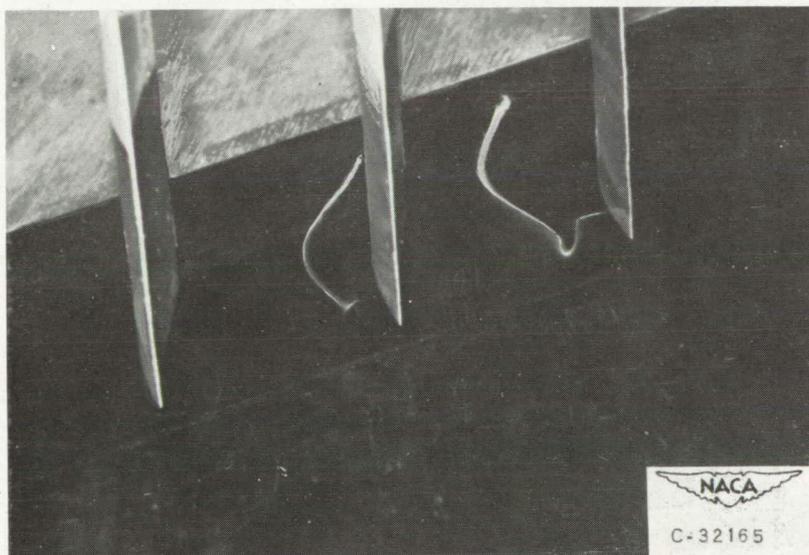
(b) Static taps at inlet near nose of blade and in midchannel positions;
    stagger angle, 45°.

Figure 37. - Streamline patterns for cascade with 0.060-inch blade tip clearance.
    Solidity, 1.5; angle of attack, 11°; aspect ratio, 2.34.
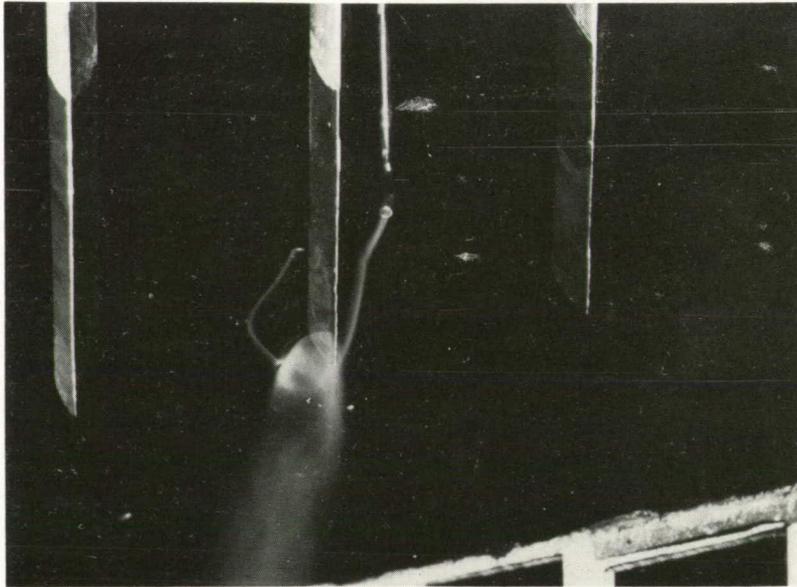
(c) Static tap near nose of blade and probe on wall near nose of blade;
     stagger angle, 45°.
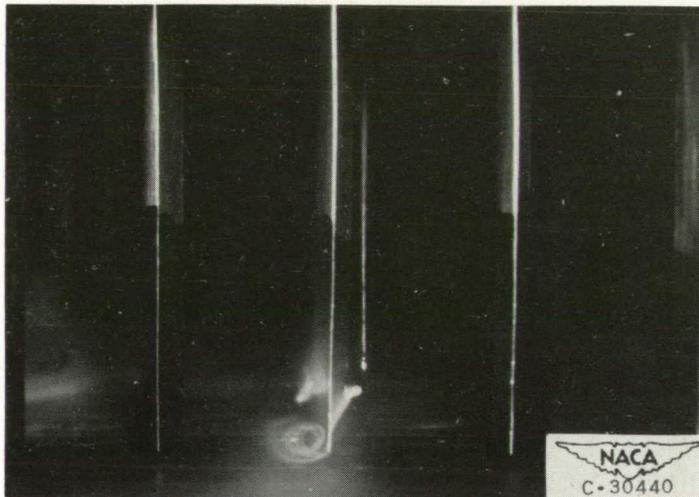
(d) Probe away from wall on nose of blade; stagger
     angle, 0°.

Figure 37. - Concluded. Streamline patterns for cascade with 0.060-inch blade tip
     clearance. Solidity, 1.5; angle of attack, 11°; aspect ratio, 2.34.
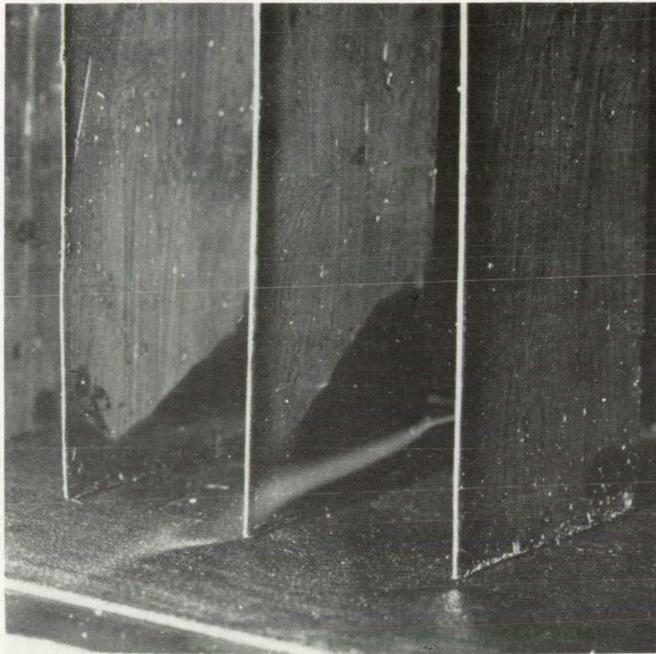
(a) Probe on nose of blade; stationary wall.
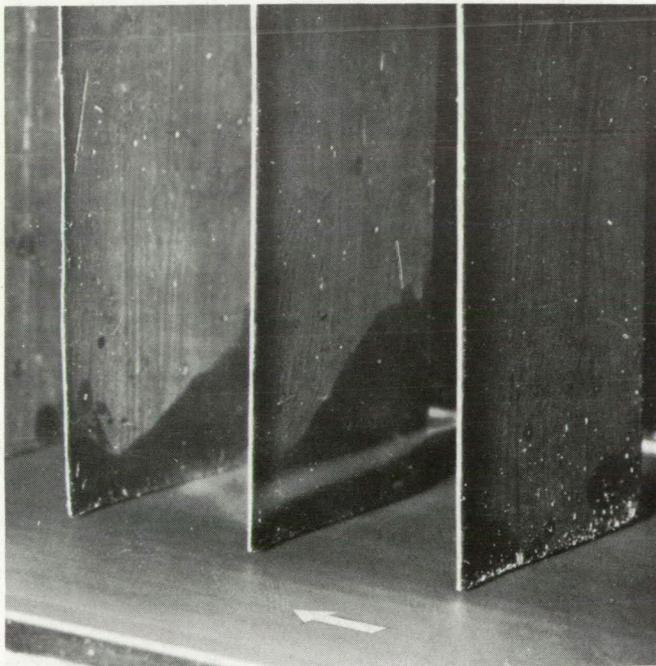
(b) Probe on nose of blade; moderate-speed wall.

Figure 38. - Streamline deflections on pressure surface of blade. Pressure surface
    leading; 0.014-inch blade tip clearance; stagger angle, 0°; solidity, 1.5; angle of
    attack, 11°; aspect ratio, 2.34.
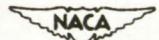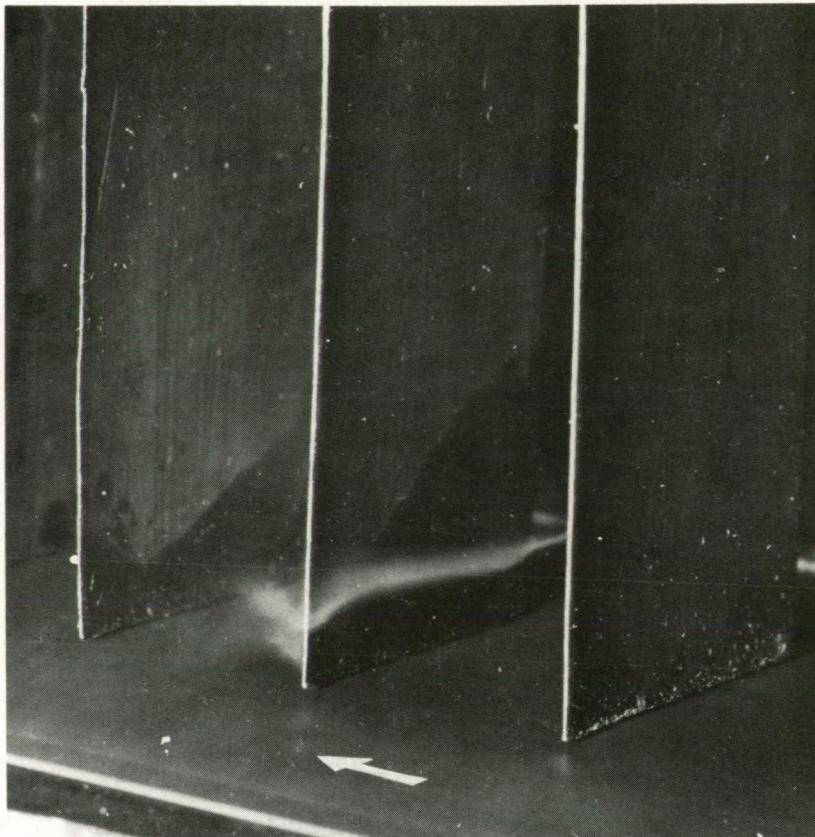
(c) Probe on nose of blade; high-speed wall.

Figure 38. - Concluded. Streamline deflections on pressure surface of blade. Pressure
surface leading; 0.014-inch blade tip clearance; stagger angle, 0°; solidity, 1.5;
angle of attack, 11°; aspect ratio, 2.34.
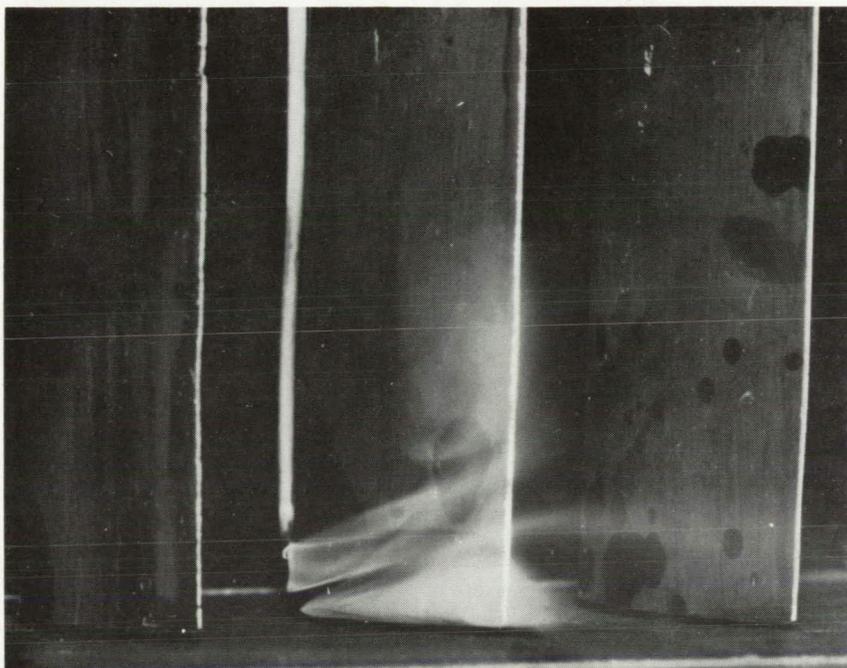
(a) Probe on nose of blade; stationary wall.
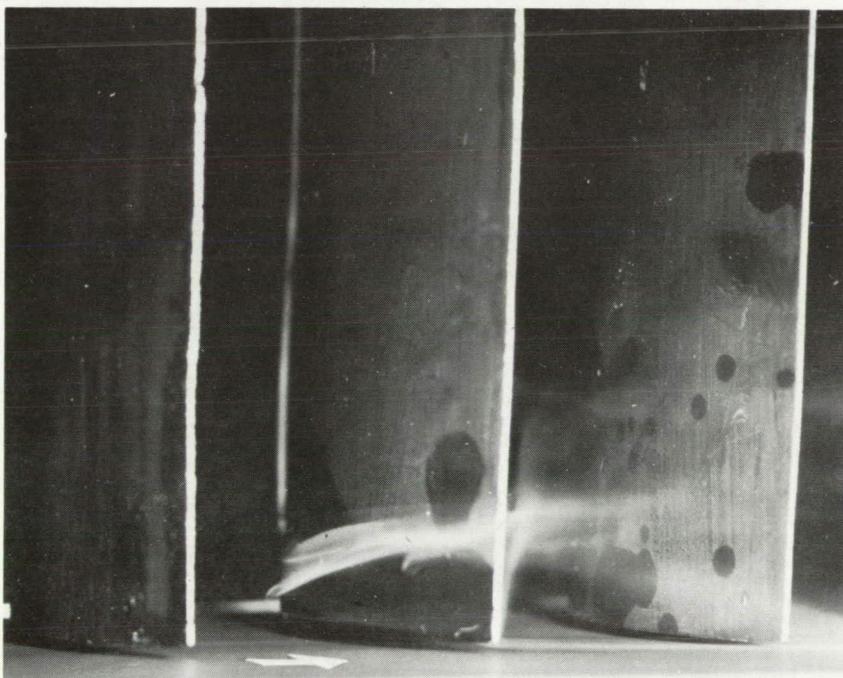
(b) Probe on nose of blade; moderate-speed wall.

Figure 39. - Streamline deflections on suction surface of blade. Suction surface lead-
   ing; 0.014-inch blade tip clearance; stagger angle, 0°; solidity, 1.5; angle of attack,
   11°; aspect ratio, 2.34.
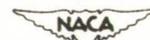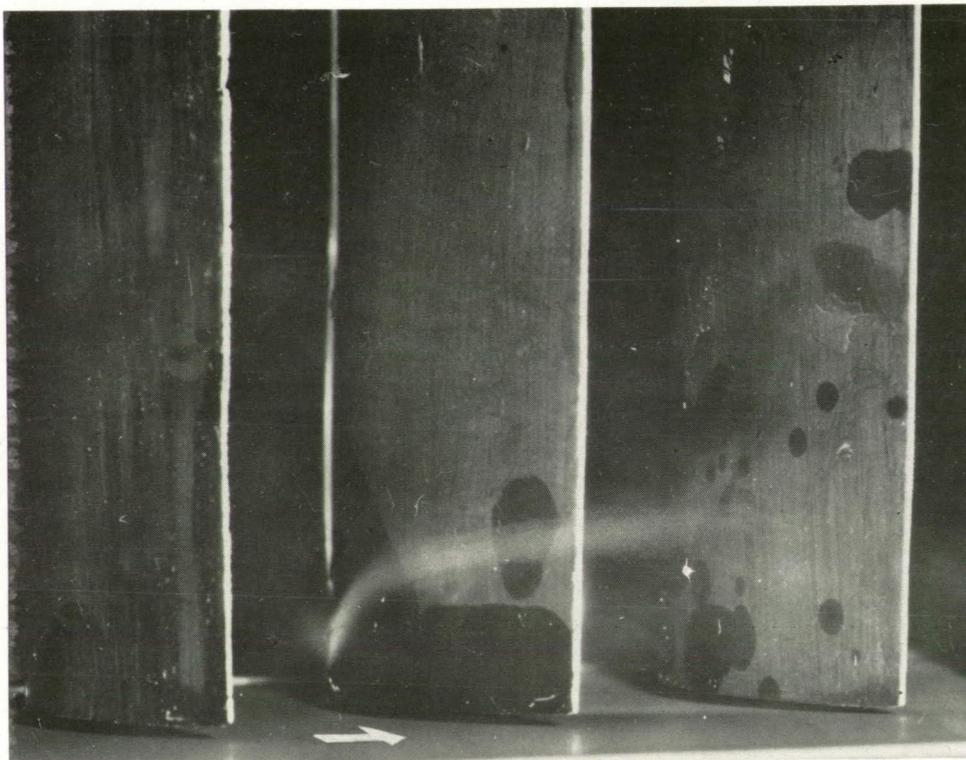
C-30444

(c) Probe on nose of blade; high-speed wall.

Figure 39. - Concluded. Streamline deflections on suction surface of blade. Suction
surface leading; 0.014-inch blade tip clearance; stagger angle, 0°; solidity, 1.5;
angle of attack, 11°; aspect ratio, 2.34.
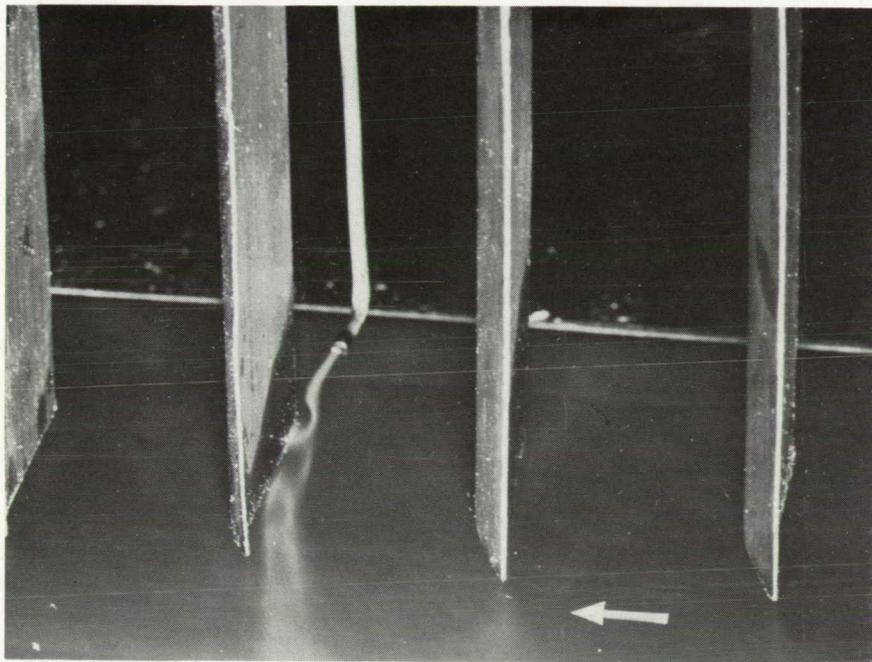
(a) Probe near pressure surface of blade; moderate-speed wall; downstream view.
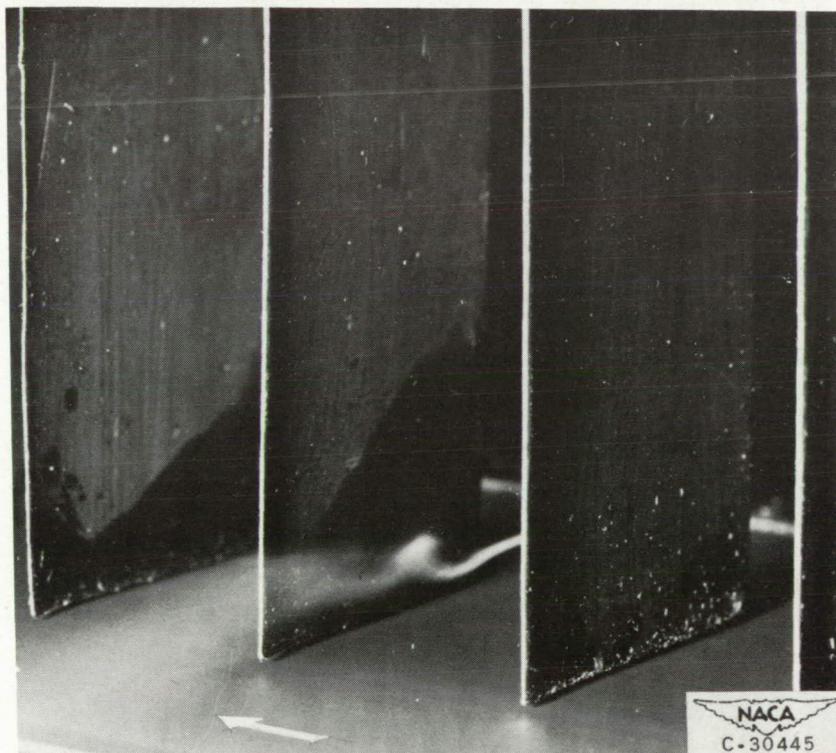
(b) Probe near pressure surface of blade; moderate-speed wall; side view.

Figure 40. - Streamline patterns showing scraping effect of blade. Pressure surface leading; 0.014-inch blade tip clearance; stagger angle, 0°; solidity, 1.5; angle of attack, 11°; aspect ratio, 2.34.
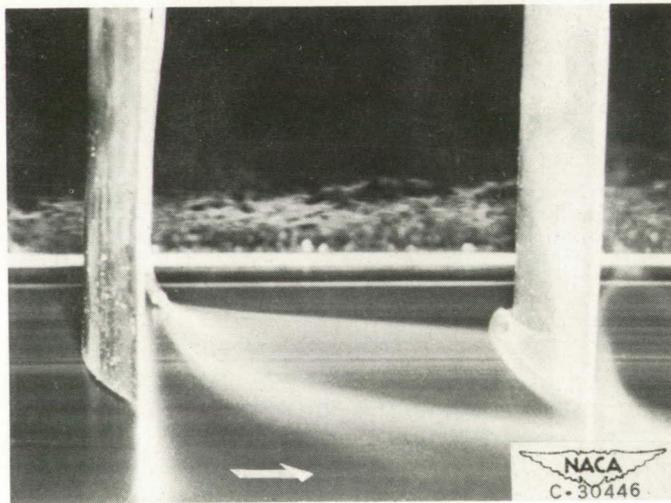
Figure 41. - Streamline patterns showing scraping effect of blade; suction surface leading.
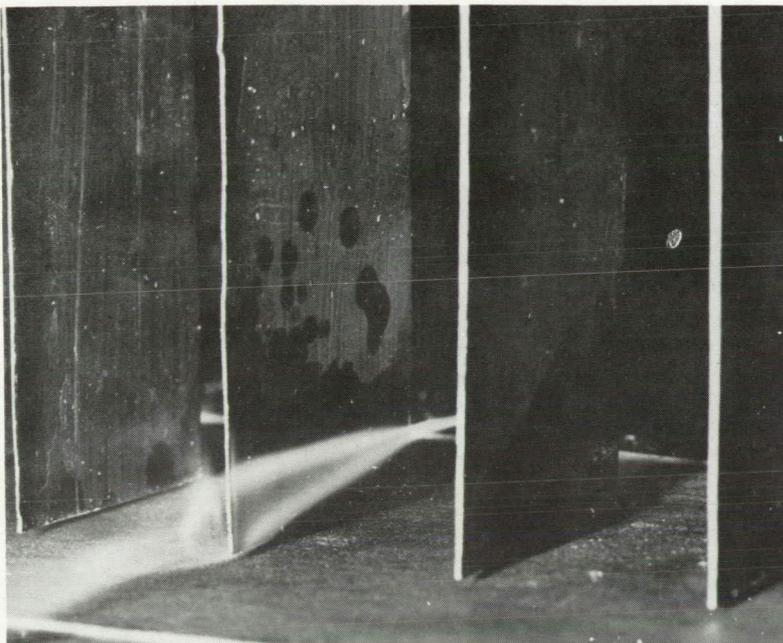
(a) Probe on nose; stationary wall.
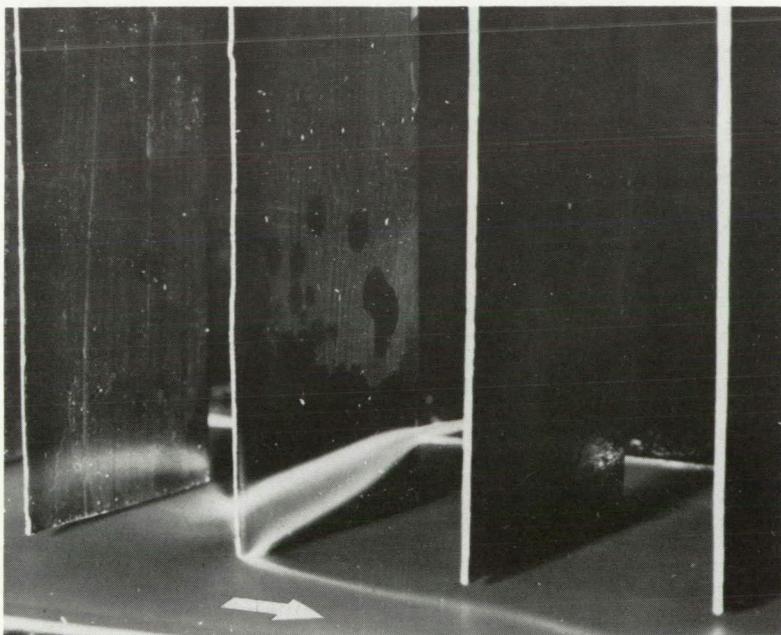
(b) Probe on nose; slow-speed wall.
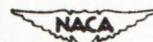
Figure 42. - Streamline deflections on pressure surface of blade. Suction surface leading; 0.014-inch blade tip clearance; stagger angle, 0°; solidity, 1.5; angle of attack, 11°; aspect ratio, 2.34.
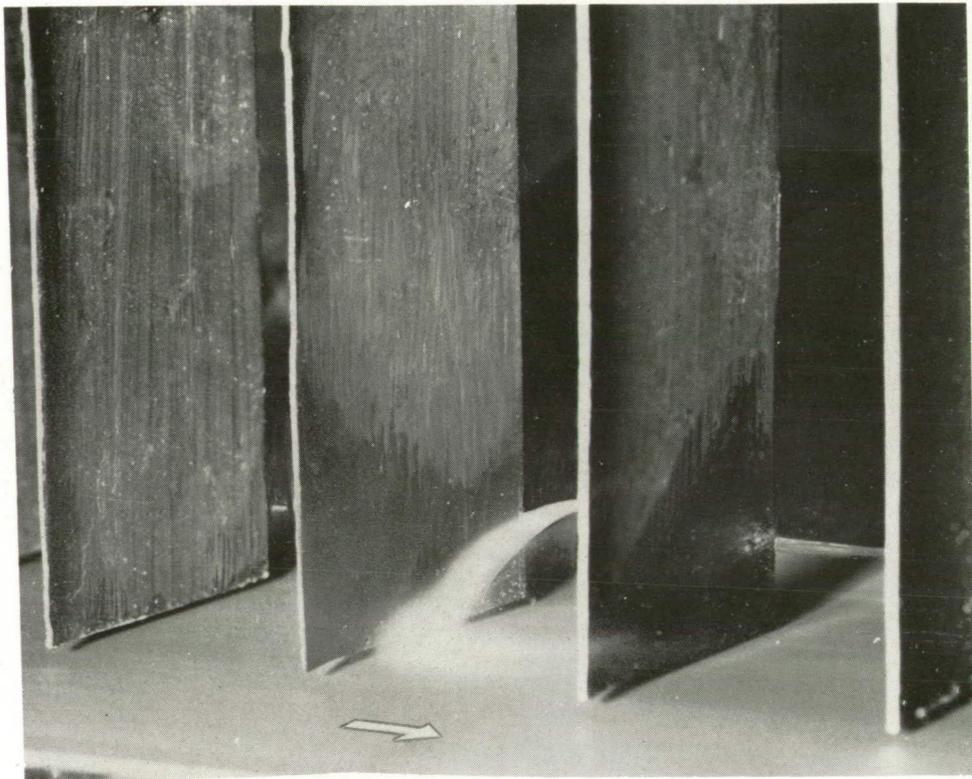
(c) Probe on nose; high-speed wall.

Figure 42. - Concluded. Streamline deflections on pressure surface of blade. Suction
   surface leading; 0.014-inch blade tip clearance; stagger angle, 0°; solidity, 1.5;
   angle of attack, 11°; aspect ratio, 2.34.
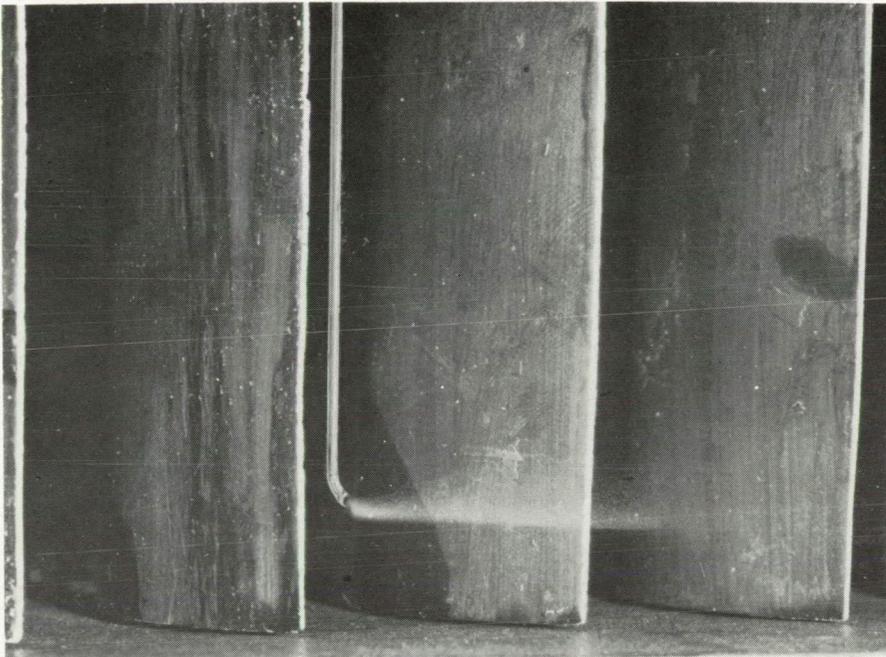
(a) Probe on nose; stationary wall.
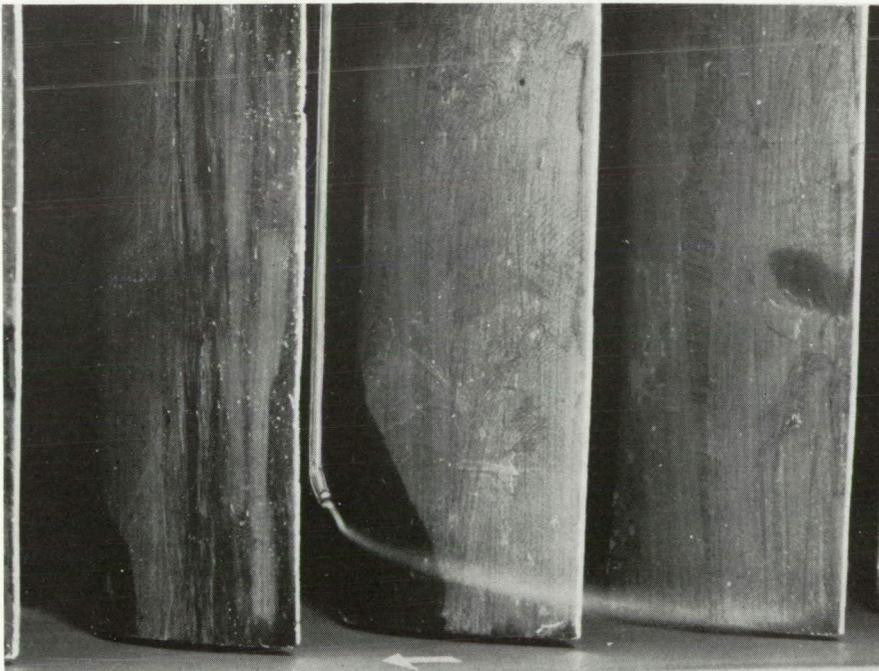
(b) Probe on nose; moderate-speed wall.

Figure 43. - Streamline deflection on suction surface of blade. Pressure surface
leading; 0.014-inch blade tip clearance; stagger angle, 0°; solidity, 1.5; angle
of attack, 11°; aspect ratio, 2.34.
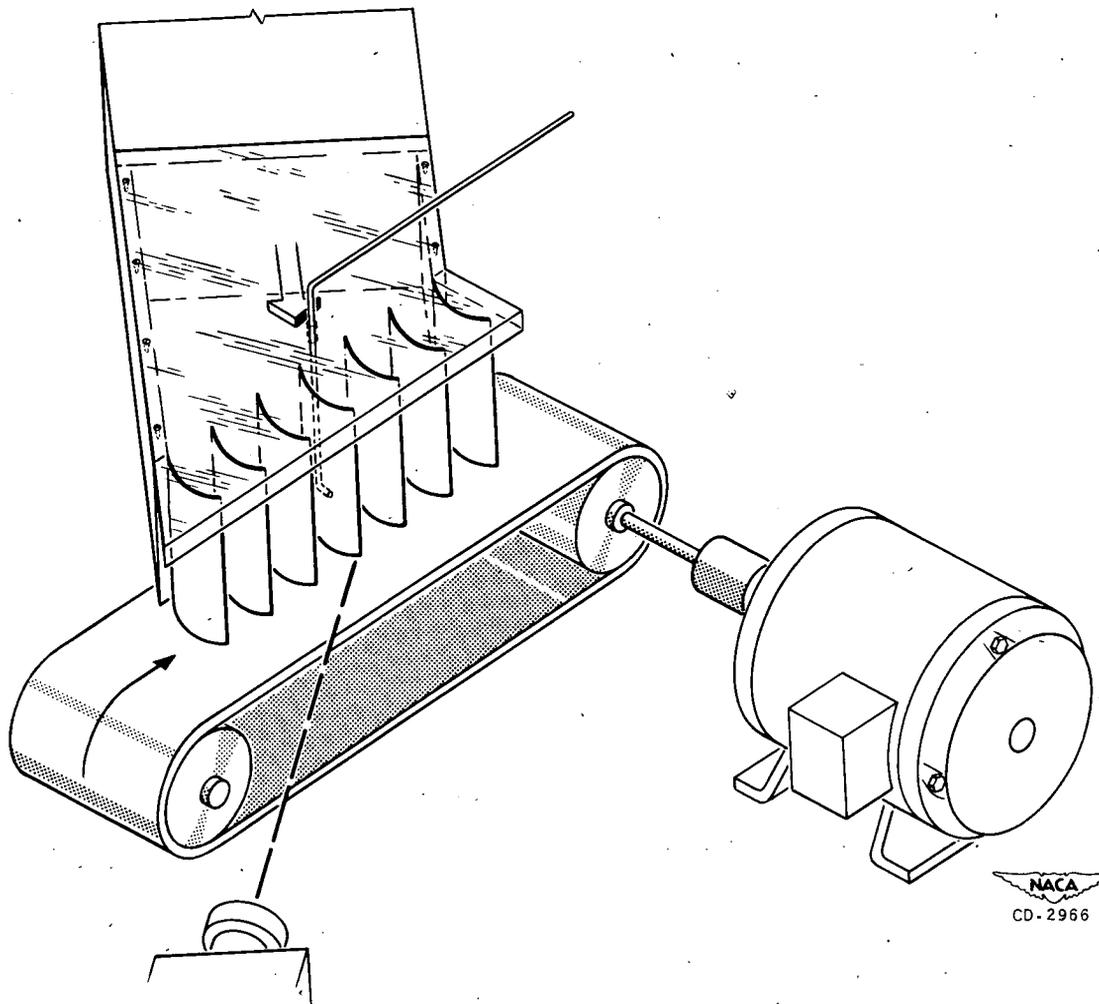
(a) Schematic diagram of apparatus.

Figure 44. - Tip-clearance effects with relative motion between wall and high-turning
blades. Smoke introduced on pressure surface of middle blade.

(b) Stationary wall.

Figure 44. - Continued. Tip-clearance effects with relative motion between wall and high-turning blades. Smoke introduced on pressure surface of middle blade.
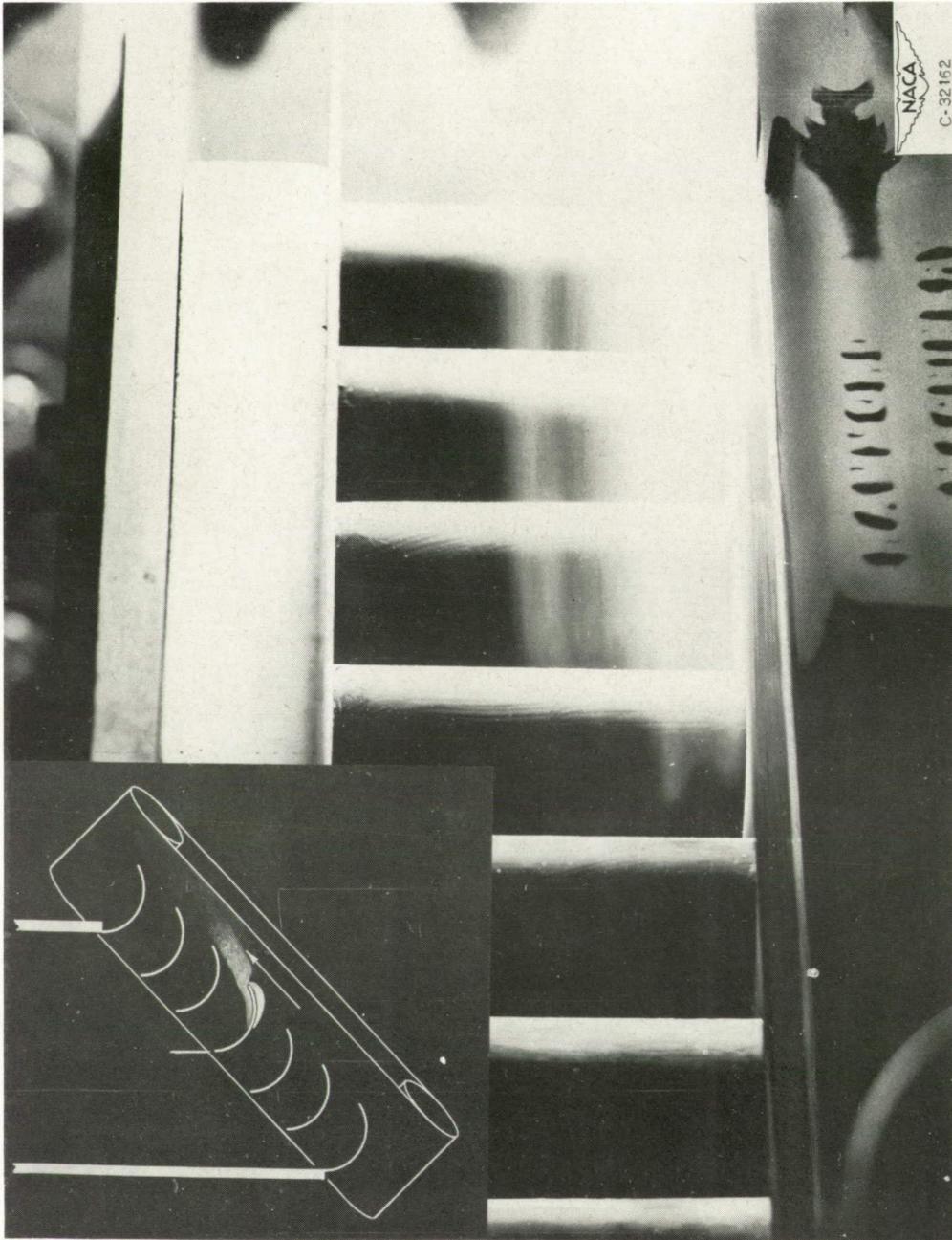
(c) Moderate-speed wall.

Figure 44. - Continued. Tip-clearance effects with relative motion between wall and high-turning blades. Smoke introduced on pressure surface of middle blade.
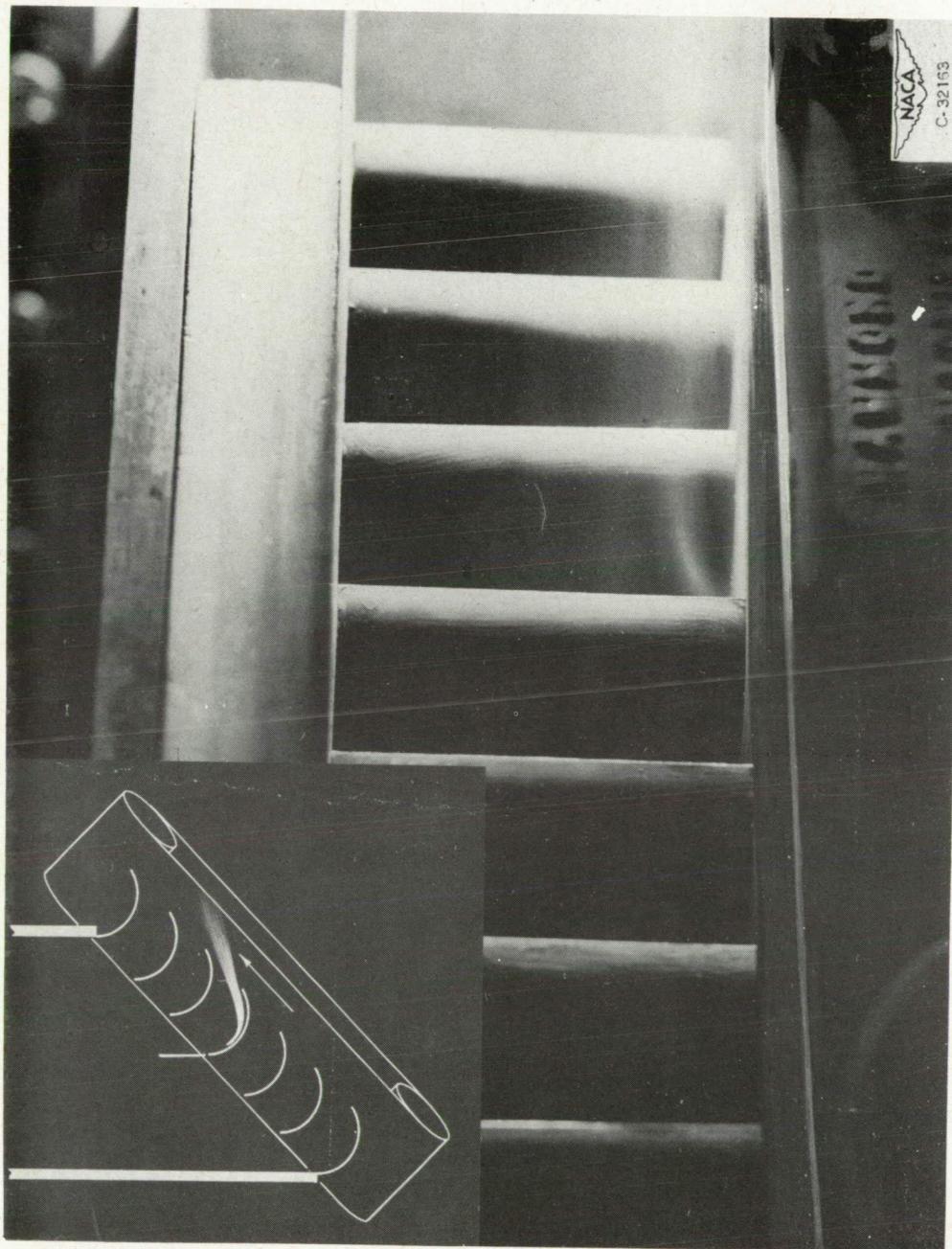
(d) High-speed wall.

Figure 44. - Concluded. Tip-clearance effects with relative motion between wall and high-turning blades. Smoke introduced on pressure surface of middle blade.
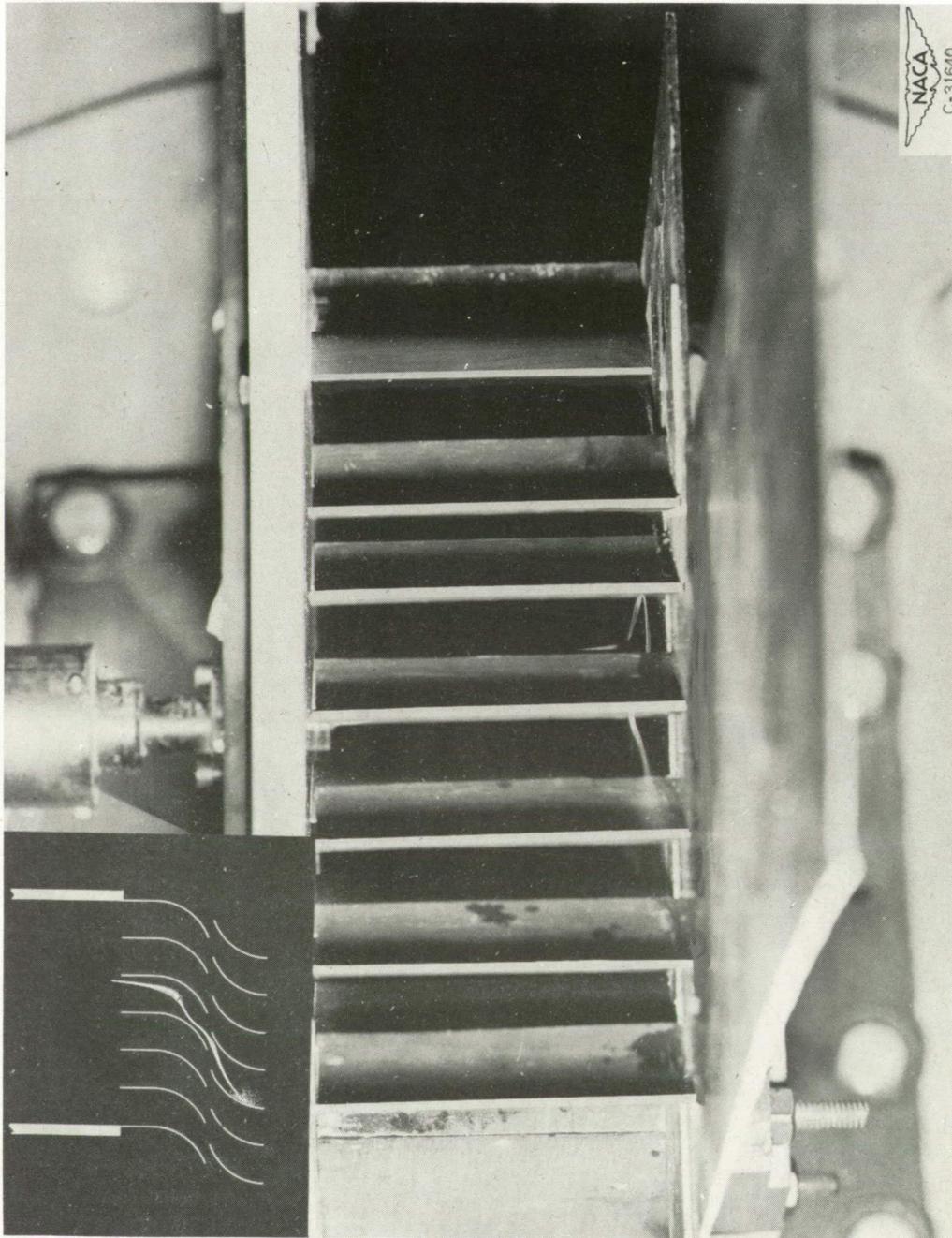
(a) Probe on wall at inlet to upstream cascade near pressure surface.

Figure 45. - Passage vortex generated by upstream cascade striking pressure surface of blade in downstream cascade.
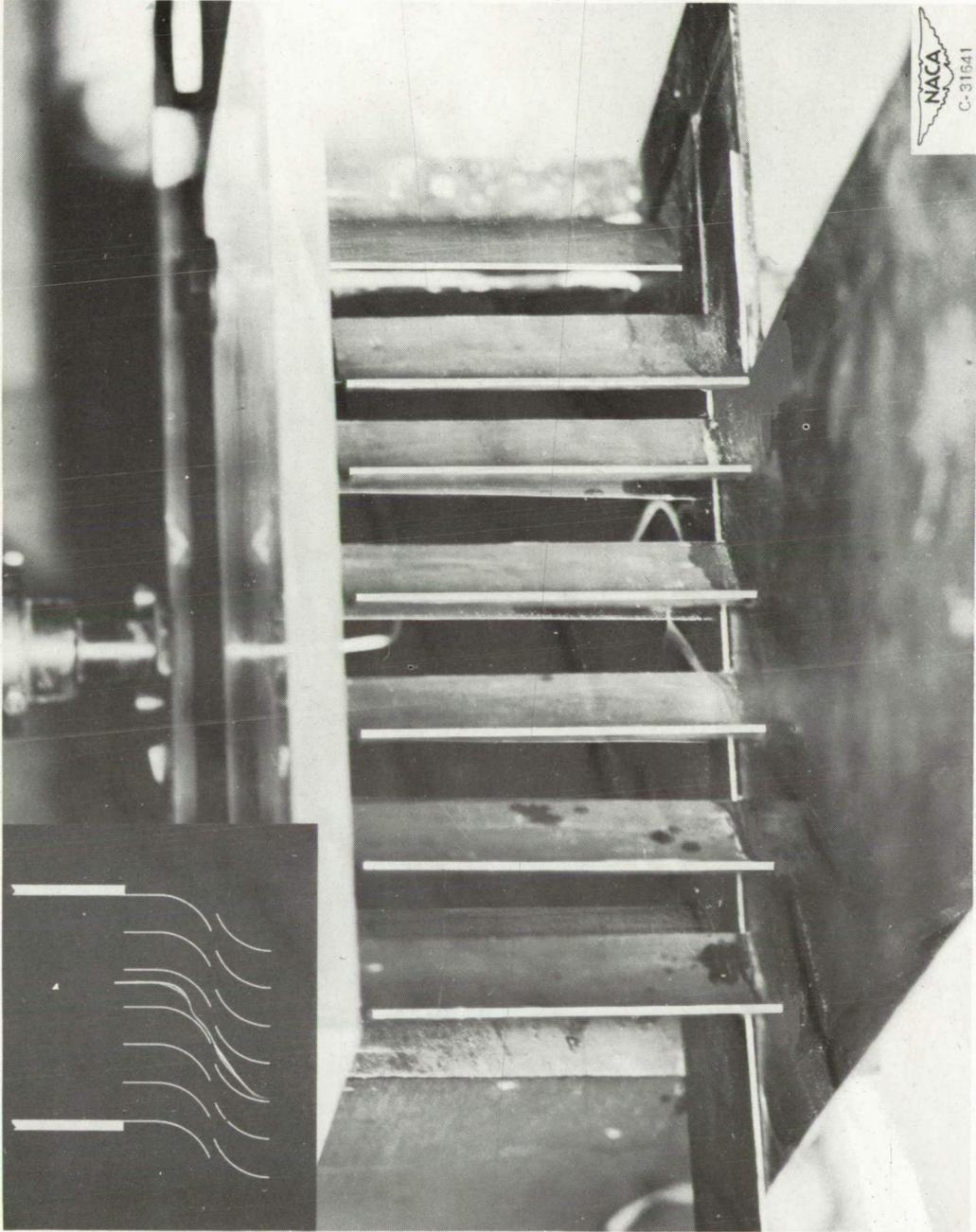
(b) Probe on wall at inlet to upstream cascade near suction surface.

Figure 45. - Concluded. Passage vortex generated by upstream cascade striking pressure surface of blade in downstream cascade.